

**Hierarchical Control and Management Strategy
of Microgrid with Hybrid Energy Resources**

BY
Tawfiq Naji T. Kameel

A Thesis Presented to the
DEANSHIP OF GRADUATE STUDIES

KING FAHD UNIVERSITY OF PETROLEUM & MINERALS
DHAHRAN, SAUDI ARABIA

In Partial Fulfillment of the
Requirements for the Degree of

MASTER OF SCIENCE
In
ELECTRICAL ENGINEERING

May, 2014



KING FAHD UNIVERSITY OF PETROLEUM & MINERALS

DHAHRAN- 31261, SAUDI ARABIA

DEANSHIP OF GRADUATE STUDIES

This thesis, written by **TAWFIQ NAJI KAMEEL** under the direction his thesis advisor and approved by his thesis committee, has been presented and accepted by the Dean of Graduate Studies, in partial fulfillment of the requirements for the degree of **MASTER OF SCIENCE IN ELECTRICAL ENGINEERING**.



Dr. ALI AHMAD AL-SHAIKHI
Department Chairman



Dr. SALAM A. ZUMMO
Dean of Graduate Studies

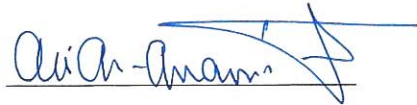
26/5/14
Date



Dr. MOHAMMED ALI ABIDO
(Advisor)



Dr. IBRAHIM EL-AMIN
(Member)



Dr. ALI T. AL-AWAMI
(Member)

TAWFIQ NAJI TAWFIQ KAMEEL

2014

DEDICATION

بِسْمِ اللَّهِ الرَّحْمَنِ الرَّحِيمِ

قُلْ إِنَّ صَلَاتِي وَنُسُكِي وَمَحْيَايَ وَمَمَاتِي لِلَّهِ رَبِّ الْعَالَمِينَ

To the soul of my dear father

To my mother

To my brothers and sisters

To my Fiancé

To all friends and colleagues

To every one works in this field

To all of them,

I dedicate this work

ACKNOWLEDGMENTS

To begin with, I thank the one and only Almighty Allah for giving me more than I can ever deserve and for guiding me in my life journey to where I have reached.

I would like to start out my acknowledgement by expressing my deep appreciation to my academic advisor **Prof. Mohammed A. Abido** for helping me with all his capabilities till the completion of this work. I thank him for all the effort and valuable time he spent helping me.

I would like to send a special thanks to the Electrical Engineering Department represented by the chairman **Dr. Ali A. Al-Shaikhi**. I would also like to thank the committee members, **Prof. Ibrahim M. El-Amin** and **Dr. ALI T. AL-AWAMI** for their suggestions and interest in my work.

Furthermore I would also like to thank the Research Institute and especially the Center of Engineering Research director **Dr. Luai M. Al-Hadrami** for supporting me in my studies.

Thanks to KFUPM for accepting me and for giving me the opportunity of a life time. I am honored to have studied in this great university. Last of all, I would like to express my adoration to my family and friends for always standing by my side and being there. I am indebted to them for all the hardships they had to go through in order for me to succeed. I would never have reached to where I am without their prayers and their help.

TABLE OF CONTENTS

<i>DEDICATION</i>	IV
ACKNOWLEDGMENTS.....	V
TABLE OF CONTENTS.....	VI
LIST OF TABLES.....	IX
LIST OF FIGURES.....	X
LIST OF ABBREVIATIONS.....	XIII
ABSTRACT.....	XVI
ملخص الرسالة.....	XVIII
CHAPTER 1 INTRODUCTION.....	1
1.1 Background.....	1
1.2 Thesis Motivation	2
1.3 Thesis Objectives	5
1.4 Thesis Contribution	6
1.5 Thesis Organization.....	7
CHAPTER 2 LITERATURE REVIEW.....	8
2.1 MG Control Strategies.....	8
2.1.1 Centralized Control of MG	8
2.1.2 Distributed Control of MG	9
2.1.3 Hierarchical Control of MG	14
2.2 MAS Applications in MG Management and Control	15

2.3	MPPT Techniques.....	20
2.4	Control of Micro-Hydro Generation System	23
CHAPTER 3 MICROGRID MODELING		25
3.1	MG Structure	25
3.2	Battery and Charging/Discharging Controller Modeling	27
3.3	PV Panel and MPPT controller modeling.....	31
3.4	Control of MG inverter	36
3.5	Micro Hydro modeling	44
3.6	Diesel Generator Modeling	48
CHAPTER 4 PROPOSED CONTROL AND MANAGEMENT STRATEGY.....		50
4.1	Hierarchy of proposed strategy	50
4.2	Flow Chart and Description of EMS.....	51
CHAPTER 5 PROPOSED MULTI-AGENT SYSTEM (MAS) DEVELOPMENT		60
5.1	Agent and MAS Definition	60
5.2	Multi-Agents Communication and Coordination	62
5.3	Creating Agents Environment	63
5.4	Proposed MAS Architecture	65
5.5	Zonal Control	72
5.6	Interfacing MAS with MG network Model	74
CHAPTER 6 RESULTS AND DISCUSSION		78
6.1	Simulation of Power and Control Circuits.....	78
6.1.1	Simulation of Battery Controller	78
6.1.2	Simulation of PV model and MPPT controller.....	81
6.1.3	Simulation of Inverter	83

6.2	Online Optimal Generation Schedule.....	87
6.3	Simulation of MAS	94
6.4	Simulation Complete Control and Management System	97
6.4.1	Simulation of Scenario 1.....	98
6.4.2	Simulation of Scenario 2.....	104
6.4.3	Simulation of Scenario 3.....	110
6.5	Simulation of Zonal Control of MH.....	112
CHAPTER 7 CONCLUSION AND FUTURE WORK.....		115
7.1	Conclusion	115
7.2	Future Work.....	116
APPENDEX		117
REFERENCES.....		120
VITAE.....		132

LIST OF TABLES

Table 6-1 Simulation Parameter for Battery and its Controller	80
Table 6-2 Simulation Parameters of PV model	82
Table 6-3 Inverter Test Parameters	85
Table 6-4 Power Contribution Percentage from Different DGs	93
Table 6-5 Total Energy Supplied from Different DGs in One Day	93
Table A-1 Data for Wadi Baisha Dam	117
Table A-2 Hydraulic Turbine and Speed Controller Parameters	118
Table A-3 Diesel Generator Parameters	118

LIST OF FIGURES

Figure 2-1	Flowchart of P&O Technique.....	21
Figure 2-2	Flowchart of IC Technique.....	22
Figure 3-1	Schematic Circuit of Studied MG.....	27
Figure 3-2	Battery Model.....	28
Figure 3-3	Bidirectional Converter Circuit.....	29
Figure 3-4	Block Diagram of Battery Voltage Controller.....	30
Figure 3-5	Schematic Circuit of PV Model.....	31
Figure 3-6	P-V Curves of PV at Different Irradiance Values.....	33
Figure 3-7	I-V Curves of PV at Different Irradiance Values.....	33
Figure 3-8	P-V Curves of PV at Different Temperatures.....	34
Figure 3-9	I-V Curves of PV at Different Temperatures.....	34
Figure 3-10	Schematic Circuit of Boost Converter.....	35
Figure 3-11	Parallel Connection of PV and Battery.....	36
Figure 3-12	Three-phase Inverter.....	37
Figure 3-13	Block Diagram of VSI.....	38
Figure 3-14	Block Diagram of Power Controller.....	39
Figure 3-15	Block Diagram of Voltage Controller.....	41
Figure 3-16	Block Diagram of Current Controller.....	42
Figure 3-17	Block Diagram of PQ Inverter.....	43
Figure 3-18	PQ Controller.....	43
Figure 3-19	Mode Transition of Inverter Operation.....	44
Figure 3-20	Block Diagram of Hydroelectric Generation Control System.....	47
Figure 3-21	Block Diagram of Servo-Motor.....	47
Figure 3-22	Block Diagram of Hydraulic Turbine.....	48
Figure 3-23	Diesel Generator Model.....	49
Figure 4-1	Hierarchy of Control and Management Strategy.....	51
Figure 4-2	Flow Chart of EMS.....	53
Figure 4-3	The Flowchart of Gradual Start up.....	57
Figure 4-4	The Flow Chart of Gradual Shut Down.....	58
Figure 5-1	Platforms and Container of MAS [162].....	65
Figure 5-2	Single Line Diagram of MG.....	67
Figure 5-3	Information Flow between Agents.....	69
Figure 5-4	Data Exchange between Simulink and JADE.....	75
Figure 5-5	Interfacing Agents with MG Buses through UDP Ports.....	76
Figure 5-6	MATLAB GUI.....	77
Figure 6-1	Simulink Model of Battery with Charging/Discharging Controller.....	79
Figure 6-2	Plot of Battery DC link Voltage.....	80
Figure 6-3	Plot of Battery Current.....	81
Figure 6-4	SIMULINK MODEL of PV and MPPT.....	82

Figure 6-5	Plot of irradiance, PV Power, and PV Voltage.....	83
Figure 6-6	Simulink Model of Inverter and its Controllers.....	84
Figure 6-7	Simulink Model of Inverter Voltage controller.....	84
Figure 6-8	Simulink Model of Inverter Current Controller.....	85
Figure 6-9	Load Voltage Waveform.....	86
Figure 6-10	Load Current Waveform.....	87
Figure 6-11	Solar Irradiance Curve for a Typical Day in summer.....	89
Figure 6-12	24 hours Generation Schedule for June, 1 st Obtain from EMS.....	90
Figure 6-13	Solar Irradiance Curve for a Typical Day in winter.....	90
Figure 6-14	24 hours Generation Schedule for Jan, 1 st Obtain from EMS.....	91
Figure 6-15	24 hours Generation Schedule for Jan, 1 st Obtain from EMS with Reduced MH Working Hours.....	94
Figure 6-16	Snapshot of JADE GUI Showing Seven Agents created in Main container	95
Figure 6-17	Snapshot from JADE Sniffer during Construction of Spanning Tree.....	95
Figure 6-18	Information Flow between Agents.....	97
Figure 6-19	Irradiance Curve for Scenario 1.....	99
Figure 6-20	Generation Schedule using MAS for Scenario 1.....	100
Figure 6-21	PV Inverter Current Waveform (Scenario 1).....	100
Figure 6-22	PV Generator Voltage during Transition from VSI Mode to PQ Mode (Scenario 1).....	101
Figure 6-23	Battery-1 DC Current (Scenario 1).....	101
Figure 6-24	Battery-2 DC Current (Scenario 1).....	102
Figure 6-25	Battery Inverter Current during Transitions between Different States (Scenario 1).....	102
Figure 6-26	Load 3 Current Transition at Time =4 sec (Scenario 1).....	103
Figure 6-27	Load Flowing From PV Generator.....	103
Figure 6-28	Load Following from HH Generator.....	104
Figure 6-29	Sun Irradiance Curve (Scenario 2).....	106
Figure 6-30	Output Power from Different DGs (Scenario 2).....	106
Figure 6-31	PV Inverter Voltage during Switching from PQ Mode to VSI Mode....	107
Figure 6-32	MH Generator Current during Shutting Down.....	107
Figure 6-33	Generation Output of MH and PV during Gradual Shut Down.....	108
Figure 6-34	PV Generator Voltage during Transition from PQ Inverter to VSI in Gradual Shut Down.....	108
Figure 6-35	MH Generator Current during Gradual Shut Down.....	109
Figure 6-36	BSS DC Current during Gradual Shut Down.....	109
Figure 6-37	Sun Irradiance Curve (Scenario 3).....	111
Figure 6-38	Output Generation from Different DGs (Scenario 3).....	111
Figure 6-39	Diesel Generator Current during Start up (Scenario 3).....	112

Figure 6-40	Diesel Generator Current during Shut down (Scenario 3).....	112
Figure 6-41	Load and Generation curves in Zonal Control.....	113
Figure 6-42	Plots of LA3 Load and BA Generation in zone 1	114
Figure 6-43	Load and Generation plots for Agents in Zone 2.....	114
Figure A-1	Typical Fuel Consumption Curve for 120 KVA Diesel Generator	119

LIST OF ABBREVIATIONS

AGC	:	Automatic Generation Control
ANN	:	Artificial Neural Network
BA	:	Battery Agent
BSS	:	Battery Storage System
BVL	:	Bus Level Voltage
CCC	:	Current Controlled Chain
DA	:	Diesel Agent
DFIG	:	Double Fed Induction Generator
DG	:	Distributed Generator
DMS	:	Demand Side Management
EI-DGs	:	Electronically Interfaced Distributed Generator
EMS	:	Energy Management System
FIPA	:	Foundation of Intelligent Physical Agent
JADE	:	Java Agent Development Environment
IACS	:	Instantaneous Average Current Sharing
IC	:	Incremental Conductance
IP	:	Internet Protocol

GA	:	Generation Agent
LA	:	Load Agent
MAS	:	Multi-Agents System
MH	:	Micro Hydro
MHA	:	Micro Hydro Agent
MG	:	Microgrid
MPPT	:	Maximum Power Point Tracking
MSC	:	Master Slave Current
MSO	:	Multi Master Operation
PCC	:	Point of Common Coupling
PMSG	:	Permanent Magnet Synchronous Generator
P&O	:	Perturb and Observe
PV	:	Photovoltaic
PVBA	:	PV-Battery Agent
RA	:	Regional Agent
RES	:	Renewable Energy Resources
SA	:	Service Agent

SC	:	Scheduler Agent
SG	:	Synchronous Generator
SSO	:	Single Master Operation
UDP	:	User Datagram Protocol
VSI	:	Voltage Source Inverter

ABSTRACT

Full Name : Tawfiq Naji Kameel
Thesis Title : Hierarchical Control And Management Strategy Of Microgrid With Hybrid Energy Resources
Major Field : Electrical Engineering
Date of Degree : [May 2014]

The increasing energy need requires integrating and harnessing any available energy resources, especially renewable energy resources (RES) which considered as cheap and clean source of energy. Small scale hydro generation and photovoltaic (PV) generation plants can be constructed to electrify the off-grid loads located in remote areas. This generation system can be supported by energy storage system and back up diesel generator to form a microgrid (MG) capable of standalone operation. The different characteristics for different types of generators in the aforementioned MG require an efficient and reliable energy management strategy to optimally operate the MG. This thesis proposes an online multi agent-based hierarchical control and management strategy for (MG) comprising PV generation, micro-hydro (MH) generation, diesel generation, and battery storage system (BSS). The proposed strategy is composed of two layers. The upper layer is a decentralized online multi agent management system, and the lower layer is a physical layer composed of local controllers for the different type of distributed generators (DG) in the system.

The energy management system represented by multi-agents aims to maximize the utilization of renewable energy resources and energy storage in order to minimize the operational cost of MG. Moreover, the proposed strategy automatically handles the mode

of operation transitions and reconfiguration of MG. Furthermore, the proposed management strategy handles unit commitment operation. Also, an adaptive dynamic communication and coordination approach resulting in zonal (regional) control of MG is proposed in this thesis. A dynamic model for each component of MG is developed and implemented in SIMULINK environment and this will represent the physical layer of control strategy, while multi-agents system (MAS) is designed and implemented in Java Agent Development Environment (JADE).

In order to validate the proposed strategy, first of all the optimal generation schedule is obtained by online scheduling using MAS. Secondly, MAS-based management system interfaced with physical local controllers built in SIMULINK is tested and simulated for different scenarios for load and weather changes to examine its efficiency and robustness. The results show the effectiveness of the proposed energy management strategy and its capability of automatic handling of different tasks including power allocation, unit commitment, and transition between different modes of operations.

ملخص الرسالة

الاسم الكامل: توفيق ناجي توفيق كميل

عنوان الرسالة: نظام تحكم وإدارة هرمي للشبكات الصغيرة المحتوية على مصادر طاقة هجينة

التخصص: هندسة كهربائية

تاريخ الدرجة العلمية: أيار 2014

إن الزيادة في الطلب على الطاقة الكهربائية تتطلب دمج وتسخير جميع مصادر الطاقة المتاحة، وخاصة مصادر الطاقة المتجددة (RES) التي تعتبر مصادر رخيصة ونظيفة للطاقة. يمكن إنشاء محطات توليد مائية صغيرة ومولدات الطاقة الشمسية لتزويد الاحمال الكهربائية في المناطق النائية خارج نطاق الشبكة الكهربائية الرئيسية. ويكمن دعم نظام التوليد الكهربائي بنظام تخزين للطاقة ومولد ديزل احتياطي لتشكيل شبكة كهربائية صغيرة قادرة على العمل بشكل مستقل. الخصائص المختلفة لأنواع توليد الكهرباء في الشبكة الصغيرة المذكورة اعلاه تتطلب استراتيجية فعالة و موثوقة لإدارة الطاقة من أجل تشغيل الشبكة الصغيرة في الحالة المثلى. هذه الرسالة تقترح إستراتيجية آتية هرمية مستندة للعملاء المتعددين للإدارة والتحكم في الشبكات الكهربائية الصغيرة التي تضم مولد الطاقة الشمسية، مولد الطاقة المائية الصغير، ومولد الديزل و نظام تخزين بالبطاريات. تتكون الاستراتيجية المقترحة من طبقتين: الطبقة العليا عبارة عن نظام لامركزي وأني لإدارة الطاقة الكهربائية يستند الى نظام العملاء المتعددين. أما الطبقة السفلى فهي طبقة مادية تتكون من وحدات تحكم محلية للمولدات الكهربائية الموزعة المختلفة في النظام. تهدف إستراتيجية إدارة الطاقة المقترحة الى تعظيم استغلال مصادر الطاقة المتجددة من أجل تقليل الكلفة التشغيلية للشبكة الصغيرة. علاوة على ذلك فإن الاستراتيجية المقترحة تتكفل تلقائياً بالانتقالات بين اوضاع التشغيل المختلفة وإعادة تشكيل الشبكة الصغيرة. في هذه الاطروحة ايضا تم اقتراح نهج ديناميكي تكفي للتواصل والتنسيق ينجم عنه نظام تحكم مناطقي (إقليمي) للشبكة الصغيرة (MG). تم تطوير نموذج ديناميكي لكل مكون من مكونات (MG) وتنفيذها في بيئة (SIMULINK)، ويمثل هذا النموذج الطبقة المادية من استراتيجية التحكم، في حين تم تصميم نظام العملاء المتعددين (MAS) وتنفيذه في بيئة تطوير جافا (JADE).

للتحقق من صحة الاستراتيجية المقترحة، أولاً وقبل كل شيء تم الحصول على جدول التوليد الزمني الأمثل باستخدام الجدولة الانية المستندة على (MAS). ثانياً، تم اختبار نظام الإدارة القائمة على (MAS) مربوطاً مع وحدات التحكم المحلية المادية التي بنيت في SIMULINK ومحاكاة لسيناريوهات مختلفة للاحمال الكهربائية وتغيرات الطقس

لدراسة كفاءة ومثانة النظام. أظهرت النتائج فعالية الاستراتيجية المقترحة لإدارة الطاقة وقدرتها على التعامل التلقائي مع مهام مختلفة بما في ذلك تخصيص القدرة، و جدولة تشغيل الوحدات، والانتقال بين اوضاع التشغيل المختلفة.

CHAPTER 1

INTRODUCTION

1.1 Background

The increase in population and the extension of inhabited geographical spots require expansion of production of electric power and extension of network to meet the new needs. In fact, reliance on fossil fuels for energy production leads to a significant reduction in the stock of global energy, not to mention the environmental pollution caused by the burning of such kind of fuel, prompting many researchers to seek for alternative sources of cheap and clean electric energy represented in renewable energy such as wind and solar energy. Involving renewable resources in electricity generation system resulted in evolving of concept of distributed generator (DG) and microgrid (MG) where small or medium scale generation takes place at distribution level at medium voltage or low voltage. Despite the fact that renewable generation provides clean and cheap source of energy, the penetration of renewable energy increased the complexity of the power system. Also, the intermittent nature and weather dependency for most type of renewable resources threads the system stability and makes the fluctuation not only at load side but also at generation side. In addition, the renewable generators are not directly coupled to the grid. They are interfaced with electronic devices generating undesired high order harmonics yielding to voltage distortion and poor power quality. Renewable energy

resources can be classified as controllable/dispatchable and uncontrollable resources. While most types of these resources cannot be controlled, few of them can be controlled such as hydro generation, biomass, and concentrated solar thermal energy. When dealing with variable renewable generation, the objective is to harvest the maximum power available at different weather conditions, and that requires maximum power point tracking (MPPT) techniques. The special nature of MG containing renewable resource made traditional control techniques employed in conventional large power system insufficient and granted the need for different and special techniques to insure system stability and reliability, and enhanced power quality without wasting any available energy. In this thesis, Hierarchical control and management strategy is developed for a standalone MG combining micro hydro (MH), photovoltaic (PV), and diesel generates with battery storage system (BSS). The proposed strategy is simulated for different scenarios to evaluate its efficiency, effectiveness, and robustness.

1.2 Thesis Motivation

The increasing demand with limited energy resources has motivated researchers to seek for alternative energy resources that are mostly presented in renewable energy resources (RES). RES are clean and cheap source of energy. The penetration of RES in power systems developed the concept of distributed generation and MG making power system more complex and the conventional methods of control inefficient, thus many efforts have been shown to evolve the control strategies with the help of advances in power electronics technology to tackle the new issues in modern power system. However, many gaps need to be filled in this area to define a comprehensive strategy to efficiently

controlling MG. Distributed control approaches are characterized by simplicity and not requiring communication link, but lacks the accuracy, flexibility, optimality, and comprehensiveness considering its dependency on limited local information disregarding that the rule might be played by other global parameters in the MG.

On the other hand, centralizing the control mechanism improves the accuracy of the control and drives the operation into optimal region by considering many variables in the system, but the total reliance on high bandwidth communication link not only requires additional cost, but also makes the whole system collapse possible by communication system failure. Therefore, hierarchical control was proposed to compromise between centralized and decentralized control. However, most of proposed hierarchical control techniques are not generalized and disregarded the type of energy source which significantly affects the features of control approach.

Besides, several researches in this field assume dispatchable DGs which are usually not true as most of the energy sources are intermittent renewable energy. Different load and generation conditions require different control modes and the mode reconfiguration process has to be automated based on MG available information. This objective can be achieved by employing some sort of advisor in the control strategy of MG which is lacked by most of control and management strategies proposed in the literature.

Recently, multi-agent system (MAS) has been used for MG control, to make MG smarter and interactive. MAS has decentralized nature and is characterized by intelligence, speed and flexibility. MAS has been applied in various fields of electrical engineering, but none of conducted researches have addressed application of MAS in the

studied generation system. Besides that, most of the proposed systems are centralized MAS, and they are limited to management part without addressing control part.

What was mentioned so far, are the motives for choosing the proposed strategy. We still need to mention the reasons for studying energy management for the specific types of generation in this work. The entire electric power generation in the Kingdom of Saudi Arabia (KSA) is obtained by burning fossil fuels. Despite the fact that KSA is a huge oil producer; using oil to generate electricity is very expensive taking in consideration the international price of oil barrel. In addition, such type of generation results in global warming and environment pollution. Furthermore, consuming crude oil at that massive rate resulted in stress on consumable resources that is required for other applications, mainly transportation, and military applications. In other words the larger the rate of consumption, the smaller the period of availability.

Obviously the penetration of renewable energy in KSA generation system and harnessing any available alternative source of energy even at small scale is strongly needed. KSA has the potential for some renewable energy resources, such as wind generation, solar generation including concentrated thermal and photovoltaic, and small scale hydro generation.

In KSA, there are remote areas off-grid and electrified by diesel generators; this type of generation has the same disadvantages of the conventional thermal Generation in KSA, and is even worse considering the cost perspective. Expansion of transmission network to supply these remote areas is not a practical or feasible solution, but supplying these areas by available renewable resources seems to be the best solution. In the south western regions of KSA, there are a number of dams used to store the rain water, to avoid

the flood that could destroy the nearby villages, and to supply the irrigation water to these villages in organized manner. The irrigation water flow could be utilized to generate electricity to supply the local loads. On the other hand, the high levels of solar irradiance in KSA make PV generators very attractive and feasible energy solution.

Few researches addressed the issues related to integrating PV generation with MH generation which have different generation peak time on both long term or short term. Those who addressed the problem merely describes approaches for operation of this hybrid system without any details on control implementation. This thesis proposes a multi-agents based hierarchical control strategy applied for MG with PV, micro-hydro, diesel, and battery to manage energy economically and to automatically handle control and operation mode transitions and unit commitment.

1.3 Thesis Objectives

This thesis proposes a hierarchical control strategy to control MG with hybrid energy resources including electronically interfaced distributed generators, (EI-DGs), and directly coupled DG. That is to say, the generation system consists of renewable and conventional generation with energy storage system. The renewable energy resources (RES) shall include controllable generation represented by small scale hydro generation, and uncontrolled generation represented by PV generator. Diesel generator is the conventional type of generation in MG, and battery bank is the energy storage system. The objectives of the thesis are as follows:

Objective 1: To develop a dynamic model of MG consisting of PV, micro-hydro, diesel, battery system.

Objective 2: To identify the proper size for each type of generation based on the connected load.

Objective 3: To obtain optimal generation schedule for MG.

Objective 4: To design and implement a local controller for each type of generators.

Objective 5: To create MAS in JAVA Agent Development Environment (JADE), to act as energy management layer in the proposed strategy.

Objective 6: To propose, design, and implement a two layers multi-agent based hierarchical control strategy for MG. The first layer (primary layer), presents the local controllers responsible for power sharing and voltage and frequency regulation. The settings for real and reactive power and mode of operation for each DG are received from the second control layer. The second layer determines the setting of real power (P) and reactive power (Q), mode of operation for each type of generation, and charging/discharging mode for BSS. In addition, it handles generation unit startup and shut down operation.

Objective 7: To propose Zonal control approach for MG considered MG.

1.4 Thesis Contribution

This thesis has the following contributions:

- Using decentralized MAS to manage and control MG with generations system comprising PV generator, MH generator, diesel generator, and BSS
- Employing MAS to manage interactive operation of PV and MH generation

- Handling unit commitment operation including start-up and shut down of generation units by MAS
- Using decentralized MAS for online reconfiguration and operation mode transitions of MG.
- Developing new efficient communication and information flow scheme to enable different agents to properly coordinate with each other and make the right decisions to operate MG optimally.
- Proposing a zonal control approach to deal with power contingencies and communication failure in MG.

1.5 Thesis Organization

This Thesis is organized in seven chapters; the first chapter which has been already introduced, contains an introduction about the topic of the thesis, the reasons for selecting this topic, and the thesis objective. In the second chapter a comprehensive literature review on the related researches is presented. The literature review highlights different researches conducted on MG control strategies, MAS application, MH generation system, and MPPT techniques. A detailed model for different components of MG is presented in chapter 3. While in chapter 4, the architecture of proposed energy and control strategy is described. In chapter five, the proposed MAS is introduced. In chapter six the results are shown and discussed. Finally, conclusion and future work are presented in chapter seven.

CHAPTER 2

LITERATURE REVIEW

2.1 MG Control Strategies

MG control strategies can be classified as centralized control, distributed control, and hierarchical control strategies. These different control strategies vary in complexity, efficiency, speed, and accuracy. In the next sections different researches conducted on different control strategies are presented.

2.1.1 Centralized Control of MG

In centralized control scheme; load measurements such as current, voltage, or power depending on control approach are sensed and inputted to a central controller to generate control signals for each DG unit. This type of control requires communication channels to gather information from MG and to send dispatch signal to each DG unit. The communication channel could be of high bandwidth, or low bandwidth depending on the frequency content of the control and measurement signals that are of concern. In case the interest is in low frequency component of a control signal, a low bandwidth channel is sufficient. For example, economic dispatch operation or optimal power flow in MG are centralized operations that require a central controller. However, voltage and frequency can be regulated using local distributed controller like droop controller. In fact, energy management and power sharing process can be fully centralized by sending current or voltage settings to each individual DG unit from the central controller. Usually central

control leads to economic operation and accuracy in load sharing as it takes in consideration the network configurations, parameters, and technical constraints and acts accordingly. However, the necessity for communication requires additional cost [1-11]. Besides, losing communication will lead to lose the entire control system which eventually results in system collapse.

2.1.2 Distributed Control of MG

To avoid embedding communication system in MG control scheme; several researches focused on distributed control methods, which requires only local measurements, and depends mainly on voltage and frequency as an agent of control. There are three main distributed control techniques to share load demand between different DGs in MG i.e. droop techniques, current sharing techniques.

The droop controller is a simple and efficient technique to share real and reactive power between multiple DGs. It emulates the droop characteristics of synchronous generator. In Conventional droop controller; the real power can be shared by controlling frequency, and reactive power can be shared by controlling voltage magnitude, this is known as P - f and Q - V droop controller [12-16], and can be expressed by following equations:

$$f = f_{rated} - m_p(P - P_{rated}) \quad (2.1)$$

$$V = V_{rated} - n_q(Q - Q_{rated}) \quad (2.2)$$

Where m_p, n_q are droop coefficients for real power and reactive power respectively. The droop coefficients are chosen according to DG capacity, maximum allowable frequency deviation Δf_{max} , and maximum allowable voltage deviation ΔV_{max} :

$$m_{p1} \cdot P_{rated1} = m_{p2} \cdot P_{rated2} = m_{pn} P_{ratedn} = \Delta f_{max} \quad (2.3)$$

$$n_{q1} \cdot V_{rated1} = n_{q2} \cdot V_{rated2} = n_{qn} V_{ratedn} = \Delta V_{max} \quad (2.4)$$

The conventional P - f / Q - V droop controller is accurate when line impedances of MG are inductive which is not true for low voltage network where the impedances are highly resistive. Therefore, in low voltage network it is more accurate to control real power by adjusting voltage magnitude, and reactive power by controlling frequency using P - V / Q - f droop controller [17]. When DG inverter is modeled as a current source the voltage magnitude can be drooped against direct current component I_d to control real power, and the frequency can be boosted against quadrature current component I_q to control reactive power resulting in V - P Droop f - Q boost controller [18]. The controller is complicated, but it is efficient and accurate to jointly share real and reactive power between multiple DGs.

The aforementioned droop controllers have slow response, poor capability to reduce voltage and frequency disturbances resulted from mode transition and switching operations, poor harmonic sharing, poor current sharing and voltage regulation [19]. Its dose does not account for line impedance, local loads, grid impedance, nonlinear load, and voltage imbalances. It is also very sensitive to error in current and voltage measurements[20]. Besides, when scheduling droop coefficients, stability issues must be taken in consideration. Moreover, the output impedance of DG inverters can be resistive, inductive, or complex; and depending on its nature it has different impact on power control which adversely affects the accuracy of droop controller. The previous issues are motives to improve the conventional droop controller to enhance its dynamic behavior, and increase its accuracy. To enhance dynamic behavior, transient response, and relative

stability of MG adaptive droop controller is developed. In grid-connected operation the coefficient of droop controller can be updated based on grid impedance, voltage, and frequency estimation to obtain accurate decoupled real and reactive power [21]. This method might be accurate but it greatly relies on the estimation of parameters, and so, errors in estimation could lead to inaccuracy in control. In addition, if the MG's DG units are separated by large distances this control scheme might need a communication channel especially since the measurement needed to estimate grid parameters are collected at PCC. First derivative of real power and reactive power can be added to droop controller converting it to *PI* controller.

$$f = f_{rated} - m_p(P - P_{rated}) - \hat{m}_p \frac{dP}{dt} \quad (2.5)$$

$$V = V_{rated} - n_q(Q - Q_{rated}) - \hat{n}_q \frac{dQ}{dt} \quad (2.6)$$

Where \hat{m}_p, \hat{n}_q are adaptive droop gain [22, 23]. This method enhanced transient response of the droop controller without affecting its power sharing. As the output voltage of the DG inverter is affected by real and reactive power flow in the line, this will causes a voltage drop and leads to error in reactive power sharing and voltage deviation. The voltage droop controller can be modified to be a function of real and reactive power to compensate for power flow. Thus, the effect of line impedance whether it resistive, inductive, or complex is overridden [24].

$$V = V_{rated} + k_r \frac{rP}{V_{rated}} + k_x \frac{xQ}{V_{rated}} - (n_p + k_q Q^2 + k_p P^2)Q \quad (2.7)$$

Where r , and x are resistance and inductance of line. Clearly, the controller is nonlinear with high order variable and many parameters that need to be optimized to obtain the best performance. The system is complicated and parameters need to be adjusted for any change in network configuration.

It is true that droop controller emulates droop characteristics of synchronous generator, but it is assumed to have zero inertia. In transient time a virtual inertia based on modifying droop gain with df/dt will supply higher power when frequency is reduced. When rate of change in frequency exceed specific limit the droop gain is modified to increase inertia of inverter. This technique enhance the transient response of droop controller[25].

In conventional P-f droop controller the droop gain is constant providing constant slope for different real power operating points, and for some operating points the system might be drifted from the stability region. Instead of fixed slope, arctan power-frequency droop controller is used to set an upper and lower bound on frequency, yielding to a more stable system at higher power operating point[26, 27].

Reactive power control through voltage-droop controller allows sharing reactive power between different DGs in MG in autonomous operation mode. However, the voltage might be varied from optimal value due inaccuracy in reactive power control caused by transmission line impedances and local reactive load. Terminal voltage can be restored to reference value through $Q - \dot{V}$ droop controller [28, 29], where \dot{V} is the rate of change of voltage. Droop controller employs rate of change of voltage instead of voltage itself. $Q - \dot{V}$ controller consist of \dot{V} restoration loop which will produce a set point for reactive power, which is then fed to the droop controller to generate a reference for voltage rate of change.

In order to change output real or reactive power of DG units in MG, the droop gains are adjusted to obtain desirable power. However, stability constraints put some limitations on the values that can be given to droop gains because some values of droop

gain may drive MG to the unstable region; so scheduling droop gains process must consider stability limits[30, 31].

The control of real power and reactive power is not completely decoupled, and can be affected by each other. For that reason virtual impedance is used to decouple control of real power from reactive power control. The virtual impedance can be resistive, inductive, or complex depending on the nature lines and DGs output impedances. Usually low voltage MG lines have resistive impedance, and so, the virtual impedance should be resistive. On the other hand, medium voltage MGs has complex impedance. While in high voltage MG the lines are inductive [23, 32-35].

So far, different distributed control methods applied in AC MG were reviewed and discussed. Here, a brief discussion of DC MG control is presented. In standalone operation DC MG, DC power can be drooped against DC voltage or DC current[36]. While in grid-connected operation V_g/V_{dc} droop controller is used where real power is balanced by drooping the dc link voltage against the microgrid output voltage using V_g/V_{dc} controller. This controller changes the power flow to the grid from DG unit while keeping constant output power from DG [37]. However, this control method may cause voltage violation if the grid voltage exceeds the limits, therefore, combining P/V_g with V_g/V_{dc} controller is used to undo the voltage violation whenever it takes place [37, 38]. V_g/V_{dc} avoids frequency changes in delivered power unlike the conventional droop controller, and as previously mentioned the P/V_g controller avoids voltage violations. So, by combining the two controllers the advantages of both are obtained.

Apart from droop controllers; current sharing techniques are sometimes used for equal current sharing among different MG inverters with different capacities and output

impedance. There are three types for current sharing techniques i.e. circular chain current (CCC) technique [39, 40], master slave current (MSC) technique[41, 42], and instantaneous average current sharing technique (IACS) [43-46]. In CCC technique each inverter tracks the current of the previous one in successive manner until the last inverter flows the first inverter, so any failure of any inverter current loop will cause complete control chain failure unless detected and isolated. In MSC, one inverter acts as voltage source and the other inverters act as current source, sharing load current equally between them. Finally in IACS the currents from all inverters are summed up and their average is sent to each inverter as current set point. The current sharing methods require a simple information exchange structure between inverters.

2.1.3 Hierarchical Control of MG

As previously mentioned the centralized control of MG requires high bandwidth communication link and losing this link leads to entire control system failure. On the other hand distributed control requires no communication, but the operation of MG might not be optimal. Besides that, sharing active and reactive power might sacrifice frequency and voltage amplitude regulation to nominal values. The hierarchical control combines good features of both centralized and decentralized control by employing multi-level control. Each level of control supervises the lower level until primary control (local control) is reached. The information is exchanged between different levels via low bandwidth communication channel. In bottom level the real and reactive power are shared by a local controller such as droop controller. In the upper levels the setting for droop controller is an external signal to restore voltage and frequency to optimal value, and mode of operation for each DG inverter is determined and sent to a lower level. Loss

of communication drifts the MG from optimal operation, but MG continues to operate by the local controller. There is neither unified definition nor standard structure for hierarchical control. Furthermore, the tasks assigned to each level of control significantly vary from one control strategy to another. Some hierarchical strategies suggest that the bottom level of control is in charge of the primary voltage and frequency regulation through droop controller or other controllers. The middle layer is responsible for secondary regulation, where voltage and frequency are restored to their nominal values. Also, if MG is connected to main grid, a tertiary control in upper level is employed to control the amount of power exported or imported from the main grid. On other hand, some strategies go in completely different direction and propose a multi-layer control approach with primary level represented by local controller, second level for optimization and supervision of MG, and third level for load and weather forecasting. [47-55].[56]. In general, hierarchical control approaches provides more secure, optimal, and accurate operation of MG. MAS can be employed as an upper level of hierarchical control to handle different tasks such as energy management, optimization, economic dispatch, and islanding of MG. In the next section, the applications of MAS in MG are reviewed.

2.2 MAS Applications in MG Management and Control

Several researches addressed use MAS in controlling and managing MG. The approaches vary in complexity, reliability, and effectiveness. The different natures of MGs being investigated in terms of type of DGs and loads, and the control objectives of different researches make comparison between different researches not straight forward. Some of researches adopt central control approach, while others go for decentralized and hierarchical control approach. Load and weather forecasting, environment conditions,

energy prices, operation modes, and optimal operations are disregarded in some researches, and addressed in others.

Design of general MAS-Based control of MG was presented in [57] . The control system include energy management system (EMS), load flow analysis, automatic generation control (AGC), and other controls. AGC was taken as a specific application and simulated.

Short-time generation scheduling and load following control using MAS were presented in [58-60]. [58] depends on forecasted load performed by neural network and fuzzy controller, in addition to, real time measurement of load. A supervisory and control agent (SC) was introduced in this research to collect measurement from loads and DGs, sending them to the central controller, and receiving control settings. Therefore, the control system is still centralized and the overall contribution of MAS is minimized. Schedule coordinator agent (SC) created by MG management agent was proposed in [59, 60] to enable negotiation between DGs and Load to obtain optimal generation schedule.

Multi-agent based three layer hierarchical control for MG was presented in [50, 61]. In the upper layer an agent responsible for multi objective optimization is employed. The objectives of optimization include cost, emission, and minimization of losses. The middle layer is responsible of the assignment of modes of operation for each type generation and storage system. And finally the lower agents represent the local controller for DGs and loads. [61] adds to [50] the intelligent mode switching. Also, voltage and frequency stability were addressed in [61]. The Proposed control system in the previous two references is very complicated, and requires a lot of information about the system.

Operation mode transition and reconfiguration of MG control is also addressed in [62] where event-triggered control is proposed.

A decentralized load generation balance was presented in [63-65]. In [63] Each DG unit and load was assigned an agent. Through three step communication between neighbor agents, the total power mismatch was calculated. Using the same communication method the generation and demand was balanced. No central agent was employed to supervise the system. The optimal operation was not an objective. The load following was performed online without a future plan. The work in [63] is extended in [64]. The control strategy is arranged in three control layers. The lower layer is the local controllers, the middle layer is utilized for load-generation balance, and the upper layer is employed to perform economic dispatch. While [63] does not adopt any DG to be the master unit, [64] used a master-slave control method. [65] Introduced agents for loads, buses, generators, and feeders. The capacity of each feeder was considered. In addition, when imbalance is detected in the system, the generators are ranked according to price; then a request is sent to the generator with the lowest price, it will continue until a balance is reached, thus the economic operation in MG is fulfilled.

[66-68] introduces the concept of multi-agents reinforcement learning in MG control to deal with a large amount of variables and the stochastic environment of MG, making control of micro-grid adaptive and reactive with system changes.

In [69-73], MAS system was applied in intelligent energy management system of grid-connected and standalone MG with hybrid energy resources. The generation system in [69] comprises PV, battery, and diesel generator working in standalone mode. The proposed control system aims to minimize diesel consumption by utilizing PV and

battery efficiently. Load shedding process was employed to disconnect non-critical loads in case of surplus demand. The same system was investigated in [72] but in grid-connected operation. The performance factor for each type generation and storage system was involved in management process. Besides, the price of energy in the electricity market decides if the MG will buy energy from grid, or commits the diesel generator. In [70, 74] MAS is employed to control DC MG consisting of PV, Fuel Cell, and battery. MAS is responsible for maintaining stability of DC bus voltage by achieving generation/Load balance, and protecting battery DC voltage rise by switching PV mode of operation from maximum power point MPP to bus voltage level BVL. It is also responsible for load disconnection when generation cannot meet the load. In [71] Characteristics of different type of energy sources and storage system were considered to achieve optimal operation of a grid-connected MG with PV, Wind, fuel cell, and battery system. Weather conditions were also involved in management process. A simple centralized Agents-based load generation balance control is applied in [73] for MG with PV, wind, fuel cell, and gas turbine. An agent is created for each type generation, and a central control agent collect running parameters from all DGs and perform generation balance

Mode transition of MG using MAS were discussed in [75-79]. Intelligent agent was employed in [78] to handle transition of MG from grid-connected to islanded mode, and also to synchronize the voltage of MG with main grid prior to reconnection to main grid, to improve the performance of MG and its interaction with the main network, under grid voltage transients. Transition between grid-connected operation and islanded operation using simple control with one DG unit based on internet protocol IP and MAS

was also investigated in [75]. Similar work to [75] was applied to IDAPS MG in [76]. In addition to performing mode transition, MAS was employed to control PV generation system to secure critical load in islanded mode and activate load shedding mechanism to keep system stable in [77], and to detect and isolate faults in [79].

A description of MAS-based hybrid hierarchical/distributed control of MG was presented in [80].

Regional MAS was introduced in [81, 82] where a group of local agents LA managed by a regional agent (RA). LAs can exchange information through RA. RA can coordinate with other RAs in the system. Another type of agent is defined in [81] which is service agent SA. SA provided services to LAs such as weather forecast, and calculations. Two learning systems are adopted to perform generation scheduling i.e. online learning and offline learning. The generation schedule is obtained based day-ahead forecasting and online measurement. On the other hand no SA was used in [82], but a coordination agent CA was in charge of coordination between RAs. It is possible to relate previous researches to MAS-based multi-MGs management proposed in [83], With difference in agent types, and responsibilities, and information flow. In the same context, power system was divided into multiple MGs in normal and emergency operation was addressed in [84]. each MG seeks to supply its vital and non-vital loads, and request surplus generation from other MG when it has shortage. When MG encounters an emergency such as fault or sudden drop in renewable generation it enters restoration mode until healing and back to normal operation. In [85], optimal power flow in a group smart micro grids were obtained based on cooperative agents which allow MG to

exchange information and determine the optimal power flow locally and globally. The power flow problem was formulated using linear quadratic (LQ) method.

Demand side management (DSM) based on MAS was introduced in [86-91]. DSM agent was employed to perform load shifting and curtailment based on load forecasting, market price, and available renewable generation to achieve low operational cost and utilize renewable energy in [86]. Where in [87] A framework for DSM maintaining divisional auction market and zonal auction market for multiple MG was developed to enable end-consumer to participate in energy trading and perform load shifting. The proposed MGs contain generation and energy storage system. A multi-agents based DSM system is proposed in [88], for a building with multiple rooms to manage power consumption of air conditioners based on an auction agency considering thermal behavior of the building. Reinforcement learning is used for load shifting based on day-ahead forecasted load and online load measurements. The control system is applied to house electrical devices including electric vehicles [89]. In [90], a heuristic technique is used for load shifting with fuzzy logic-based bidding strategy. Priority index concept is introduced in [91] where consumers with large size and number of time of participation in energy market are given a lower energy cost.

2.3 MPPT Techniques

Many MPPT techniques are proposed in literature to harvest the maximum available power produced by PV arrays. These techniques vary in complexity, accuracy, speed, and cost. Perturb and observe P&O/Hill Climbing method, and incremental conductance (IC) is the most popular methods. In P&O method the voltage is increased

gradually and the power is observed. If the power is found to be increasing the voltage is increased until reaching a point where no more increase in the power. On the other hand, if incrementing voltage resulted in reducing of output power the voltage is decremented and continues to decrease until maximum power is reached [92-100]. The flow chart for P&O algorithm is depicted in Figure (2-1).

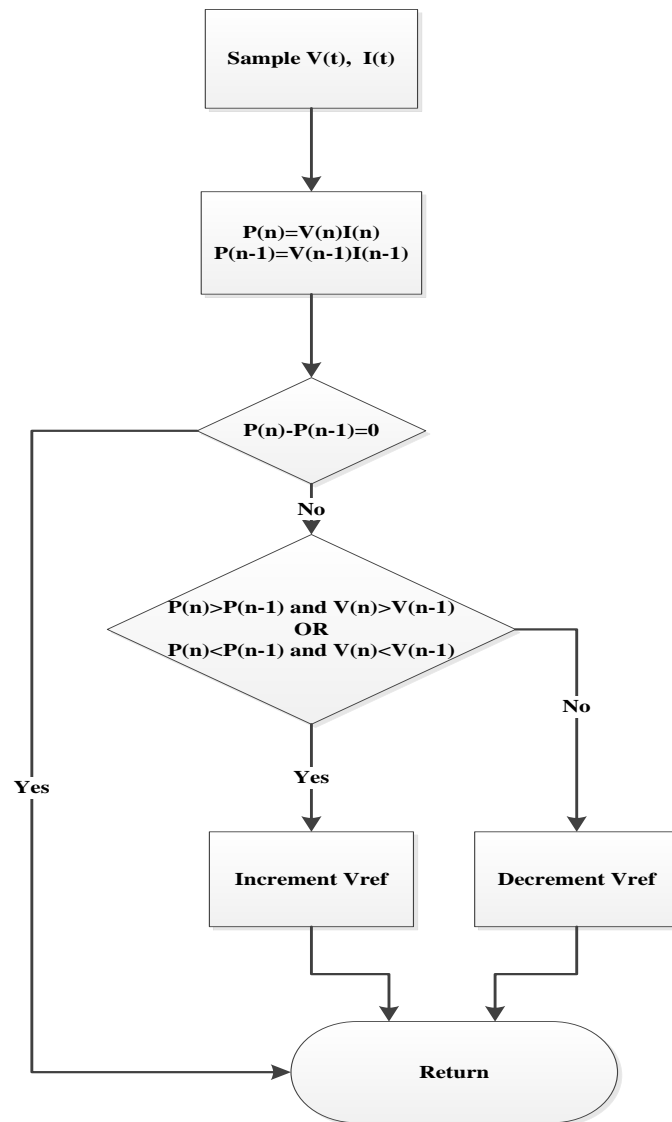


Figure 2-1 Flowchart of P&O Technique

Based on the fact that the slope of power-voltage (P-V) curve is positive to the right MPP, zero at MPP, and negative left of MPP, the IC method was developed to track maximum power by incrementing or decrementing voltage and measure conductance and incremental conductance and compare them to take the proper control action and determine whether to increase or decrease the duty cycle of DC-DC convertor or decide that the MPP has been reached [100-109]. Figure (2-2) illustrates the algorithm for IC method. P&O method is simpler and less accurate than IC method.

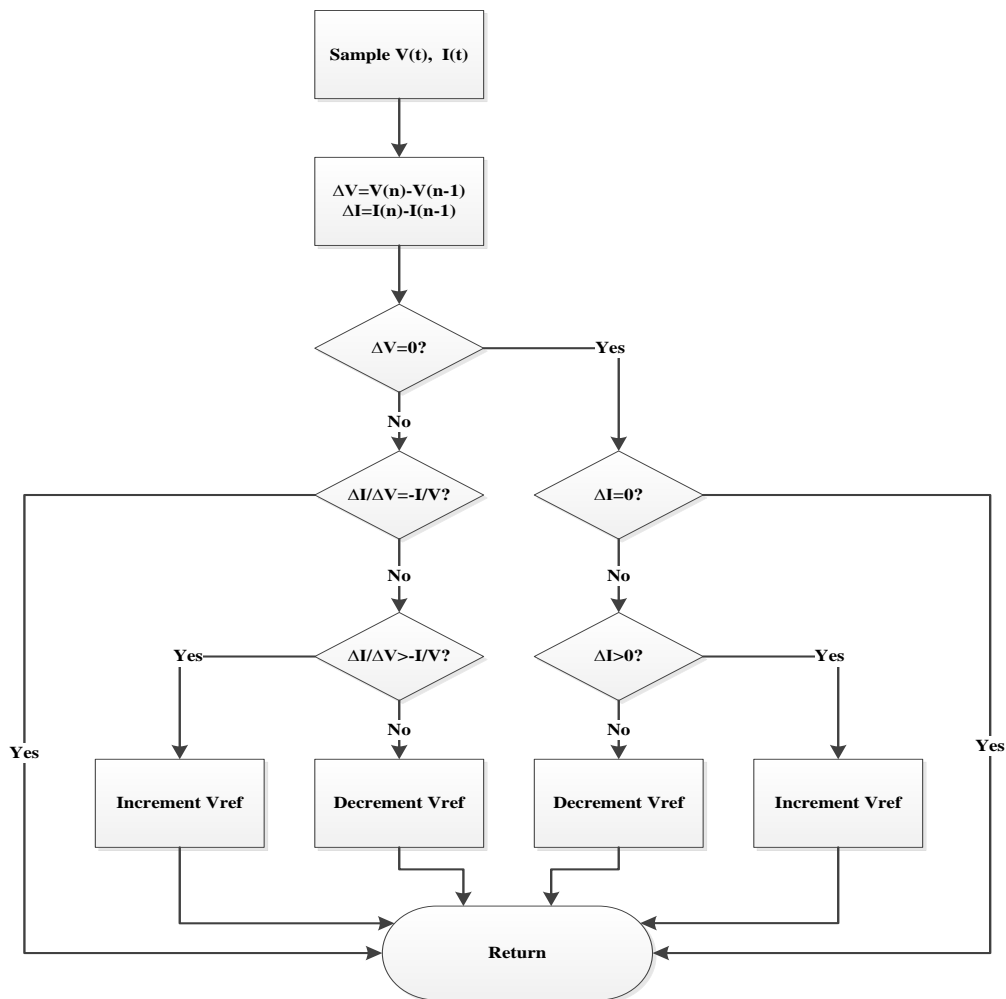


Figure 2-2 Flowchart of IC Technique

Other techniques for MPPT includes Steepest-Decent technique [110], Gauss Newton technique, intelligent techniques such as artificial neural network ANN and fuzzy logic [111-114], current sweep[115], forced oscillation[116] , constant voltage [117-119], feedback voltage or current techniques[120].[121]

2.4 Control of Micro-Hydro Generation System

Small scale hydro plants ranges from 1 KW to 15 MW, for generating capacity between 1 MW to 15 MW its classified as small hydro plants, and whenever the capacity ranges from 100 KW to 1 MW it is considered as mini hydro plant. Micro hydro units are between 10 KW to 100 KW. Plants bellow 10 KW is labeled as Pico hydro [8]. Among the advantages of small hydro generation, is that its reliability and long life cycle. It is also more predictable compared with other renewable resources, in addition to that it has limited impact on environment, and requires minimal maintenance and short construction schedule[122]. Small hydro generating system is built up of water turbine, water wheel, gear box, spillway, cross regulator, and electric generator [123, 124].

Several types of turbines are used in hydro generation, and the selection criteria for turbine are basically the head of water and speed of flow. The most common types of turbine are Pelton turbine, Francis turbine, Kaplan and propeller turbine. Pelton turbine is suitable for low specific speed and high head, whereas Kaplan turbine is used for medium specific speed and medium head, and for high speed with low head Kaplan and propeller turbine us used. Other types of turbines include bulb turbine, PIT turbine, S-type turbine, and cross flow turbine [122].

Small generated power of micro-hydro makes using synchronous generator (SG) expensive and sometime impractical. However, in order to obtain dispatchable renewable energy from hydro station, the SG is the best choice, especially when dealing with reservoir-type hydro generation. On the other hand, for variable speed hydro generation which do not require generation control, but need energy harvesting mechanism using induction generator (IG) might be a better choice considering its low cost, high efficiency, and compact size [122]. It is true that IG has no voltage regulation capability. Nevertheless, this problem can be overcome by using power factor correction capacitor bank [125], doubly fed induction generator (DFIG) [126, 127] where the output voltage is rectified and required reactive power is supplied by inverter [128], or by combining DFIG with capacitor bank to reduce the size of inverter [129]. SG can be paralleled with IG to regulate the voltage as in [130, 131]. Permanent magnet synchronous generator (PMSG) is also commonly used in micro-hydro generation with full conversion of AC power into DC power and controlling real and reactive power by PQ inverter [121, 132-134]. The full conversion of AC power into DC power can be also applied for IG [135]. Using speed governor for micro-hydro might be expensive and impractical, so in order to achieve generation/load balance in standalone operation electronic controlled load is proposed in literature to dump the excess generation and maintain the nominal frequency [136-139]. The amount of dumped energy can be reduced by reducing the amount of water flow using three pipe system control proposed in [140].

CHAPTER 3

Microgrid Modeling

3.1 MG Structure

The general structure of MG comprises DGs, energy storage system ESS, voltage and current controller, power sharing controller, synchronization algorithm, loss of main detection algorithm, and load shedding mechanism[15, 16]. DGs are mainly electronically interfaced EI-DG (PV, wind, fuel cell...*etc.*) , which are mainly variables, and uncontrollable source of generation; but conventional generation sources can also exist in MG such as diesel generator. MG could be operated in grid-connected mode or islanded mode [3, 141, 142]. When MG is operated in grid connected operation, the frequency and voltage are ruled by main grid; and MG converters are controlled as current source to supply constant power to feed local loads partially or completely, with the possibility to export and import power from and to main grid. On the other hand, when MG is disconnected from the main grid, voltage and frequency need to be controlled to maintain stability and good power quality [143-145]. Whenever the demand exceeds the rated generation capacity of MG, a load shedding mechanism must be activated to disconnect part of local load to maintain voltage and frequency stability[146, 147][148]. Loss of the main connection must be detected to take the necessary control actions; thereby the loss of main detection algorithm is required[149]. Furthermore, prior to the reconnection to the main grid, the voltage of MG should be synchronized with the main grid voltage by means of synchronization method[29, 150].

The structure of the studied MG is depicted in Figure 3-1. The considered MG has seven buses i.e. four generation buses and three load buses. PV panels with a battery bank are connected to bus 1, MHP is connected to bus 3, diesel generator is attached to bus 7, and battery bank is placed at bus 5. Bus 2, bus 4, and bus 6 are load buses. PV panel is interfaced to a dc link through boost converter which is controlled by MPPT controller to harvest maximum available solar power. The battery is responsible for smoothing output power from the PV panel, and to store PV surplus power, and supply lacking power by supervising charging/discharging rates accomplished by buck-boost converter controller. The DC output power at DC link is converted to AC power through 3-phase inverter to supply AC loads. When the battery is working alone (without PV), it is controlled to supply or store a specific amount of power. In both cases (with PV connected or disconnected), buck-boost converter maintains constant DC voltage across the capacitor all the time in order to enable proper control of the inverter. MHP consists of water reservoir represented by a water dam, hydraulic turbine, governor, exciter, and synchronous generator. Obtaining optimal size of the proposed system is out of the scope of this work. The system is sized such that RES with BSS can autonomously supply the load, with diesel as back up generation. The total connected load is assumed to be 100 KW peak with load factor of 0.45. The generation capacity for MH, PV, and diesel generator is 100 KW. BSS has 120 KWh capacity.

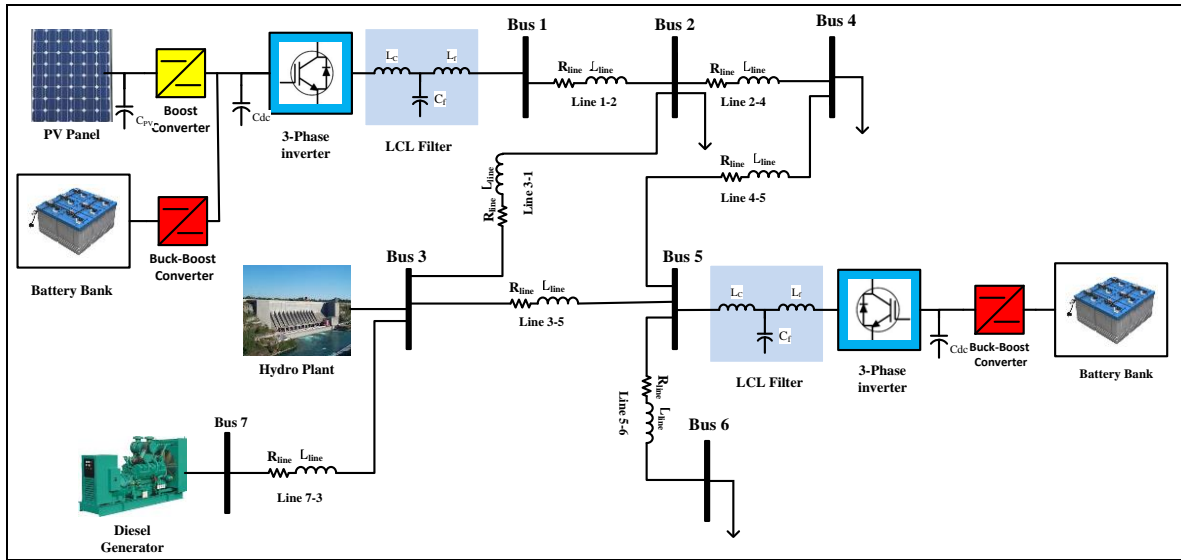


Figure 3-1 Schematic Circuit of Studied MG

3.2 Battery and Charging/Discharging Controller Modeling

The model of the battery is shown in Figure 3-2. It's merely a controlled voltage source with internal resistance. The internal voltage E of the battery is a function of extracted capacity I_t and low frequency component I^* . The internal voltage of the battery in charging mode is different from that in discharging mode. Equations (3.1) and (3.2) express the battery voltage in charging and discharging mode respectively.

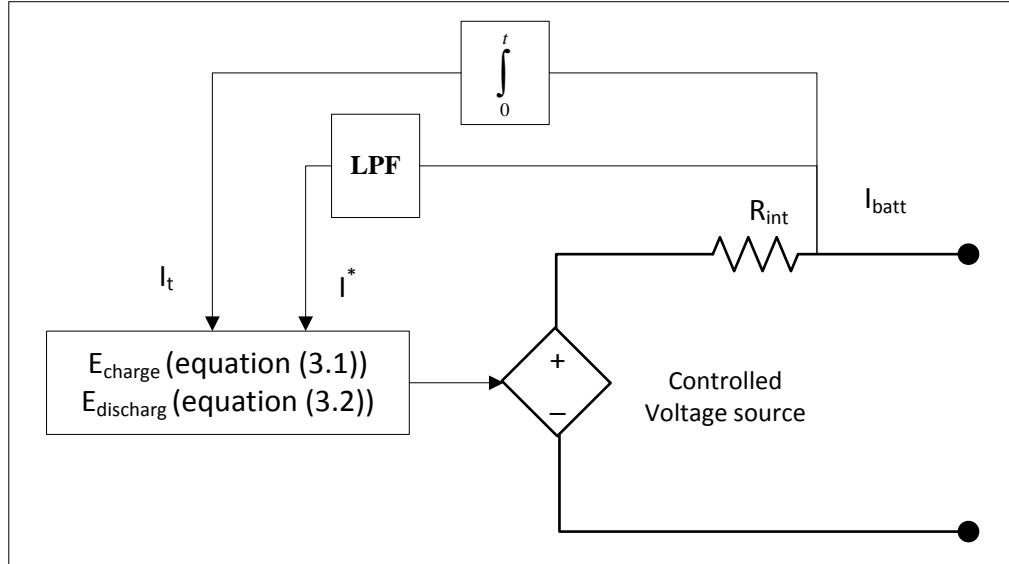


Figure 3-2 Battery Model

$$E_{charge} = E_0 - K \cdot \frac{Q}{i_t + 0.01 \cdot Q} \cdot i^* - K \cdot \frac{Q}{Q - i_t} \cdot i_t + A \cdot e^{(-B \cdot i_t)} \quad (3.1)$$

$$E_{discharge} = E_0 - K \cdot \frac{Q}{Q - i_t} \cdot i^* - K \cdot \frac{Q}{Q - i_t} \cdot i_t + A \cdot e^{(-B \cdot i_t)} \quad (3.2)$$

Where

E_0 : Battery constant voltage

K : Polarization constant (Ah^{-1}) or polarization resistance (Ω)

i^* : Low frequency current dynamics (A)

i_t : Extracted capacity (Ah)

Q : Maximum battery capacity (Ah)

A : Exponential voltage (V)

B : Exponential capacity (Ah^{-1})

To control battery in both charging and discharging mode, a converter with bidirectional power flow capability is required. In this work a half bridge buck-boost converter is used. The circuit of the converter is shown in Figure 3-3; it consists of an inductor (L_B) responsible of current smoothing and voltage boosting, followed by two transistors (T1 & T2) which are controlled to provide the desired output voltage. A capacitor (C_B) is connected at the output terminal to filter and minimize the ripple of dc output voltage. The bidirectional converter for the battery is described in equation (3.3)-(3.5)

$$V_{T1} = V_B + L_B \frac{dI_B}{dt} \quad (3.3)$$

$$V_{dc} = D_{T2} V_{T1} \quad (3.4)$$

$$I_C = C_B \frac{dV_{dc}}{dt} \quad (3.5)$$

Where V_B , V_{T1} are battery voltage and voltage across T1. D_{T2} is the duty ration of T2, and I_C is current flowing in capacitor C_B .

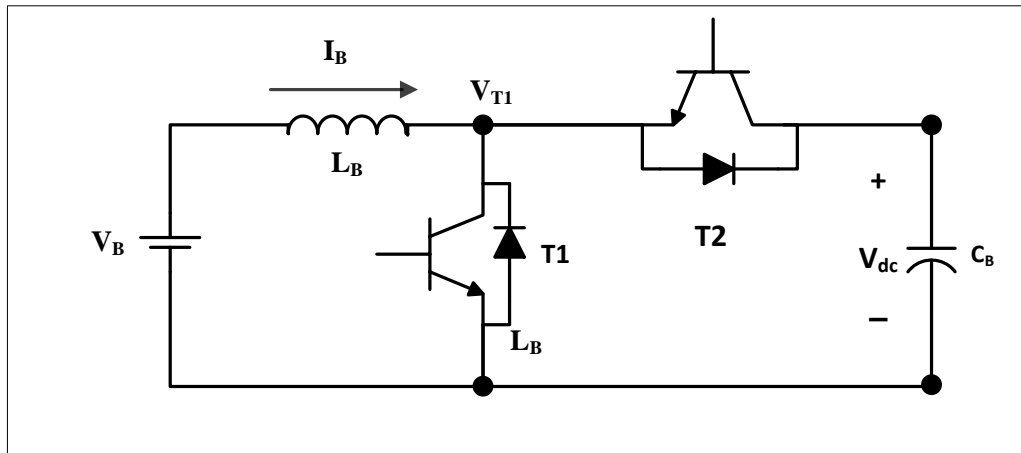


Figure 3-3 Bidirectional Converter Circuit

The battery can be controlled as the voltage source or current source depending on the application i.e. if the purpose of the control is maintaining a constant output dc voltage, then battery has to be controlled as the voltage source. On the other hand, if the battery is installed to supply specific amount of dc power, then a current controller will suit this goal. In this work, battery voltage is controlled to maintain dc link voltage at the inverter input terminals. The voltage controller block diagram is illustrated in Figure 3-4; the dc output voltage (V_{dc}) and battery current (I_B) are sensed and fed to voltage controller. The desired voltage ($V_{dc(ref)}$) is compared with the measured voltage (V_{dc}) and error is inputted to the PI controller whose output is a reference current ($I_{B(ref)}$). A second PI controller is employed to control the current by producing a proper value for the duty ratio (Duty) and feed it to a pulse generator which in turns generates the pulses that controls switching of transistors. By looking at the block diagram of the voltage controller, it can be easily noticed that both transistor are never on at the same time as the control signal for one of them is an inverted version of the other. It is worth mentioning that the extracted current from battery should not exceed the current limit. Therefore, the controller must be equipped with protection circuit against high current level.

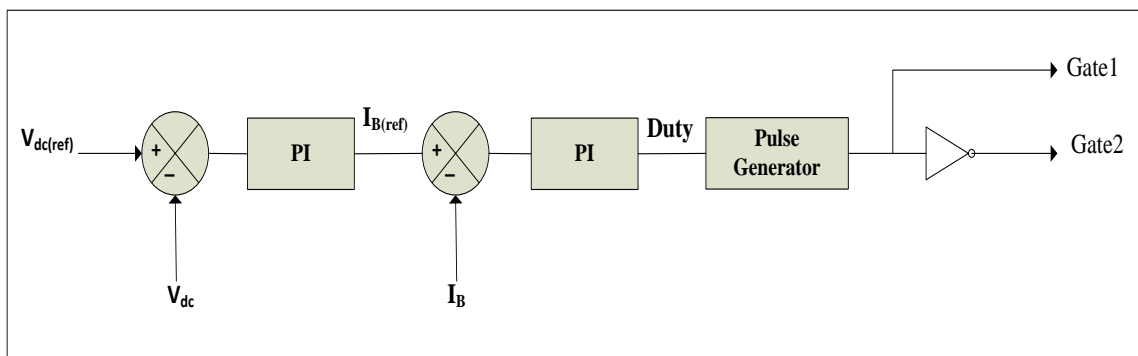


Figure 3-4 Block Diagram of Battery Voltage Controller

3.3 PV Panel and MPPT controller modeling

Photovoltaic generation has many advantages like Short lead time for designing and installing new systems, output power matching with peak load demands, static structure with no moving parts, long life, no noise, high power capacity per unit of weight, pollution free, highly mobile and portable because of its light weight, and very low operation and maintenance cost [151, 152]. The main disadvantages of photovoltaic are output fluctuation, and high investment cost [153]. One diode model is the simplest and the most popular model of PV. The schematic circuit in Figure 3-5 describes PV model; it consists of current source representing photoelectric current produced from the PV module, one diode to represent the P-N junction, and series resistance (R_s), and parallel resistance (R_p).

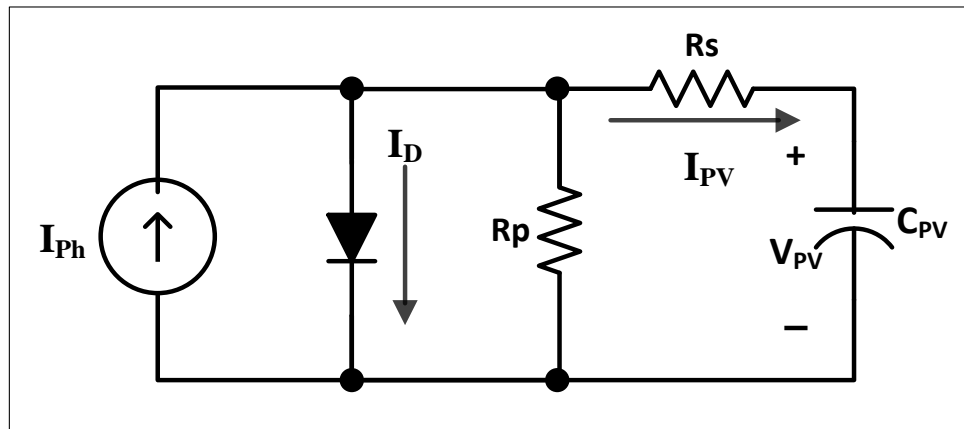


Figure 3-5 Schematic Circuit of PV Model

The PV model is described by equation (3.6)-(3.10).

$$I_{PV} = I_{ph} - I_D \quad (3.6)$$

$$I_D = I_0 \left[\exp \left(\frac{q(V+IR_s)}{\gamma K T_C} \right) - 1 \right] \quad (3.7)$$

$$I_{PV} = I_{ph} - I_o \left[\exp \left(\frac{q(V+IR_s)}{\gamma K T_C} \right) - 1 \right] \quad (3.8)$$

$$I_o = I_{o,REF} \left(\frac{T_C}{T_{C,REF}} \right)^3 \exp \left[\left(\frac{q E_g}{K \gamma} \right) \left(\frac{1}{T_{C,REF}} - \frac{1}{T_C} \right) \right] \quad (3.9)$$

$$I_L = \left(\frac{G}{G_{REF}} \right) [I_{L,REF} + \mu_{ISC} (T_C - T_{C,REF})] \quad (3.10)$$

Where;

I_D is the diode current (A)

I_{ph} is the photoelectric current (A)

V is the output voltage (V)

I_o is the saturation current (A)

T_C is the module temperature (K)

R_s is the series resistance (Ω)

E_g is energy gap (Wh)

G is the radiation W/m^2

G_{REF} is the radiation under standard condition (W/m^2)

$I_{L,REF}$ is the photoelectric current under standard condition (A)

$T_{C,REF}$ is the module temperature under standard condition (K)

μ_{ISC} is the temperature coefficient of the short circuit current [A/K]

The photoelectric current I_{ph} is directly proportional to solar irradiance, and inversely proportional to ambient temperature.

The power-voltage (P-V) curve and current-voltage (I-V) curve for different values of sun irradiance are shown in Figures 3-6 and 3-7 respectively. It is obvious that the amount of power produced by PV arrays increases as the irradiance increases. On the

other hand, a rise in the ambient temperature results in a reduction of solar generated Power as can be noticed from Figure 3-8 and 3-9 which shows P-V, and I-V curves at different values of ambient temperature. For particular values of irradiance and temperature, the amount of extracted power varies with voltage across the PV terminal, and it is maximum at a unique value of voltage called V_{mpp} .

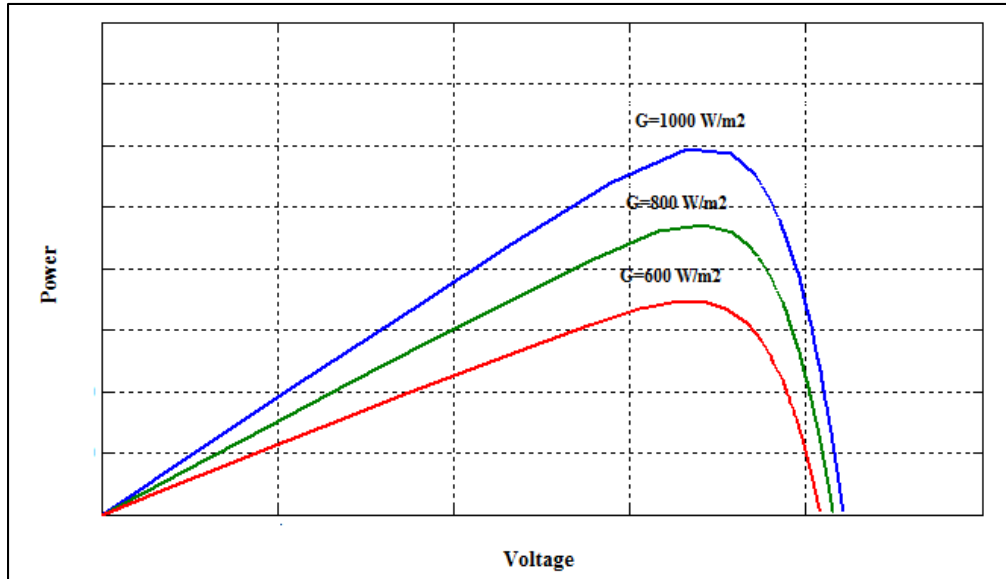


Figure 3-6 P-V Curves of PV at Different Irradiance Values

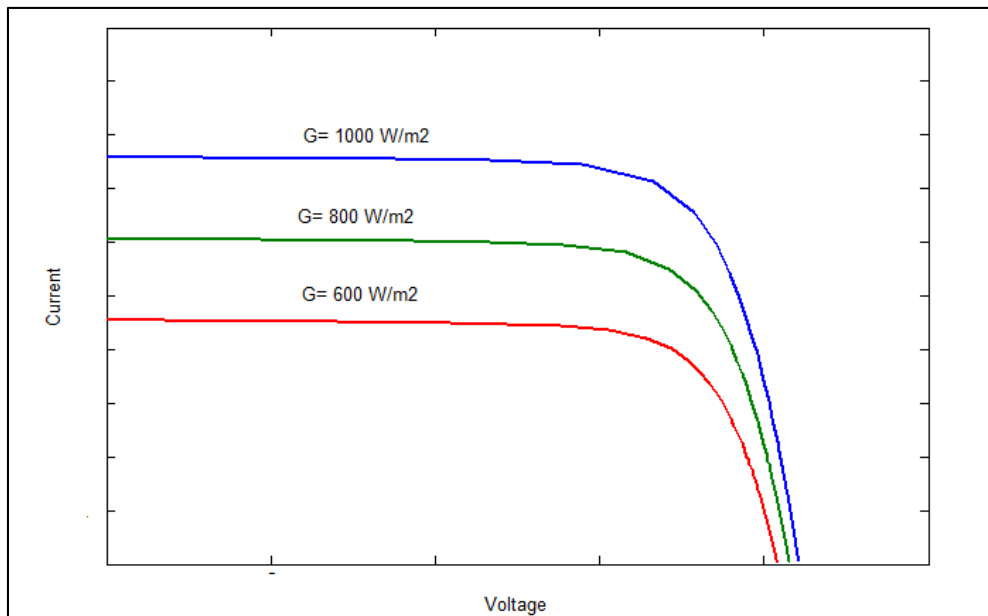


Figure 3-7 I-V Curves of PV at Different Irradiance Values

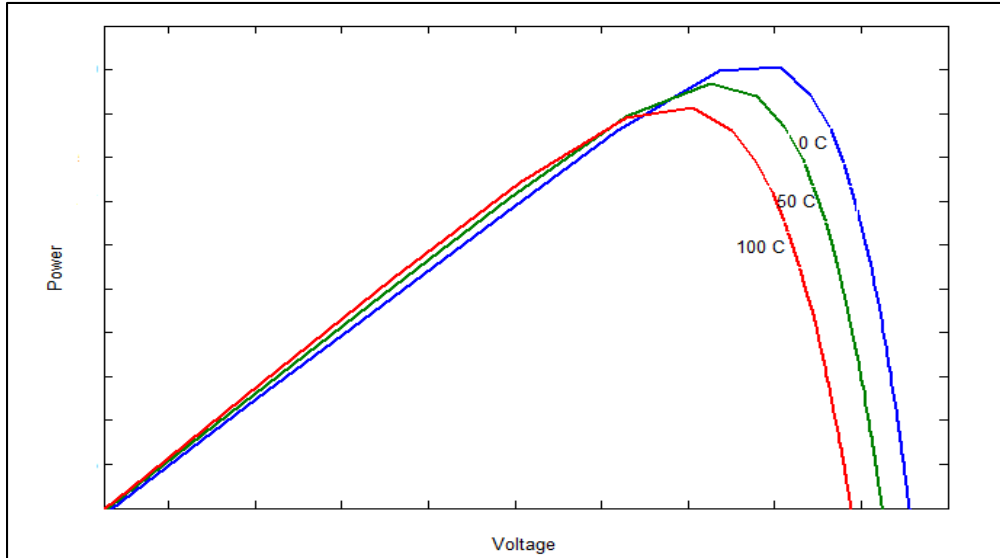


Figure 3-8 P-V Curves of PV at Different Temperatures

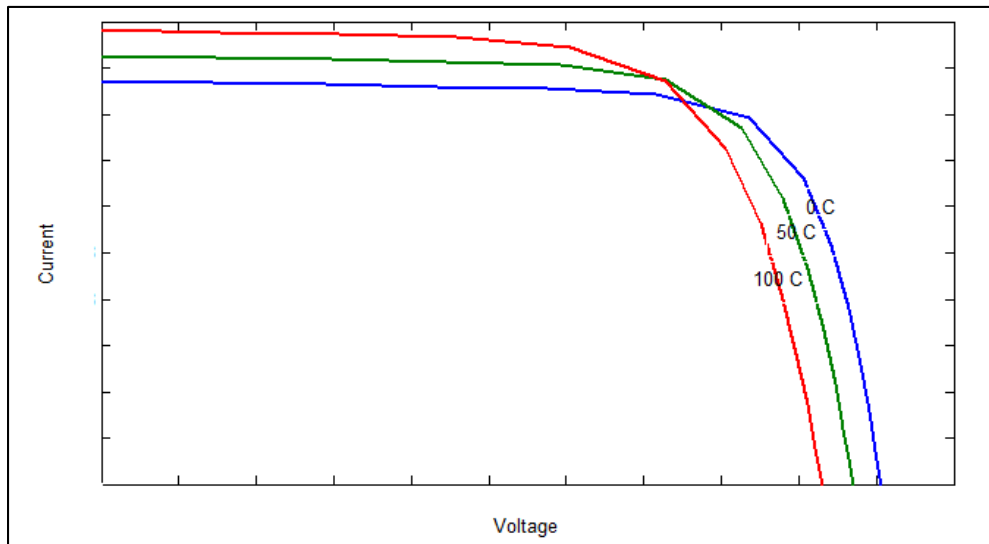


Figure 3-9 I-V Curves of PV at Different Temperatures

The maximum power that could be harvested from PV panel is called maximum power point MPP. In order to fully extract available solar power, a converter controlled by MPPT algorithm is employed. Different algorithms for MPPT were previously introduced in literature survey. Here, IC method is used due to its simplicity, and since the MPPT improvement is out of scope of this work, IC was determined to be suitable,

The converter used for controlling Ppv is a boost converter. The schematic circuit of the boost converter is shown in Figure 3-10. The circuit of the boost converter is composed of an inductor (L_{conv}) for boosting voltage and smoothing current, a transistor (T) acting as a switch, a diode, and a filtering capacitor (C_{conv}).

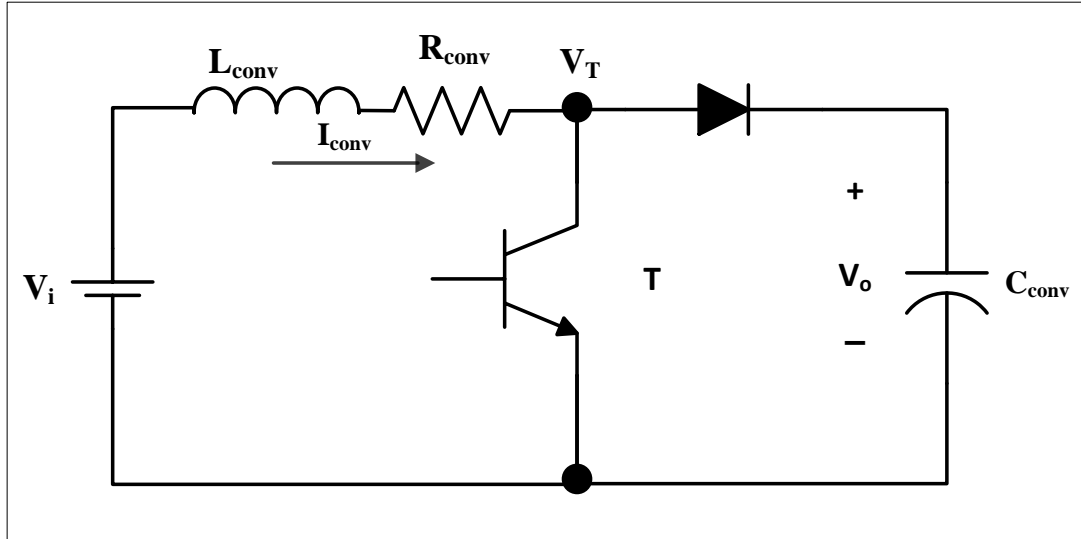


Figure 3-10 Schematic Circuit of Boost Converter

The dynamics of the converter and input/output relationship is described in equations (3.11) and (3.12).

$$V_i = V_T + L_{conv} \frac{dI_{conv}}{dt} + R_{conv} I_{conv} \quad (3.11)$$

$$V_o = V_T(1 - D) \quad (3.12)$$

Where V_i , V_T , and V_o are input voltage, transistor voltage, and output voltage respectively. D is the duty ratio of control signal of T . Figure 3-11 shows how battery and PV could be connected in parallel. Without a battery connection the voltage at C_{conv} will change according to the voltage set point generated by MPPT controller, but the output DC voltage is needed to be constant at a suitable level for proper control of the inverter. Therefore, the battery is in charge of keeping DC voltage constant. As a matter of fact, a constant voltage at DC link is achieved through matching power at the input and output

of the DC link. In other word the battery will supply or absorb power mismatch between PV output power and inverter output power.

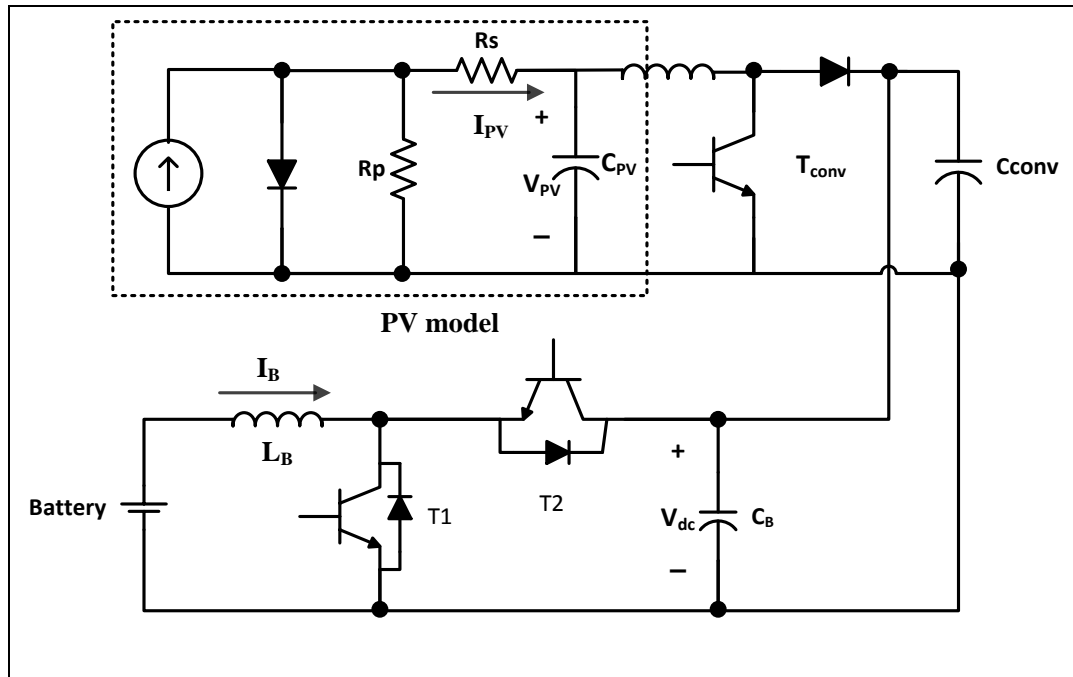


Figure 3-11 Parallel Connection of PV and Battery

3.4 Control of MG inverter

The DC output voltage from the PV and the battery is converted to a suitable AC voltage using 3-phase inverter. In this thesis the distribution voltage V_{L-L} is 380 V, and the frequency is 60 Hz. The inverter used in this work is depicted in Figure 3-12. It is composed of six IGBTs with anti-parallel diodes arranged in three half-bridges. Switching of the transistor is controlled by sinusoidal pulse width modulation (SPWM). SPWM generates firing pulses by comparing 3-phase sine wave with saw tooth signal.

The output voltage of the inverter contains high order harmonics which are filtered by LCL filter.

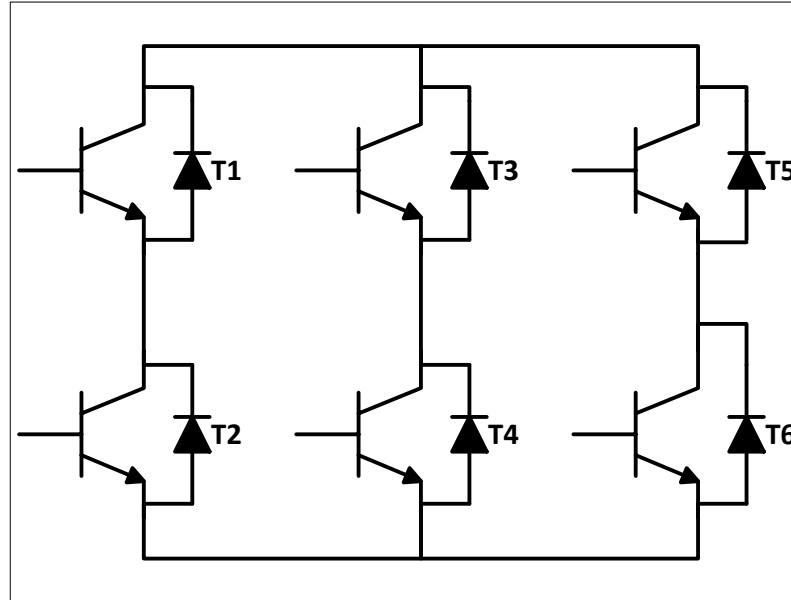


Figure 3-12 Three-phase Inverter

There are two control strategies for MG inverter i.e. PQ inverter, and voltage source inverter (VSI). PQ inverter is used to supply a given active and reactive power set-point. While VSI feeds the load with predefined values of voltage and frequency, the real and reactive power drawn from VSI is determined by the connected load. In fact, PQ control mode is used when voltage and frequency is ruled or governed by another source of energy; it could be the main-grid in case of grid-connected operation, or if MG is disconnected from grid, a diesel generator for example connected to MG network can regulate the voltage and frequency. In autonomous MG with multiple inverters, two main control strategies are possible i.e. single master operation (SMO), and multi master operation (MSO). In SMO a single inverter is operated as VSI and acts as the master providing a reference voltage for MG. Being that, all other inverters operate in PQ mode (slaves). On the other hand, MSO has more than one inverter operating as VSI (masters),

with other PQ inverters. In this thesis SMO is chosen as a control strategy. The considered MG has two inverters, and two synchronous generators used MH and diesel generator. When any of the two synchronous generators is brought online, it would act as the voltage reference, and both inverters are controlled as PQ inverters. On the other hand, when the battery and PV can withstand the load alone, and both MH and diesel generators are disconnected from network, the PV inverter acts as master leaving battery as slave.

The block diagram for the inverter controlled as VSI is illustrated in Figure 3-13. The building blocks of the VSI controller are: power controller, voltage controller, and current controller. The output current i_o , and the output voltage v_o , are measured and inputted to the droop controller and voltage controller. The output of the power controller is the voltage reference v_o^* , which is used as the input to the voltage controller which in turns produces a reference current i_l^* used by the current controller. In addition to i_l^* , current controller receive also i_l .

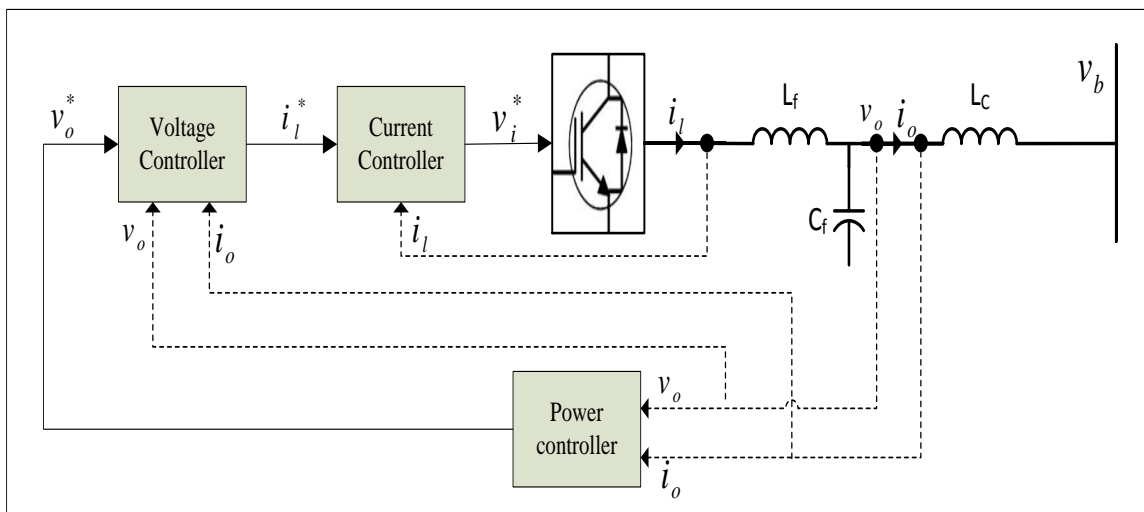


Figure 3-13 Block Diagram of VSI

The block diagram of the power controller is depicted in Figure 3-14. The power controller consists of PQ calculator, LPF, and droop controller. The droop controller mimics the governor of SG. Instantaneous real power (p) and reactive power (q) are calculated using output voltage and current. After that, p and q are passed through LPF with cutting frequency ω_c to obtain the real power P and reactive power Q. Finally, P and Q are fed to the droop controller to produce reference voltage magnitude v_{od}^* and phase angle θ . It can be seen from the block diagram that voltage and current are transformed from stationary frame (abc) in to synchronous frame (d-q) using the transformation matrix described in equation (3.13)

$$v_{dq} = \begin{bmatrix} \cos(\theta) & \cos(\theta - \frac{2\pi}{3}) & \cos(\theta + \frac{2\pi}{3}) \\ -\sin(\theta) & -\sin(\theta - \frac{2\pi}{3}) & -\sin(\theta + \frac{2\pi}{3}) \end{bmatrix} v_{abc} \quad (3.13)$$

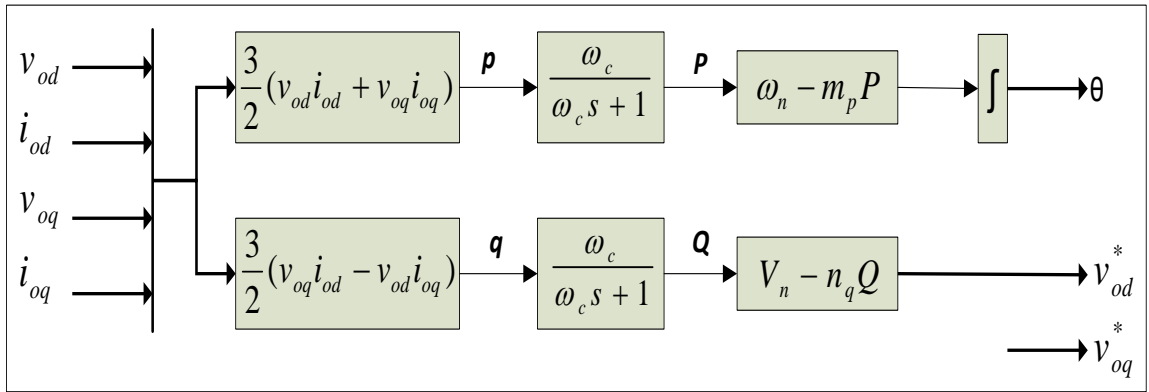


Figure 3-14 Block Diagram of Power Controller

p, and q are given by equations (3.14) and (3.15)

$$p = \frac{3}{2}(v_{od}i_{od} + v_{oq}i_{oq}) \quad (3.14)$$

$$q = \frac{3}{2}(v_{od}i_{oq} - v_{oq}i_{od}) \quad (3.15)$$

P, and Q are expressed in equation (3.16) and (3.17)

$$P = \frac{\omega_c}{s+\omega_c} p \quad (3.16)$$

$$Q = \frac{\omega_c}{s+\omega_c} q \quad (3.17)$$

The reference frequency ω obtained from P/ ω droop controller is given by:

$$\omega = \omega_n - m_p P \quad (3.18)$$

Where ω_n , is the nominal frequency and m_p , is the P/ ω droop gain. θ is obtained by integrating ω .

The reference voltage v_{od}^* is obtained from Q/V droop controller as in equation (3.19)

$$v_{od}^* = v_n - n_q Q \quad (3.19)$$

Where v_n , is the nominal voltage and n_q , is the Q/V droop gain.

The block diagram for the voltage controller is shown in Figure 3-15. It accepts reference voltage v_{odq}^* , measured output voltage v_{od} , and measured output current i_{od} as inputs and generates reference filter current i_{idq}^* . v_{od} is subtracted from v_{odq}^* , and the resulting error is fed to the PI controller. By adding a feed forward terms of v_{od} and i_{od} to the output of PI controller, i_{idq}^* is obtained. The voltage controller can be described by the state equation (3.20) and (3.21) along with algebraic equations (3.22) and (3.23)

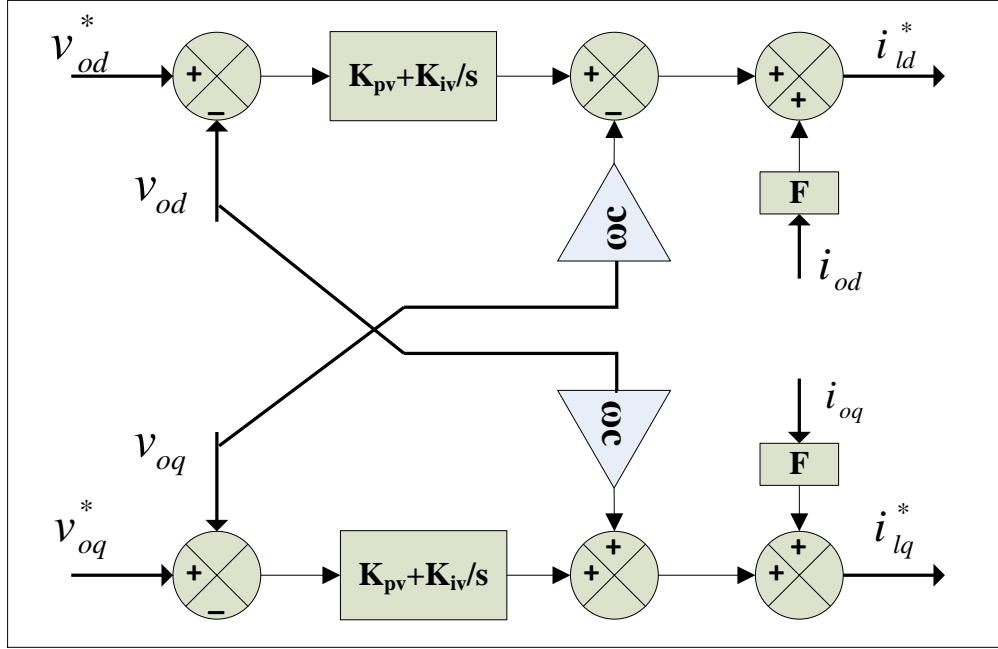


Figure 3-15 Block Diagram of Voltage Controller

$$\frac{d\phi_d}{dt} = v_{od}^* - v_{od} \quad (3.20)$$

$$\frac{d\phi_q}{dt} = v_{oq}^* - v_{oq} \quad (3.21)$$

$$i_{ld}^* = F \cdot i_{od} - \omega_n C_f v_{od} + K_{pv}(v_{od}^* - v_{od}) + K_{iv}\phi_d \quad (3.22)$$

$$i_{lq}^* = F \cdot i_{oq} + \omega_n C_f v_{oq} + K_{pv}(v_{oq}^* - v_{oq}) + K_{iv}\phi_q \quad (3.23)$$

Where F is the current feed forward gain, C_f is the filter capacitance, K_{pv} and K_{iv} are the proportional and integral gain respectively.

The structure of current controller is exposed in Figure (3-14). The corresponding state equation are:

$$\frac{d\gamma_d}{dt} = i_{ld}^* - i_{ld} \quad (3.24)$$

$$\frac{d\gamma_q}{dt} = i_{lq}^* - i_{lq} \quad (3.25)$$

Along with algebraic equation

$$i_{ld}^* = -\omega_n L_f i_{ld} + K_{pc}(i_{ld}^* - i_{ld}) + K_{ic}\gamma_d \quad (3.26)$$

$$i_{lq}^* = -\omega_n L_f i_{lq} + K_{pc}(i_{lq}^* - i_{lq}) + K_{ic}\gamma_q \quad (3.27)$$

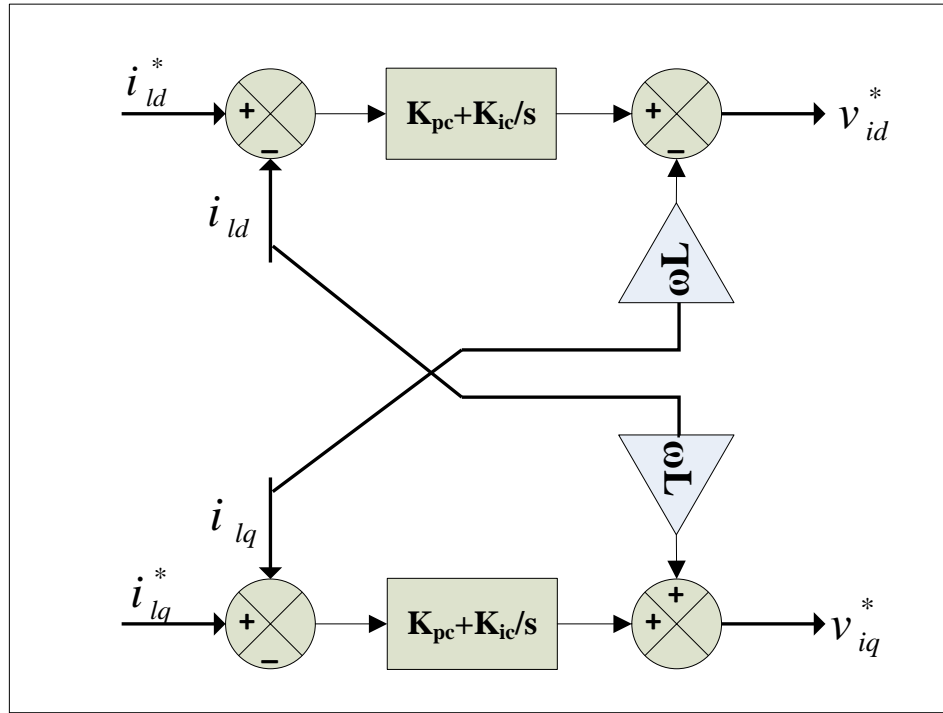


Figure 3-16 Block Diagram of Current Controller

PQ inverter block diagram is illustrated in Figure 3-17. Since the voltage is governed by another source of energy, the voltage controller is no longer needed. The PQ controller calculates the reference current i_{ldq}^* required to produce predefined PQ set-points (P^* and Q^*), and passes to the current controller. A typical PQ controller is depicted in Figure 3-18.

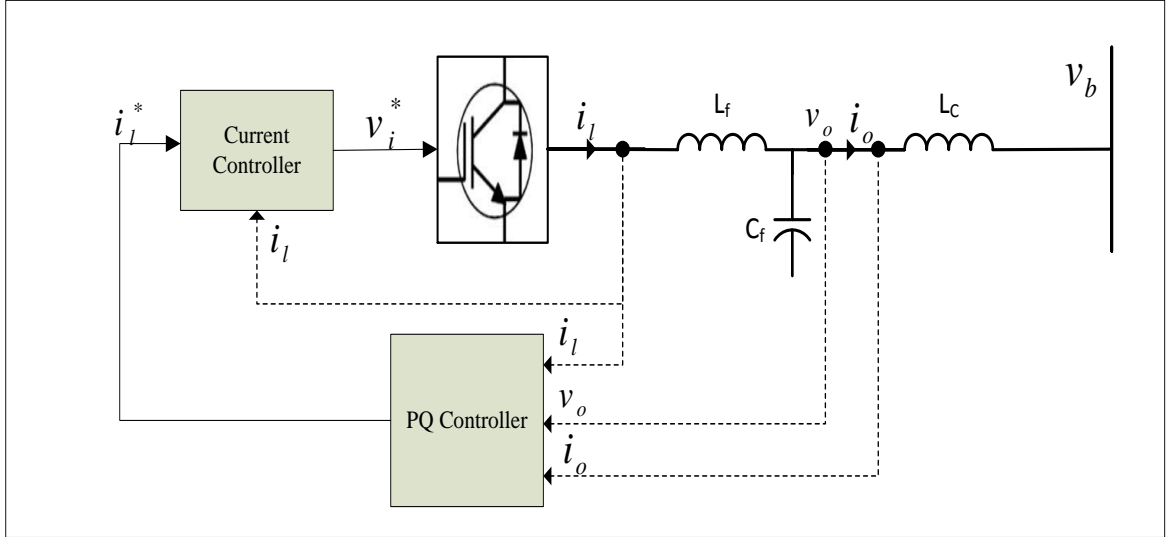


Figure 3-17 Block Diagram of PQ Inverter

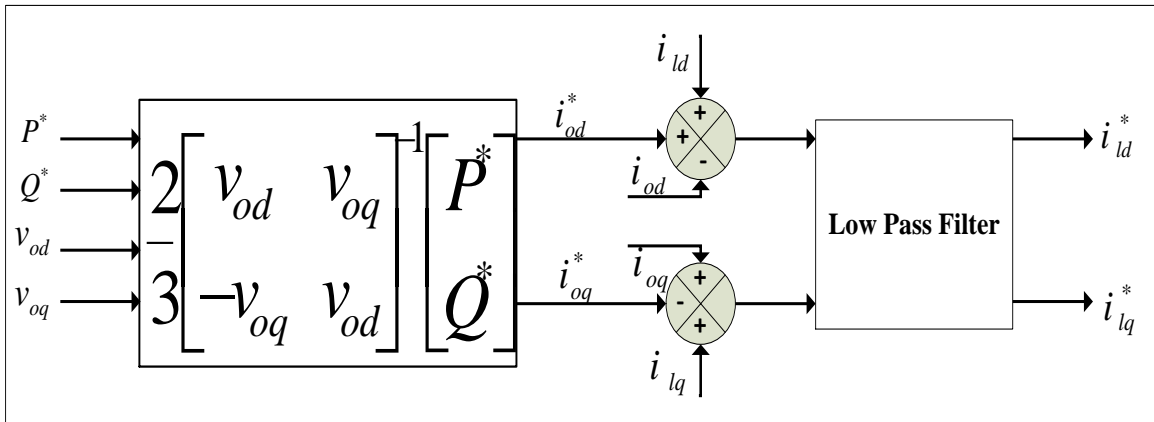


Figure 3-18 PQ Controller

The reference output currents i_{od}^* , i_{oq}^* are calculated using reference real and reactive power P^* , Q^* and measured output voltage v_{od} , v_{oq} by equations (3.26) and (3.27)

$$i_{od}^* = \frac{2}{3} \cdot \frac{v_{od}P^* - v_{oq}Q^*}{v_{od}^2 + v_{oq}^2} \quad (3.26)$$

$$i_{oq}^* = \frac{2}{3} \cdot \frac{v_{oq}P^* + v_{od}Q^*}{v_{od}^2 + v_{oq}^2} \quad (3.27)$$

The reference inductance coupling current i_d^Σ, i_q^Σ are obtained as follows:

$$i_d^\Sigma = i_{od}^* + (i_{ld} - i_{od}) \quad (3.28)$$

$$i_q^\Sigma = -i_{oq}^* + (i_{lq} + i_{oq}) \quad (3.29)$$

i_d^Σ, i_q^Σ are passed through LPF to obtain i_{ld}^*, i_{lq}^* .

As will be discussed later, the inverter will be switched from PQ inverter mode to VSI mode and vice versa as illustrated in Figure 3-19.

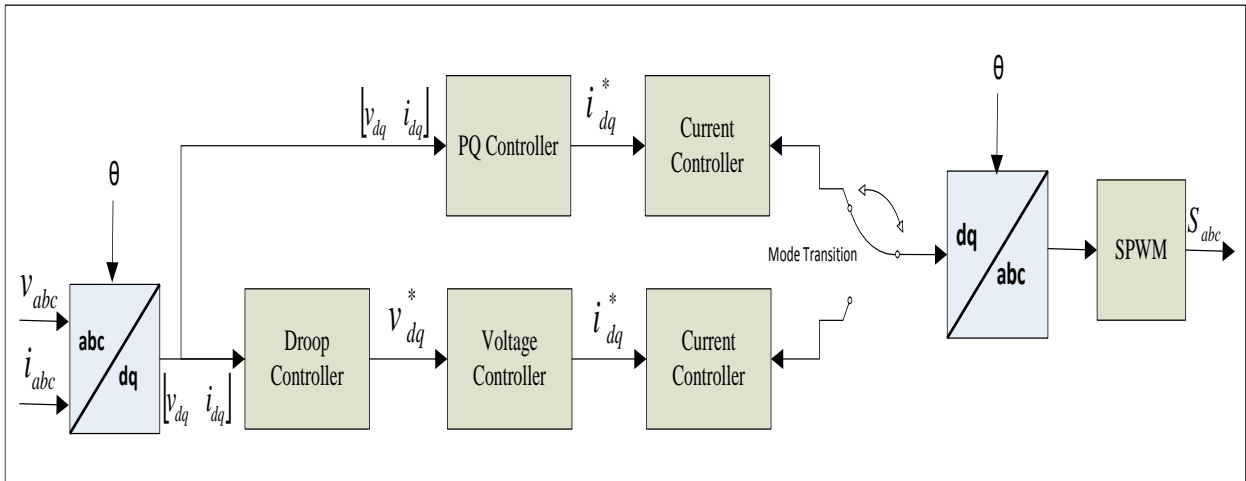


Figure 3-19 Mode Transition of Inverter Operation

3.5 Micro Hydro modeling

The principle of hydro generation is to convert potential energy of water at high level to kinetic energy by discharging water into a lower level, and then converts the resulting energy into electrical energy by using the kinetic energy of water to driver a turbine which in turns drives an electric generator. The maximum power that can be

produced depends on mainly the head of water and flow rate. The power produced by hydro-generation is given by (3.30)

$$P_H = \gamma \cdot Q \cdot H \cdot \eta_T \cdot \eta_G \quad (3.30)$$

Where:

- P_H Hydroelectric power (W)
- γ Specific weight of water (9810 N/m²)
- Q Water flow rate (m³/s),
- H Water fall height (Head) (m)
- η_T Efficiency of turbine
- η_G Efficiency of generator

For a simple hydraulic system with a water dam, water flow control system and penstock; the hydrodynamic equations are:

$$U = K_u G \sqrt{H} \quad (3.31)$$

$$P_m = K_p H U \quad (3.32)$$

$$\frac{dU}{dt} = -\frac{a_g}{L} (H - H_0) \quad (3.32)$$

$$Q = A U \quad (3.34)$$

Where:

- U : Water speed
- G : Gate opening
- H_0 : Initial steady-state value of H
- P_m : Turbine mechanical power
- L : Length of conduit
- A : Pipe Area
- a_g : Gravity acceleration

K_u, K_p constants of proportionality

Based on the rated values, (3.31)-(3.34) are normalized as follows:

$$\bar{H} = \left(\frac{\bar{U}}{\bar{G}} \right)^2 \quad (3.35)$$

$$\frac{\bar{U}}{\bar{H} - \bar{H}_0} = \frac{1}{T_w s} \quad (3.36)$$

$$T_w = \frac{LU}{a_g H_r} = \frac{LQ_r}{a_g H_r} \quad (3.37)$$

$$\bar{T}_m = \left(\frac{\omega_0}{\omega} \right) \bar{P}_m \left(\frac{P_r}{MVA_{base}} \right) = \frac{1}{\bar{w}} (\bar{U} - \bar{U}_{NL}) \bar{H} \bar{P}_r \quad (3.38)$$

$$\bar{G} = A_t \bar{g} \quad (3.39)$$

$$A_t = \frac{1}{\bar{g}_{FL} - \bar{g}_{NL}} \quad (3.40)$$

With reference to (3.30), the amount of generated power by hydro facility can be regulated by controlling the rate of water flow through the adjustment of the gate opening G . The Block diagram of hydroelectric generation control system is depicted in Figure 3-20.

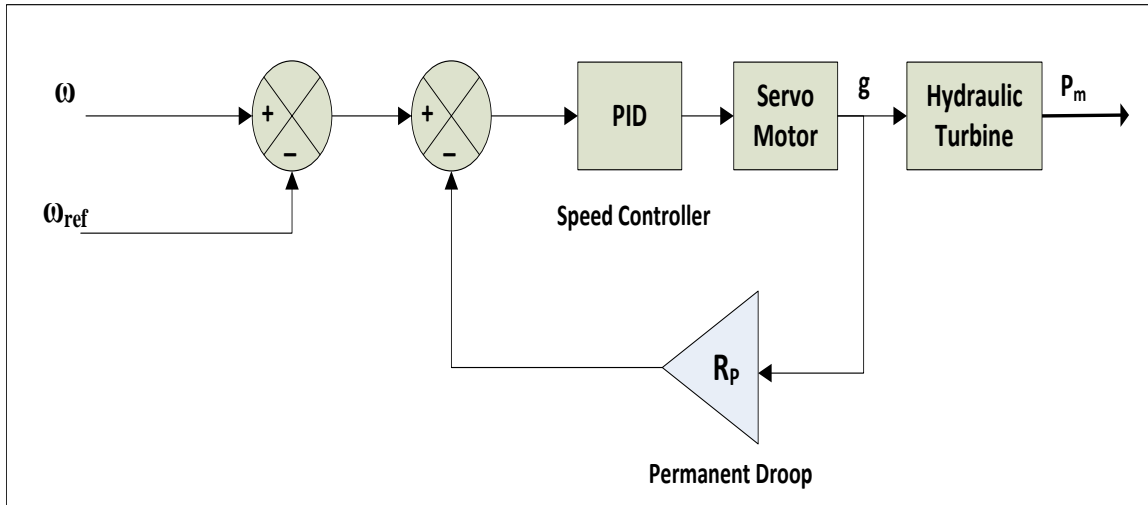


Figure 3-20 Block Diagram of Hydroelectric Generation Control System

Speed is regulated using a PID controller which drives a servo motor which in turns defines the required gate opening (g). Each value of g corresponds for a specific amount of water flow Q . The water flow drives the hydraulic turbine producing a certain mechanical power P_m used to rotate SG and produce electric power. Block diagrams of the servo motor and hydraulic turbine are shown in Figures 3-21 and 3-22 respectively.

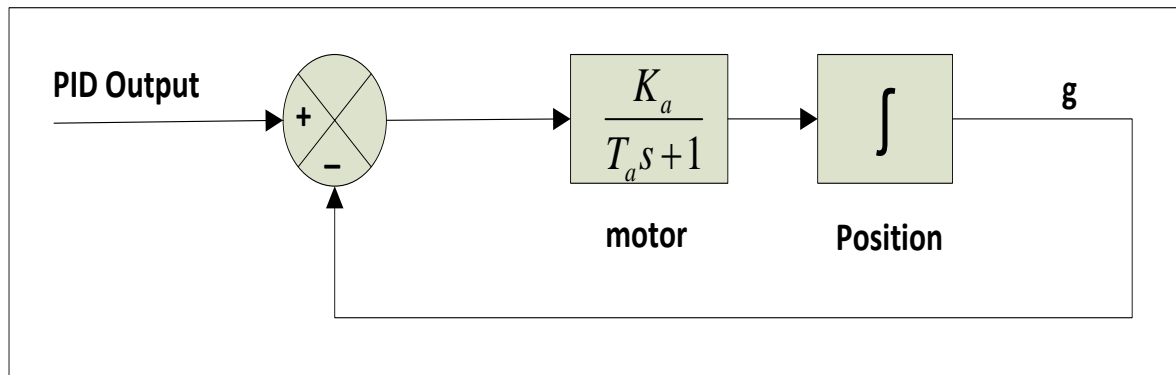


Figure 3-21 Block Diagram of Servo-Motor

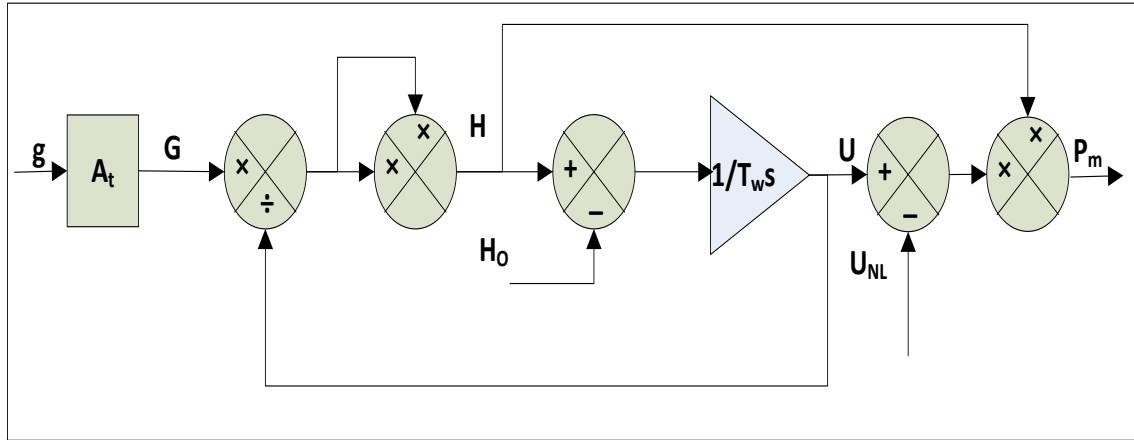


Figure 3-22 Block Diagram of Hydraulic Turbine

3.6 Diesel Generator Modeling

Diesel generator is commonly used for back up generation, as it has fast response and the output power can be regulated rapidly. It is also used to supply power to isolated and remote areas. The investment cost of Diesel generator is low. However, its running cost is high, and it is not friendly with environment [154, 155]. The Model of diesel generator is shown in Figure 3-23. The model is composed of a speed controller, actuator, and diesel engine. Speed error is fed to a speed controller which regulates the frequency of the generated voltage, and the output of the speed controller is weighted by gain K and inputted to the actuator which controls the fuel pumped to diesel engine. The diesel engine acts as a prime mover driving the SG. Speed controller and actuator are represented by second order transfer functions, while the diesel engine is modeled by a time delay T_d . T_{C1} , T_{C2} , and T_{C3} , time constants of speed controller, and T_{A1} , T_{A2} , and T_{A3} and time constants of actuator.

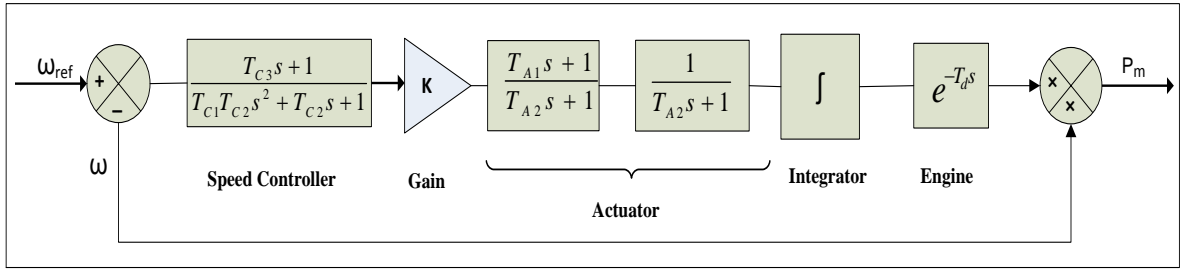


Figure 3-23 Diesel Generator Model

CHAPTER 4

Proposed Control and Management Strategy

4.1 Hierarchy of proposed strategy

The MG under study cannot be managed using distributed controllers (e.g. droop controller); it requires a supervisory controller for the following reasons:

- BSS can run out of energy and the controller has to be aware of that when it happens.
- PV generation is fluctuating and it is available during specified hours only.
- Any DG unit may encounter a technical failure, so it has to be disconnected.
- MH total generated energy in a day has to be monitored.
- Unit starting up or shutting down has to be managed.

The proposed control strategy has two levels as shown in Figure 4-1. The upper level is an online energy management system (EMS) based on MAS, and the lower level is local level, in response to power commands required by MAS. MAS will perform power balance and economic dispatch online based on system information provided by every DG and load in MG. MAS will be discussed in details in chapter 5. The local controllers for each DG in MG (described in chapter 3) will receive commands from MAS and will realize them. The information required by MAS includes P and Q demand at each load bus, available generation capacity for every DG, available solar power at any given time, SOC for batteries, and breaker status for both MH and diesel generator. On

the other hand, the commands issued by MAS include P and Q setting, mode of operation (PQ bus or PV bus), breaker open/close command, charging/discharging mode of operation for the battery. In normal conditions the total capacity MH-PV-BSS hybrid system should be sufficient to supply the total load. However, if due to unexpected weather condition or sudden failure in MH plant then the diesel generator will be started to back up generation system.

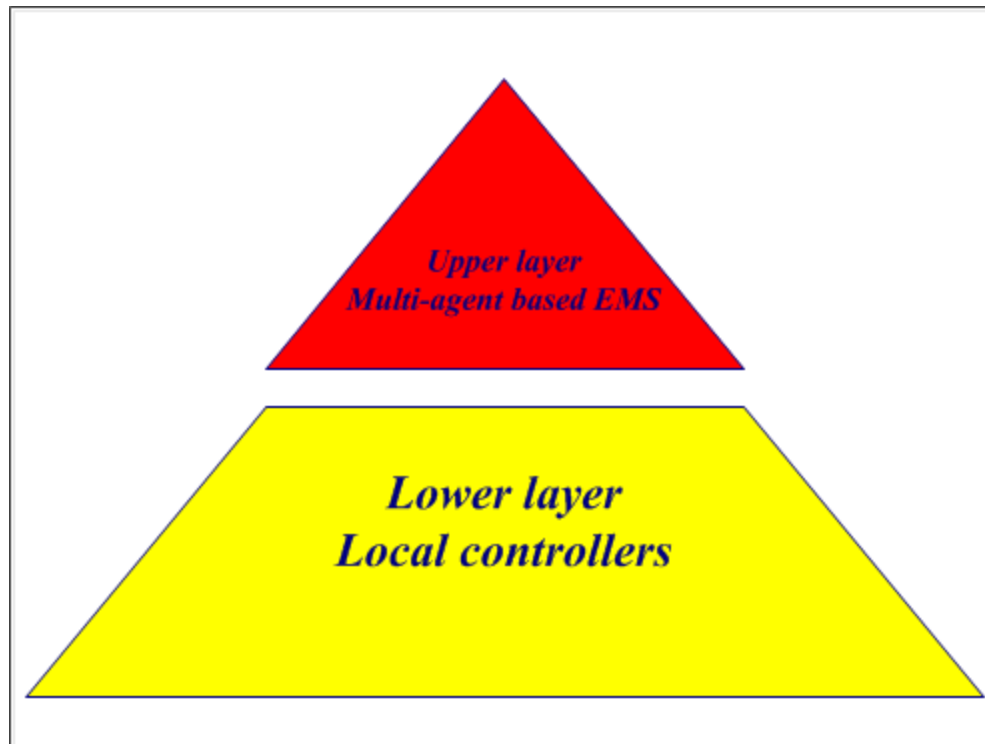


Figure 4-1 Hierarchy of Control and Management Strategy

4.2 Flow Chart and Description of EMS

The flow chart for EMS is shown in Figure 4-2. EMS receives required information as previously mentioned, then checks if the power from PV generator can meet the load demand. If yes then it will set the inverter of PV as the VSI inverter. In this

case PV will be autonomously supplying the load, and it will alone form the grid. In case the available solar power is not enough to fully electrify the total connected load, the battery is checked for available energy to support the PV generators. If it is found that energy stored in the battery is not enough then MH will be committed. When MH is committed the PV inverter will switch to PQ inverter and hydro-generation will be responsible of regulating the voltage and frequency. In addition, BSS will be switched to charging. Finally, if MH and PV cannot withstand the load, the diesel generator will be committed. In fact, when the diesel generator or MH plant is committed, then it is not reasonable to continue discharging BSS. Instead, BSS could be put in off-state to save energy and support PV generator when diesel generator or MH go offline, or in case that MH is running the hydro power can be used to charge BSS up to specific percentage. Moreover, if EMS finds that MH or diesel generators are no longer needed to be running, but they did not ran for their minimum up time, then they can be operated at their minimum output power and charge the batteries. Based on the aforementioned description proposed on EMS, it can be concluded that EMS has the following objectives:

- To minimize the operational cost by fully utilizing RES.
- To maintain voltage and frequency of MG at nominal values
- To handle interactive operation of MG
- To assign P, and Q settings for each DG in MG
- To assign operation mode for each DG in MG
- To supervise the charging/discharging operation of BSS.
- To perform unit commitment operation of MH and diesel.

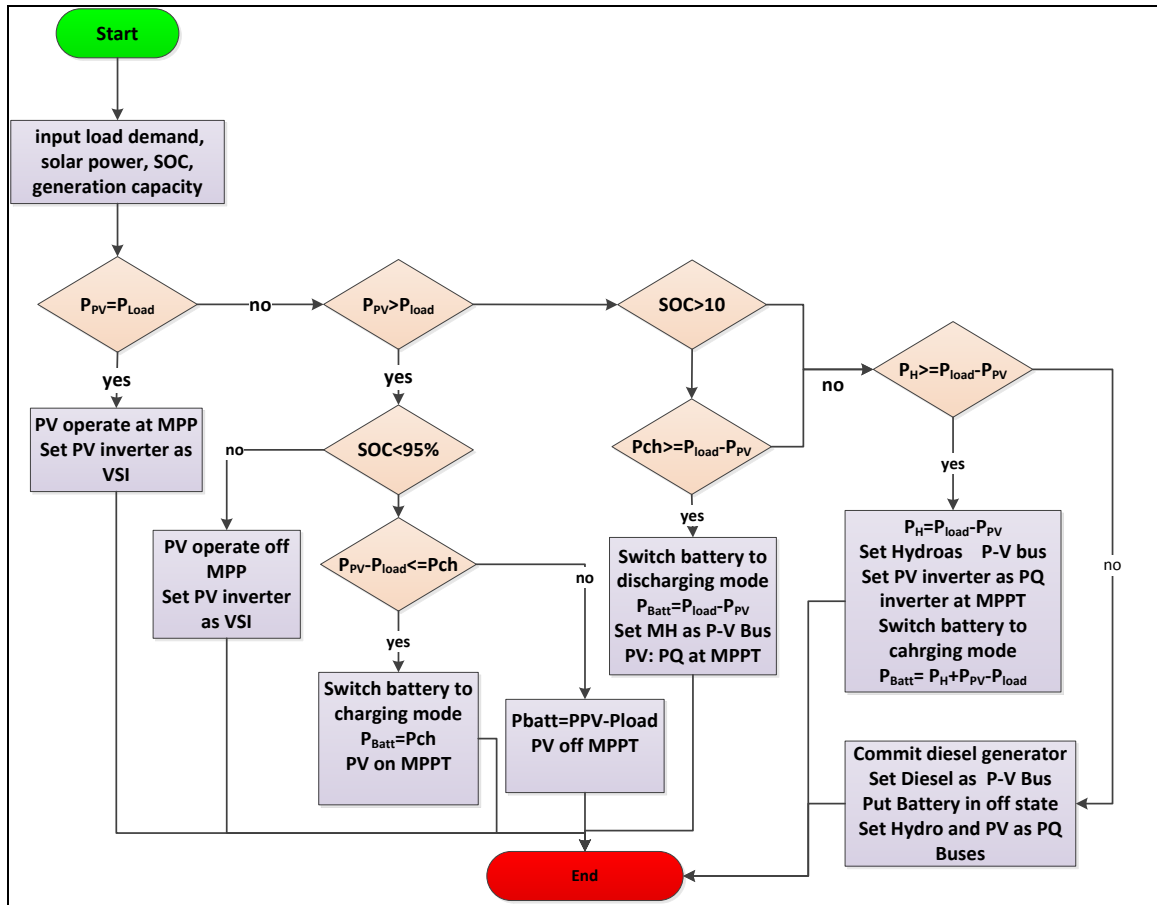


Figure 4-2 Flow Chart of EMS

In order to fully utilize the solar energy resources, the battery is installed to store or supply the mismatch between PV generation and load. That is not the only reason for deploying the battery; the battery is also used to minimize fluctuation of PV generation and shave the power. In addition, charging battery from MH will enable MH and PV to operate interactively. In fact, two operation and control strategies are possible for MH-PV system i.e. interactive operation strategy, and parallel operation strategy [14, 156]. In interactive operation, PV with aid of BSS autonomously supplies load during day time. That means, PV-BESS system has to keep voltage and frequency at nominal value. In other words, PV-BESS inverter has to be operated as VSI. During night time and early

hours in morning, MH is responsible for supplying load independently. This type of operation is preferred for dam type hydro generation to reserve the water in reservoir, especially in hot season. The other valid strategy of operation is parallel operation where PV and MH work in parallel, and this type of operation is preferred for run-off river MH. In parallel operation, there are two possibilities for regulating voltage and frequency; the first possibility is to let PV inverter act as PQ inverter, supplying predefined P and Q setting while MH forms the grid voltage reference. The second approach is to allow both MH and PV to form the grid in parallel through droop controllers. In order to operate MG interactively, the following considerations have to be taken into account:

- If the MH or diesel generators are to be committed, then the startup of these units must be gradual. Since, BSS will be discharging at maximum rate prior to starting of MH or diesel generator, then switching BSS from discharging state to off state or charging state immediately after committing MH or diesel generator in on shot, will require huge starting power from MH and diesel generator. So, BSS power better starts decreasing while MH power start increasing in small steps till BSS reaches off state or charging state. This will result in smooth starting up and smooth.
- When EMS discovers that MH and diesel generators are no longer required and PV-BSS system can withstand the load, then it is not thinkable that BSS starts discharging at maximum rate, and MH/diesel generator goes offline directly. This will cause huge disturbance in the system. Instead gradual shut down mechanism of conventional generators is activated. In this mechanism, BSS starts to discharge at low power level and conventional generators start to decrease their

power gradually till the reach minimum generation values. At that moment, the units can be shut down and the breaker can be opened.

- There has to be a spinning reserve always. So, none of DGs working autonomously is operated at maximum generation output. Also, when the committed units cannot keep the reserve, then a new unit must be brought online.
- When a new units is about to be started and connect to the existing MG, the voltage of MG and the new unit must be synchronized. To achieve that, the incoming unit is first started at no load, and the phase of its voltage is modified until the phase error between MG voltage and unit become equal or close to zero. It is possible also to alter the phase of MG by changing the phase of PV inverter until it matches the phase of new unit. In fact, the incoming units can be MH generator or diesel generator. In case that MH is the unit which is to be committed, then PV inverter controller need to receive the phase of MH generator and synchronization triggering signal to start synchronization. The same can be done to diesel generator.

The flow chart for startup operation of MH and diesel generator is shown in Figure (4-3). In the proposed MG there are two BSS; one is connected in parallel with PV generator at bus 1 (BSS-1), and another is installed at bus 5 (BSS-2). When EMS discover that PV generator and BSS maximum power are no longer enough to supply the total load, it checks for the availability of MH power, and if it is available, EMS closes the breaker of MH and decreases the output of BSS-2 by 2000 W. After that, EMS enters in waiting state for specific time using time counter. After waiting time is over, it checks if the output of BSS-2 is less than 3000 W. If yes, then EMS starts

decreasing BSS-1 output in the same manner. When output power of both BSS-1 and BSS-2 become less than 3000 KW, EMS instructs both batteries to enter off state. It is worth mentioning that with every time BSS decreases its output, MH increases its output automatically as it act as voltage reference.

The gradual shut down of conventional generation units is executed in accordance with the flow chart depicted in Figure (4-4). First, EMS has to know what generator is running and required to be shut down. This is done by checking the breakers of and the amount of generation for MH generator. If MH is running then EMS gradually starts to decrease its output until the minimum generation level is reached. At that moment EMS open the breaker of MH and transfer PV inverter from VSI to PQ. EMS does the same for diesel generator. In this work one MH an diesel generator is running at a time.

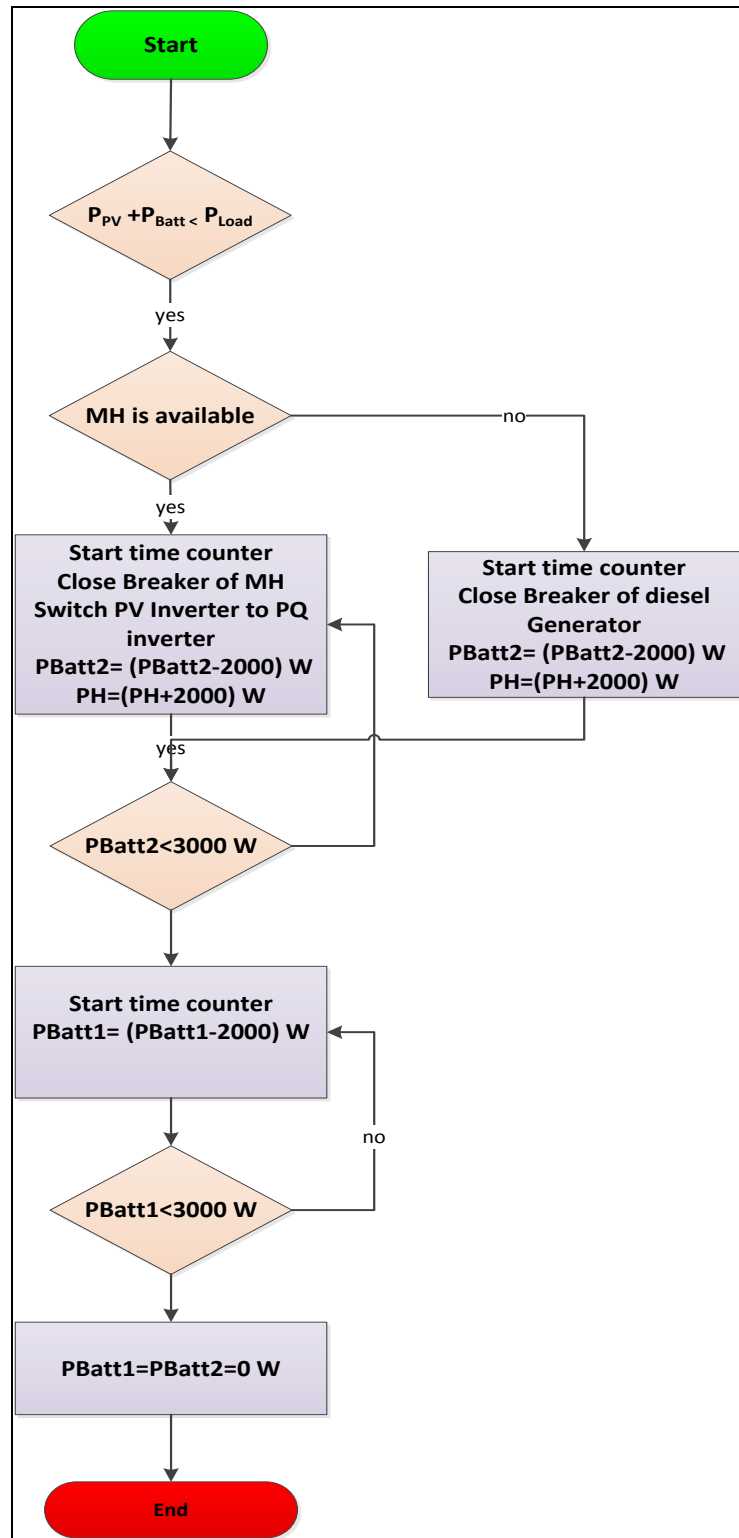


Figure 4-3 The Flowchart of Gradual Start up

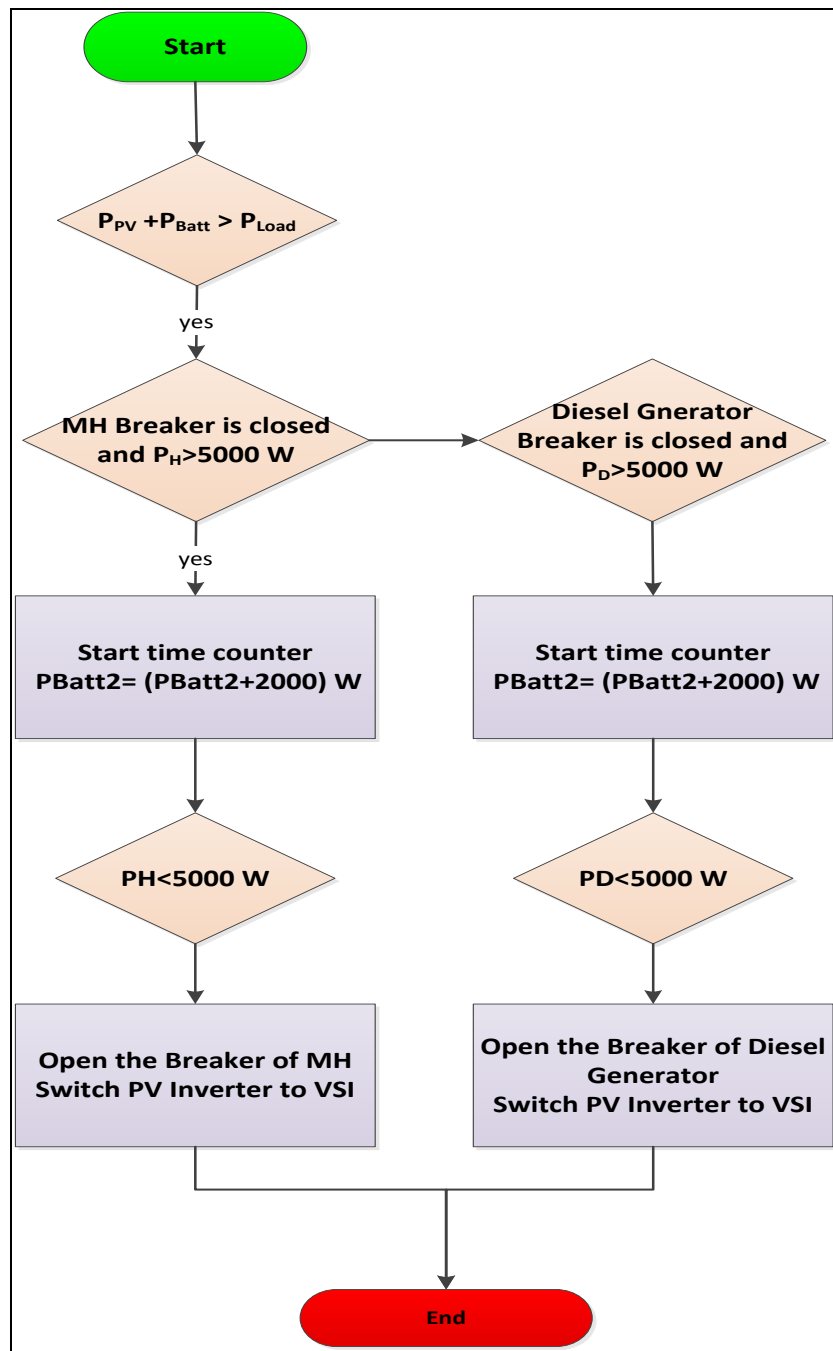


Figure 4-4 The Flow Chart of Gradual Shut Down

Online management might not be optimal as it is not planned. However, for the particular generation system proposed here, the most important issue is to obtain the best schedule for charging and discharging batteries. Nevertheless, for the studied system, we can tell when to charge or discharge the batteries. For example, in interactive operation mode, the battery is supposed to be discharged when PV generation cannot meet the load and charged when PV generation is greater than the load. The battery can be charged also during working hours of MH to store energy enough to make PV-BSS system able to withstand the load autonomously and shut down MH plant.

CHAPTER 5

Proposed Multi-Agent System (MAS) Development

5.1 Agent and MAS Definition

Several different definitions were produced to an agent by the computer science community. The fact that several definitions were proposed creates difficulty of defining notion for agency. In spite of the fact that the definitions of the agents differ from each other, they all share a basic set of concepts. The well-known definitions that clearly describe and reveal the identity of the agent belongs to Maes, Wooldridge, and Russell and Norvig. Maes quotes that “Agents are computational systems that inhabit some complex, dynamic environment, sense and act autonomously in this environment, and by doing so realize a set of goals or tasks for which they are designed” [157]. According to Wooldridge an agent is merely “a software (or hardware) entity that is situated in some *environment* and is able to *autonomously* react to changes in that *environment*.” [158]. The *environment* is simply everything external to the agent. Russell and Norvig go further, by requiring the scheduling of actions to be in response to some change in the environment, and not simply the result of the agent’s in-built knowledge. For an agent to be situated in the environment, at least part of this environment should be observable or alterable by agent [159].

An analogy between a living person in a human society and an agent situated in a software or hardware environment can be made, a member of society can observe the

events that took place around him and by taking certain actions he might alter the reality of society.

As many are convinced that agents are no different from existing systems, Wooldridge extended the definition of an agent to an intelligent agent to give a distinguished definition to agent. The intelligent agent has the following properties:

-Reactivity: an intelligent agent is able to react to changes in its environment in a timely fashion, and takes some action based on those changes and the function it is designed to achieve.

-Pro-activeness: intelligent agents exhibit goal-directed behavior. Goal-directed behavior connotes that an agent will dynamically change its behavior in order to achieve its goals. For example, if an agent loses communication with another agent whose services are required to fulfill its goals, it will search for another agent that provides the same services

-Social ability: intelligent agents are able to interact with other intelligent agents. Social ability connotes more than the simple passing of data between different software and hardware entities, something many traditional systems do. It connotes the ability to negotiate and interact in a cooperative manner

Now, if more than one agent exists in the same environment they compose MAS. Therefore, MAS is simply a system comprising two or more *agents* or *intelligent agents*. The system has an overall goal which is fulfilled by the cooperation of all agents. These agents exchange information, commands, and interact with each other. However, each individual agent has its own local goal and pursues to achieve it through a sequence of decisions and actions [160].

5.2 Multi-Agents Communication and Coordination

Agents need to communicate with each other in order to cooperate and negotiate. In fact, agents need also to make contact with user and system resource. In particular, agents interact with each other using some special languages, called agent communication languages (ACL). Among the messaging languages standards, the standards defined by the Foundation of Intelligent Physical Agent (FIPA) are widely used. FIPA ACL supports different content languages and provides managed conversation through interaction protocols. Agents must coordinate with each other to ensure that a group of agents in some environment act in consistent manner. The necessity of coordination can be justified by a number of reasons; one reason is that separate agents' objectives may conflict with each other, that is to say, a particular agent might take some action to achieve its goal without coordination and affect other agents adversely. Another reason is that agents' goal might be dependent. Besides, agent may have different capabilities and different knowledge so they need coordination to share knowledge and help each other. Moreover, coordination can help achieving the goals of agents more rapidly.

Many approaches can be used to handle agent coordination including organizational structuring, and multi-agent planning. In organizational structuring the simplest way is to use a master agent to gather information from a group of slave agents, create plans and assign tasks to each individual slave agent. This approach is difficult to realize in practice, and conflicts with decentralized nature of MAS. Another technique used in organizational structuring is contracting net protocol (CNP). It is a very useful

and efficient technique for allocation of resources and tasks among agents. CNP is based on decentralized market structure. Each agent does not solve its local problem using its local resources and knowledge, but instead it seeks for help from other agents. An agent announces a contract through a manager agent, submits its bids through contractor agents, and evaluates the bids of the other agents received through the contractor agent, and decides which offer is the best.

The other way to deal with coordination problem is to treat it as a planning problem. Multi-agents can plan their actions to avoid inconsistency between the different agents' local goals. This can be done in centralized manner where a coordination agent receives local plans and future actions and modifies them to eliminate any conflict. Also, an agent can communicate with each other directly or indirectly (through other agents) in decentralized manner without a need for a coordinator, and they can agree on the plans that guarantee coherence. In This Thesis the decentralized communication is used [161].

5.3 Creating Agents Environment

In order to build agents, a platform or a software environment compliant with FIPA standards is required. In this work Java Agent Development Environment (JADE) is used. JADE is a software framework fully implemented in Java language. It simplifies the implementation of multi-agent systems through a middle-ware that complies with the FIPA specifications and through a set of graphical tools that supports the debugging and deployment phases. In order to generate and execute the required Java code, a java-based open source platform called Eclipse is used. Eclipse allows creating customized development environment (IDE) from plug-in components. To build agents, first the

main container is launched activating JADE management GUI (-gui). Other containers can be built and registered to the main container in the same platform. Agents are created or terminated in the main container or in another normal container. The main container holds two special types of agents, namely Agent Management System (AMS), and Directory Facilitator (DF). AMS provide naming services i.e. each agent will have a unique name. It also represents the authority in the platform. On the other hand, DF provides yellow page service to enable different agents to find each other and make contact. Other main containers can be started in other platform and the agents with can be found and contacted using their unique names. Figure 5-1 illustrated an example of containers and platforms; two main containers are launched within two separate platforms. Two other normal containers are started in the first platform and register to main container. A1-A5 represents agents' names created in different containers.

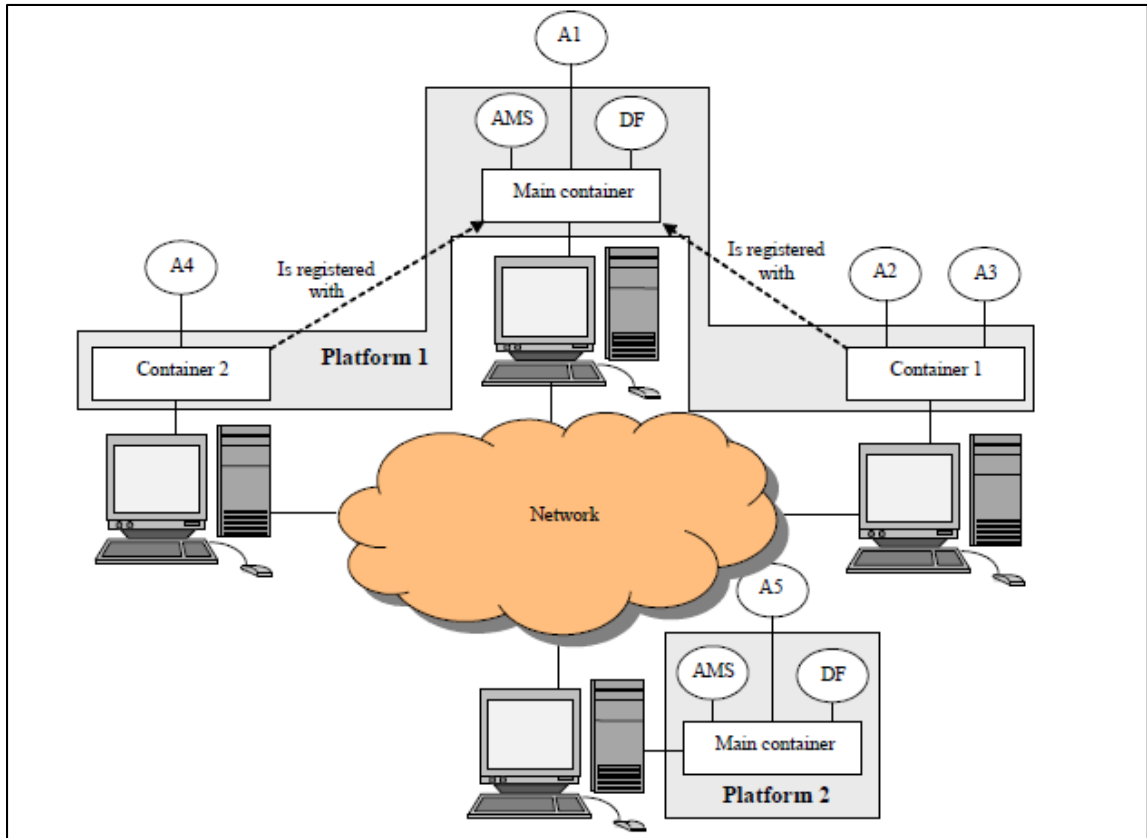


Figure 5-1 Platforms and Container of MAS [162]

Once the agent platform is built, agents can communicate with each other and exchange messages containing information, requests, or commands. In JADE there are various message template formats such as CPF (call for proposal), PROPOSE, REQUEST-PROPOSAL, ACCEPT, REFUSE, and INFORM.

5.4 Proposed MAS Architecture

MG under study was described in chapter 3. As MG has 7 buses, then 7 agents have to be created. Each individual agent corresponds to a particular bus. MAS will contain three load agents (LA), and four generation agents (GA). GAs are further classified according to the type of generation attached at their corresponding buses, PV

agent (PVA), battery agent (BA), micro-hydro agent (MHA), and diesel generator agent (DGA). In addition, service agent (SA) can be built to provide load and weather forecasting services required for energy management process. As mentioned before, agents need to communicate and coordinate with each other to achieve local and global goals which in this case maximize the utilization of renewable energy resources. In other words, MAS aims to minimize cost of operation by coordinating between different agents in the system. Control and management strategy was detailed in chapter 4. As previously mentioned, the communication approach adopted in this work is a decentralized approach, with no coordinator agent existing. To accomplish communication, first a communication tree (spanning tree) is formed, so every agent knows agents that can be contacted for exchanging information and commands. This means that the information flow route is established to enable proper flow of messages between different agents of the system. Figure 5-2 shows a simplified single line diagram of the proposed MG. It is assumed that only agents whose corresponding buses are interconnected can construct direct link of communication between them. Furthermore, agents with direct link need to have what is called parent/child relationship where the child agent reports its local view of the system to its parent agent which in turns sends commands or action request to its child. Agent can have only one parent and multiple children. Once two agents have established Parent/child relationship, each of the two agents store its parent's or child ID.

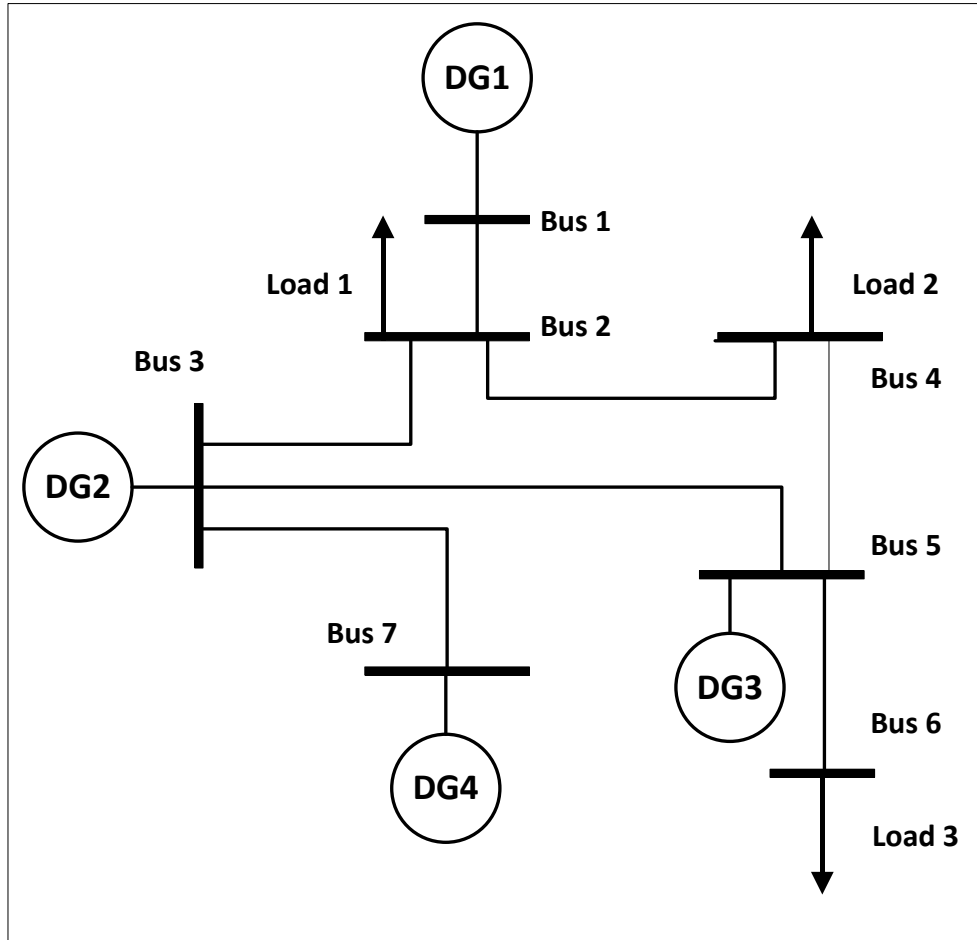


Figure 5-2 Single Line Diagram of MG

In the stage of establishing a communication tree, any agent can possibly be the starting agent. Taking PVA for example as a starting agent, the procedure for forming a complete communication tree can be described as follows:

- PVA sends a contact request to LA1, and LA1 accepts it if it is possible. PVA stores LA1 ID as its children, and LA1 stores PVA ID as its parent.
- LA sends two communication requests; one for LA2, and another for MHA. In case nothing prevents this communication link from being constructed, then LA2 will have two children; LA2 and MHA. Consequently, LA2, MHA have LA1 as their parents.

- LA2 send request to BA, so the second one becomes a child of the first one. As a matter of fact, BA receives another request from MHA, as they have their buses interconnected. However, it chooses to refuse it, since it can have only one parent. Nevertheless, both of LA2 and MHA in this case, are always potential parents. What decides which agent will be accepted as a parent is simply the time of request reception. In other words, an agent accepts the first received request and reject all other coming next.
- The outcome of the remaining steps can be easily concluded; BA becomes a parent of LA3 and DGA becomes a child of MHA.

After the spanning tree is completed, the flow of information between the agents starts as depicted in Figure 5-3. Every agent sends its local system view to its parent, and when any agent receive view from its child it combines it with its local view and send a new data package to its parent. This procedure continues until a starting agent is reached. In fact, the starting agent can see the whole system view and can process the system information to issue commands to different agents in order to achieve system global goal. The content of messages and message format sent by a particular agent depends on the type of agent. All agents have to send their ID and type along with other information. The type of each agent is denoted by a letter, for example LA is denoted by 'L', and battery is denoted by the letter 'B' and so on. A description of messages sent by each agent is presented as follows:

- PVA sends available solar power P_{PV} , SOC of battery, total real Power P_G and reactive power Q_G capacities. The message format is <ID,PVB, P_G , Q_G , P_{PV} , SOC>

- LAs sends real and reactive power demand P_L , Q_L . The message format is $\langle ID, L, P_L, Q_L \rangle$
- DGA: real and reactive power capacity, breaker status (BRK), running time (RT),
The message format is $\langle ID, D, P_G, Q_G, BRK, RT \rangle$
- MHA: real and reactive power capacity, breaker status. The message format is $\langle ID, H, P_G, Q_G, BRK, RT \rangle$
- BA: SOC of battery, real and reactive power capacity. The message format is $\langle ID, B, P_G, Q_G, SOC \rangle$

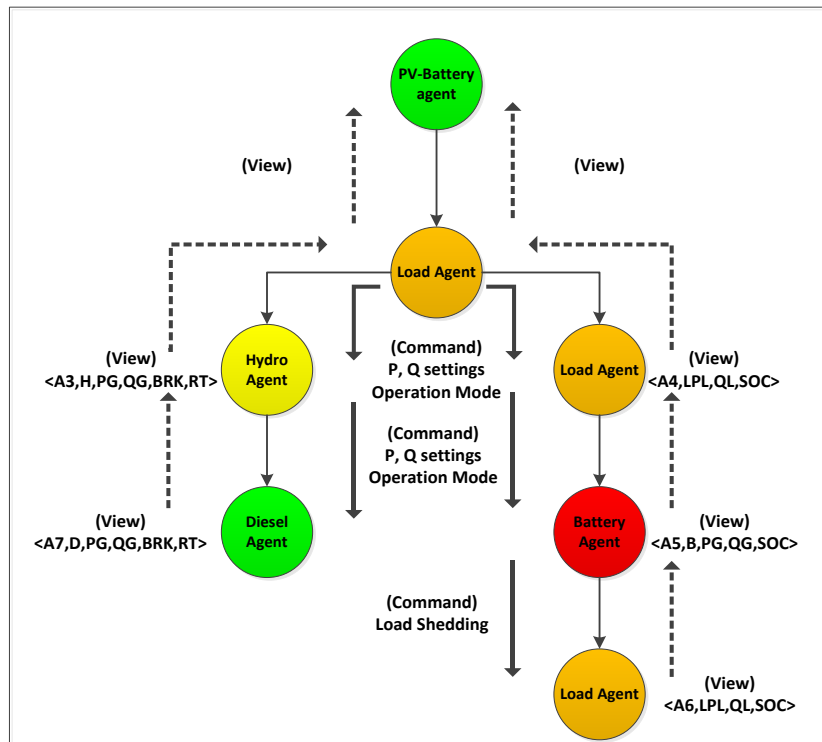


Figure 5-3 Information Flow between Agents

RT is necessary for handling unit commitment of diesel and MHP; it is not acceptable for the hydro station or diesel generator to start and stop repeatedly every short period. If the MHP or diesel generator is started and a load drop takes place right after that, then the

MHP or diesel generator will be used to charge batteries. In order to achieve this task, after each unit commitment the MHA and DGA start a time counter to let the starting agent know the running time and consider it. The previous message formatting enables the starting agent to identify every agent ID and type of agent, whether it is a load or generator. In case it is a generation agent, the starting agent has to know the type of generation. After that, the starting agent processes system information using EMS flow chart described in chapter 4, and sends commands to every agent and adds agent IDs at the starting of its corresponding commands. This is so that the receiving agents can extract the commands related to it, and this will be the third stage of communication. Assuming again that the starting agent is PVBA, the procedure for processing the system information and issuing commands are described as follows:

- Once PVBA has the complete system view, it conducts an online optimization process based on the flowchart illustrated in Figure 4-2 to obtain P, Q settings, mode of operation, and breaker open close command.
- PVBA merges all command in one message, and add agent IDs at the beginning of the commands corresponding to that agent
- PVBA passes the message containing all commands to its Child LA1, and LA1 searches for its ID and extracts the information that belongs to it and eliminates them from the message obtaining a new message.
- LA1 sends the new message to its child, and since it has two children (LA2 and MHA) it will send the same message for both of them. LA2 and MHA can search for their commands, extract them, and delete them.
- This procedure continues until the last agent receives its command.

Different types of agents receive different command packages due to their disparities in control requirements. For example, in addition to P and Q settings, PVBA receives inverter mode of operation (PQ or VSI). In general, all generation agents receive breaker open/close commands to allow MAS to isolate any generation unit if required. The commands formats for the different types of agents in the system are as follows:

- PVBA receives P, Q settings, inverter mode of operation (MOD) breaker open/close command (BRK). The package sent to PVBA from starting agents has the following format <ID,P,Q,MOD,BRK>

- LAs receive the same values of P and Q that were sent by them. In case load shedding is required, the amount of required load shed is cut from the original P and Q values and sent to LA. The message format is <ID, P, Q>

- BA receives P, Q setting, MOD, charging/discharging mode selection (MOCH), and BRK. The message format is <ID, P, Q, MOD, MOCH, BRK >

- MHA and DGA receive P, Q setting, and BRK and their commands are arranged in the following format <ID, P, Q, BRK>

Once every agent receives its commands, it will send them to their corresponding control system, and this will be the end of the three stages or sweeps of communication. This procedure is continuously repeated to keep EMS updated. Important issues regarding the previous procedure have to be highlighted which are the possibility of failure in completion of the spanning tree or information flow and the impact of this failure on the system. In fact, communication failure is probable, and this may cause one agent or group of agents to lose the communication of the system, and if they have no alternative

communication path, this will lead to incompleteness of flow information process. With lack of information the starting agent will not be able to have the right decisions. An alternative plan has to exist to deal with such situation. In this case, adaptive communication and zonal control is introduced to fix this problem.

5.5 Zonal Control

First of all, we have to explain how an agent can recognize that it is a starting agent. In fact, the agent with no parents can realize that it is a starting agent. After the spanning tree construction stage or information flow stage, more than one starting agent can be found, this will be due to partial failure in the communication network. Any starting agent has to process whatever information it receives and issue proper commands for other agents in contact. This means that the communication system is dynamic and adaptive, and if more than one starting agents exist in the system this means that the management system is divided into zones. The group of agents contained in each zone act based on partial information they have and construct the best possible operation plan. The complete system view in this case will not be available for any starting agent, so the operation schedule will not be optimal. Nevertheless, the MG will be running in suboptimal operation until the communication system is recovered. The communication failure is not the only case that requires zonal management and control; a fault can occur in some feeder or at a particular bus. This will cause the breaker to operate and isolate parts of the system from the others. In that case automatic zonal formation is very useful as it provides an alternative temporary plan for MG management. However, there are a number of limitations and constraints faced by zonal control. Among these limitations, we can mention the type of agents contained by a particulate zone. If all of the agents in the

zone are of generation type or load type then those agent are out of options and no proposed plan is available. Nevertheless, the opportunity for this case to happen becomes less as MG becomes larger and the number of agents increases. Moreover, avoiding the similarity of adjacent agents (neighbor agents) will minimize or even eliminate the possibility of having zones out of plans. There is another issue to care about when applying zonal control which are the voltage and frequency reference. Since MG is operated in SMO, and as zones are caused by either power failure, communication failure or both, then there should be something to indicate the reason of zone formation; this is because when there is a fault isolating the zone from the source that's providing the voltage reference, then the agents within the zone have to manage themselves in order to provide their own voltage reference. On the other hand, if there is no power isolation and just communication isolation, then the objective of control would be only load/generation balance in zone. Due to the small size of proposed MG and number of agents there will be not much options or alternative plans for zonal control, so, a single scenario will be simulated to show the validity of this proposed approach. The case that is going to be simulated is when BA loses communication with LA2. In this case BA will search for an alternative communication path. Fortunately, MAS enables the agent to search online for other agents. In our system BA will find MHA and send a communication request, and if the link is successfully built, then the problem is solved and everything is back to normal. However, due to some reason the connection could not be established between BA and MHA, or we can assume that there was no physical communication channel between the two agents in the first place. In this situation, BA will process the system view it has which is in this case BA generation capacity with SOC and load demand received from

LA3. Suppose that BA is not capable of supplying the whole load demand at bus 6. In that situation BA instructs LA3 to curtail part of the load. The remaining part of the complete system will act based on the information they have. MG might not be operated optimally under such conditions, and possibly the battery at bus 5 was supposed to be charged at the time of isolation.

5.6 Interfacing MAS with MG network Model

As previously mentioned MAS is developed in JADE, while the model for MG including different generation systems models, load model, and controllers' model etc. are implemented in SIMULINK environment. The agents need not only to communicate with each other, but also to exchange information with system resources which are in this case the loads, and generators with their control system located at different buses. In other words a mean of communication between JADE and Simulink is required to allow bidirectional information flow as in Figure 5-4. For that purpose UDP ports are used to link each agent with its corresponding bus as illustrated in Figure 5-5. A single UDP port is assigned to one particular agent to exchange data between SIMULINK model at one bus and one JADE agent. In order to manage the information flow between SIMULINK and JADE, a MATLAB code was generated to receive data from SIMULINK via 'listeners' every specific time and send them to JADE through UDP socket. Once all agents in JADE receive their data they will start internal information exchange, and whenever they receive the commands they upload it to their dedicated UPD sockets. Then MATLAB will read the content of UDPs and apply them to SIMULINK by modifying the model parameters. In addition to managing and organizing information exchange, the

developed code generates a graphical user interface (GUI) which enables user to monitor the different system measurement such as RMS voltage, frequency, and loads. In addition, the GUI plots the waveforms of the output real power for each type of generator. At the same time, it plots the voltages and currents waveforms at any bus. Moreover, GUI gives the user the option to change the load and the sun irradiance to examine the impacts of these changes on the system and how EMS responds to them. A snapshot of GUI is shown in Figure 5-6.



Figure 5-4 Data Exchange between Simulink and JADE

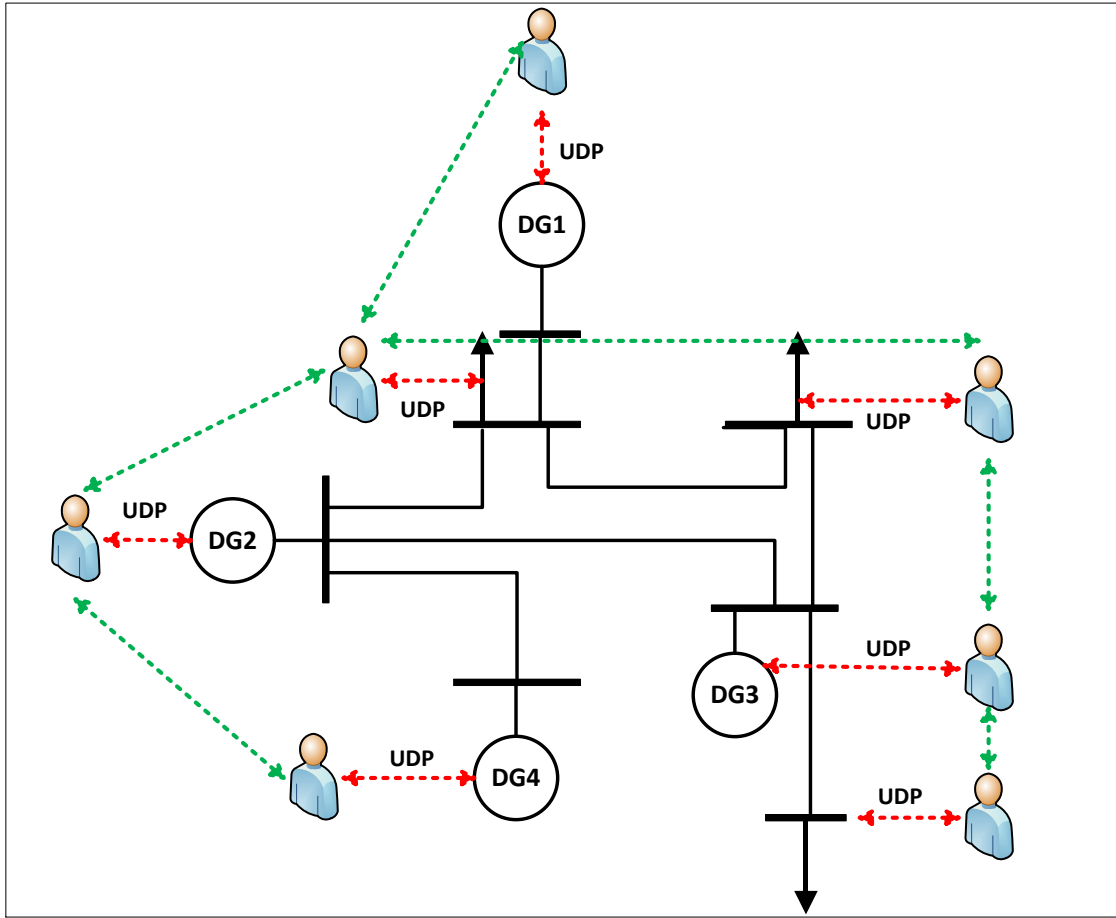


Figure 5-5 Interfacing Agents with MG Buses through UDP Ports

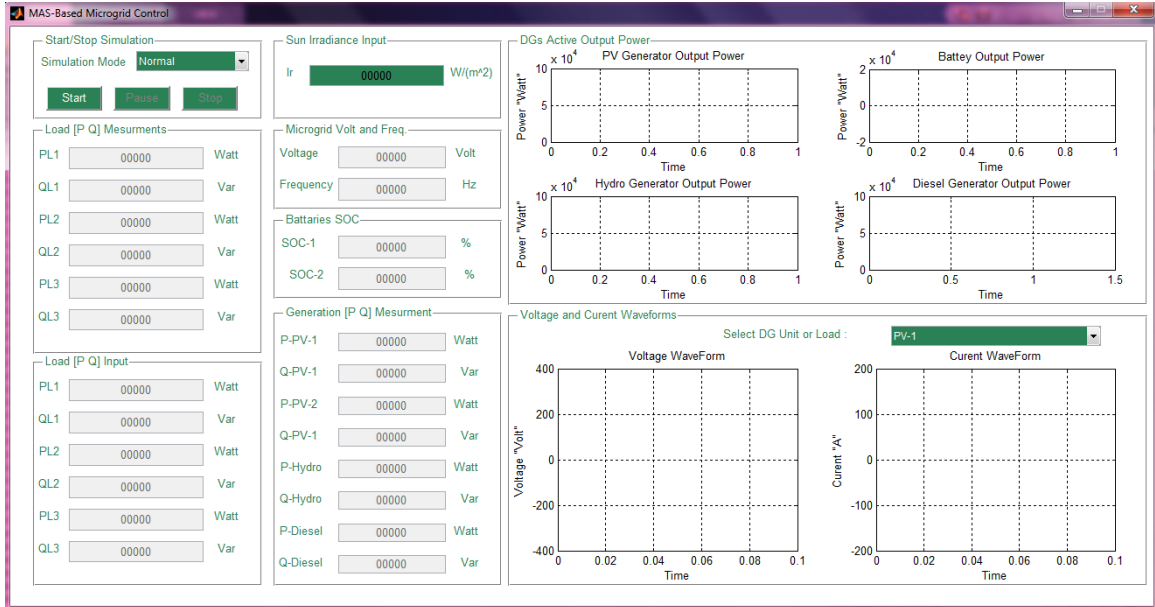


Figure 5-6 MATLAB GUI

CHAPTER 6

RESULTS AND DISCUSSION

In order to test the proposed control and management strategy, MG power and control circuit models were built in SIMULINK environment. The MAS was created in JADE by generating the required Java code. In order to verify the validity of the proposed system, first, 24 hours generation schedule is obtained for the different days in the year using online EMS described in Figure (4-2). The next step in testing the system is to check the functionality of interface between Simulink and JADE, and show that controllers can execute the commands received from MAS.

The data for MH generation and diesel generation are show in Appendix A

6.1 Simulation of Power and Control Circuits

In this section, Simulink model, controller parameters and gains with some simulation results for EI-DGs (PV, battery) and Inverter are shown.

6.1.1 Simulation of Battery Controller

The model used for battery is built in SIMULINK environment. The circuit of bidirectional converter was implemented using discrete elements including IGBT, diodes, capacitor and inductor. The controller of the converter was also built from discrete blocks including PI controllers and summing junctions. The complete SIMULINK model composed of battery, bidirectional converter, and voltage controller is shown in Figure 6-1.

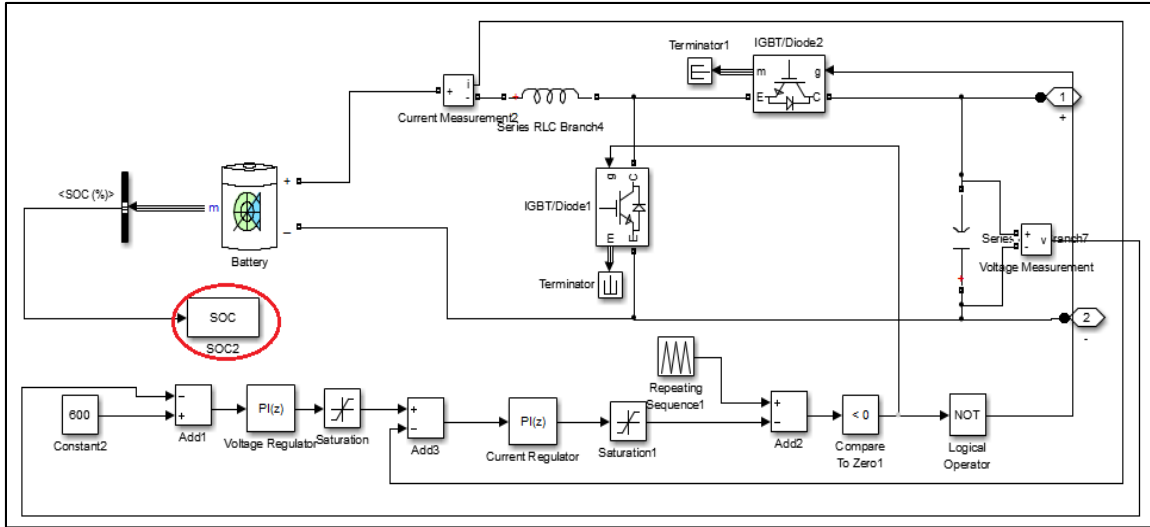


Figure 6-1 Simulink Model of Battery with Charging/Discharging Controller

As mentioned before, there are two batteries in the system; one is connected parallel with PV panel, and the other is working alone. Here the standalone battery is simulated. The simulation parameters are shown in Table 6-1. The battery controller is expected to maintain DC voltage at capacitor at constant value for variable loads. Figure 6-2 depicts the voltage at capacitor link. While Figure 6-3 shows the current drawn from battery. Initially resistive load of $100\ \Omega$ was connected at output terminals, and at time 0.8 sec the load was doubled by reducing the resistance to half. As expected the controller was able to restore the DC voltage to nominal value (600 V). We can observe the increase in the load by looking at current plot. The current drawn by battery was stepped up indicating a load stepping up. The block named 'SOC2' is used to send SOC value to work space so MATLAB m file can read it.

Table 6-1 Simulation Parameter for Battery and its Controller

Parameter	Value
Battery nominal voltage	280 V
Rated Capacity	285 Ah
Nominal Discharge Current	75 A
Reference DC voltage	600 V
DC link Capacitance	3000 μ F
Battery coil inductance	1 mH
Voltage regulator proportional gain	1
Voltage regulator integral gain	10
Voltage regulator proportional gain	1
Voltage regulator integral gain	20

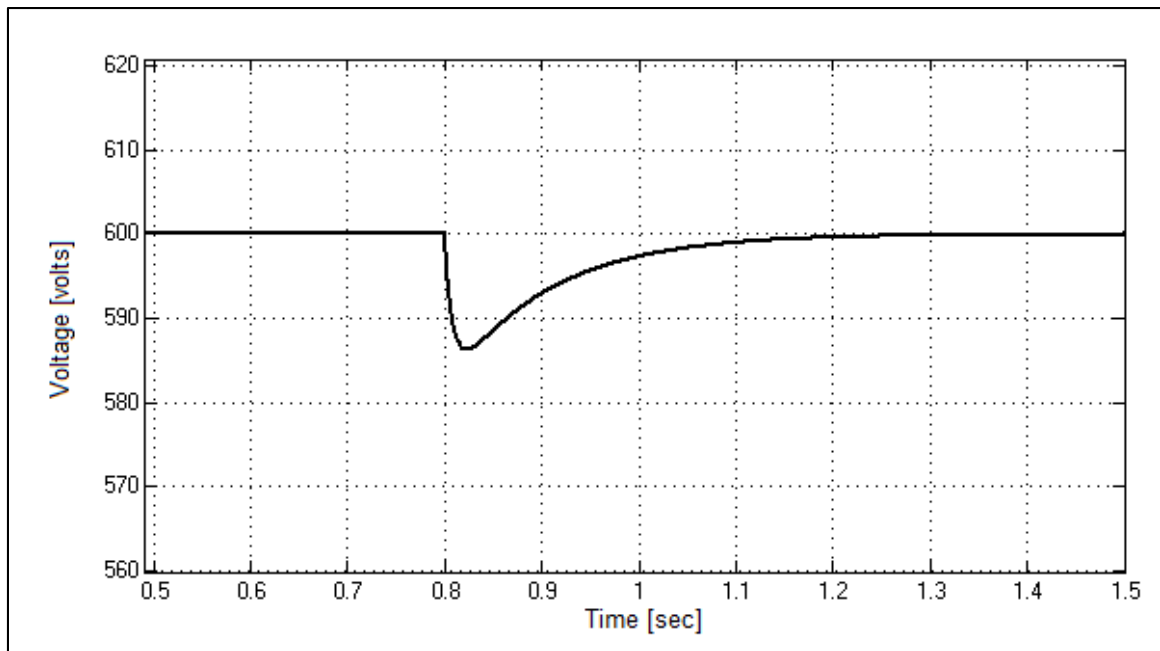


Figure 6-2 Plot of Battery DC link Voltage

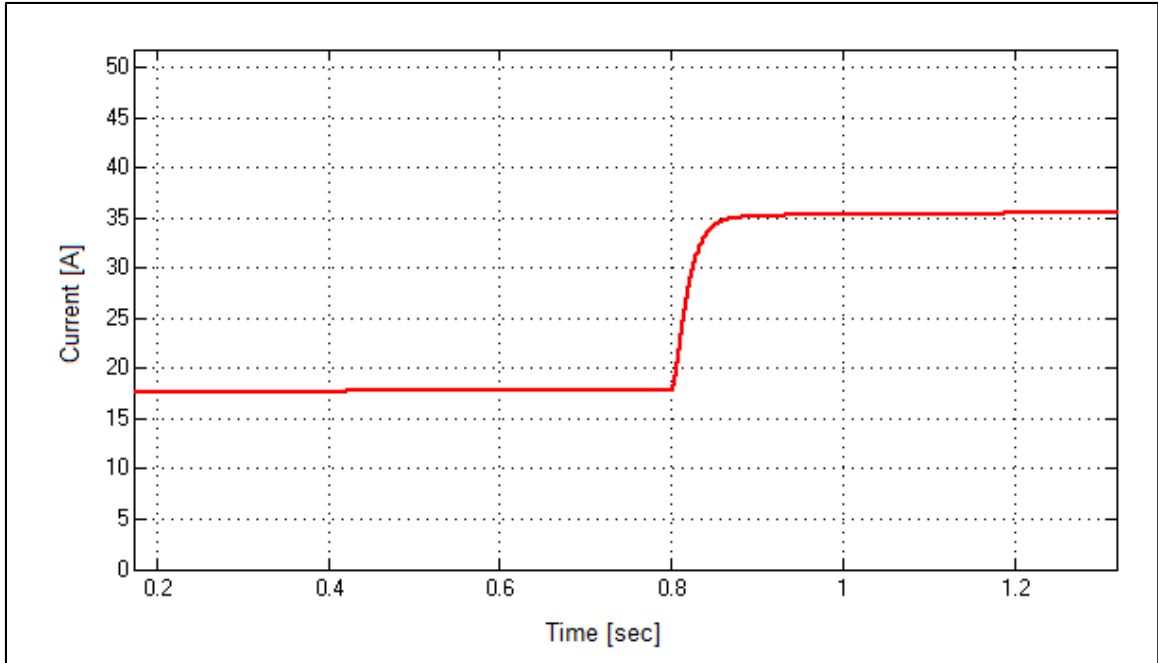


Figure 6-3 Plot of Battery Current

6.1.2 Simulation of PV model and MPPT controller

The PV model is built using algebraic equation (3.6)-(3.10), and the boost converter circuit is assembled from discrete electrical components. MPPT controller is developed with reference to Figure 2-2. The complete system model consisting of PV panel, boost converter and MPPT controller is exposed in Figure 6-4. The simulation parameter is shown in Table 6-2. In order to test MPPT controller, different values of irradiance are inputted to PV module and the PV output power is obtained. Figure 6-5 shows plots for irradiance, extracted solar power, and PV DC voltage. MPPT keep tracking the maximum power by searching for V_{mp} value and force the PV output voltage to follow that value, and as the PV voltage keep changing, the DC link voltage is also changing. However, DC link voltage must kept constant at reference value in order for the inverter to work

properly. Therefore a battery is connected in parallel with PV array to regulate the DC voltage.

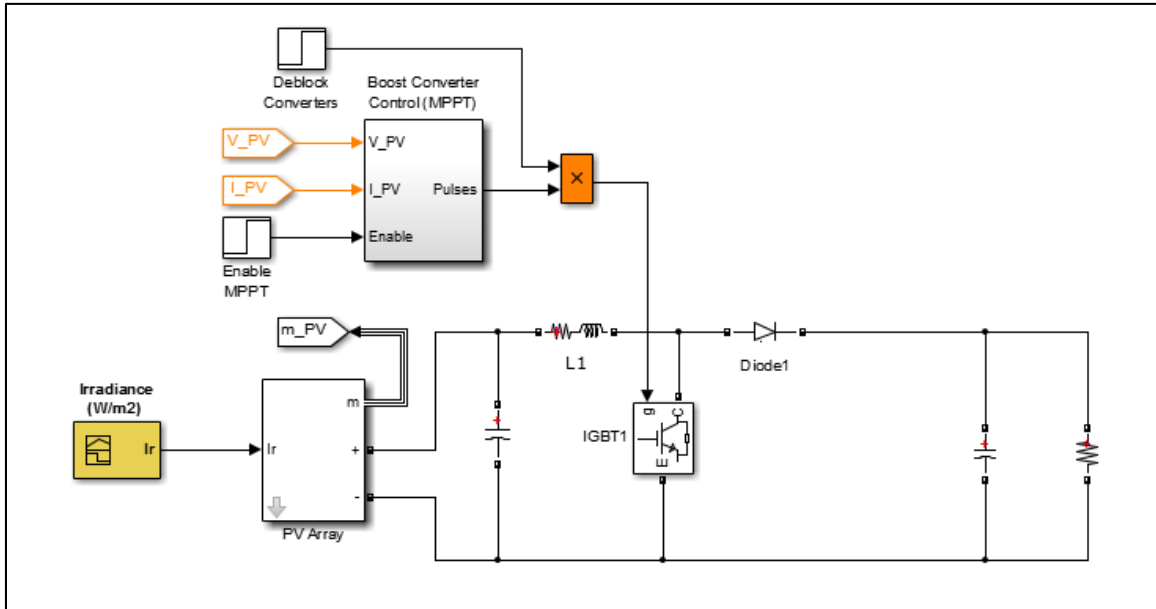


Figure 6-4 SIMULINK MODEL of PV and MPPT

Table 6-2 Simulation Parameters of PV model

Module open circuit voltage, V_{oc}	64.2 V
Module short circuit current, I_{OC}	5.96 A
PV array rated output power	100 KW
PV array open circuit voltage, V_{OC}	500
PV array Short circuit current, I_{OC}	400 A
Number of module in series	8
Number of modules in parallel	42
PV capacitor	100 μ F
DC link Capacitor	600 μ F
Boost converter inductance	5 mH

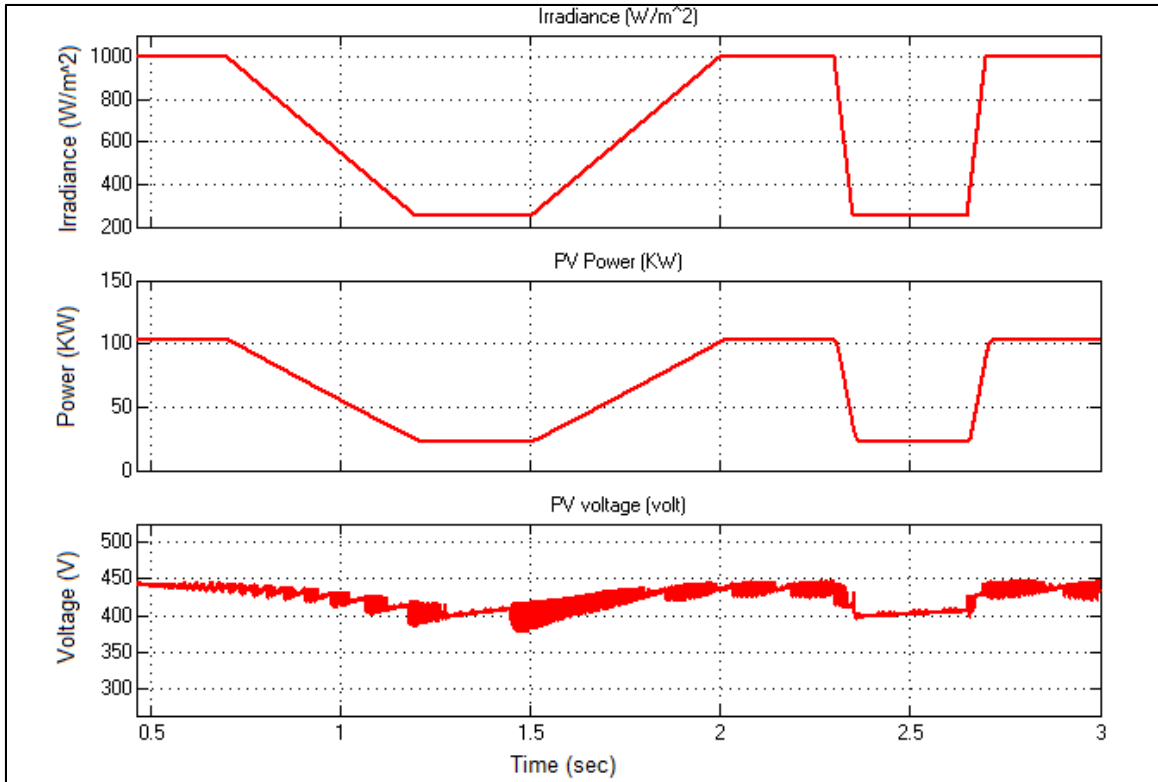


Figure 6-5 Plot of irradiance, PV Power, and PV Voltage

6.1.3 Simulation of Inverter

The complete simulation model for Inverter is illustrated in Figure 6-6; it is composed of six IGBTs, LCL filter, PQ controller, droop controller, voltage controller, current controller, and PWM generator. The block with name 'PVmode' receives its parameter value from MAS to set the mode of operation for inverter (PQ inverter or VSI). Figures (6-6)-(6-8) depict voltage controller, and current controller respectively. The controllers gains and the simulation parameters are illustrated in Table 6-4. When inverter is working in standalone mode it must be controlled as VSI to maintain voltage and frequency at nominal values. A resistive load of 10 KW was connected to inverter and VSI was simulated to obtain load voltage and current waveforms. Figures (6-9)–(6-10) show plots of load voltage and current respectively. At time =0.5 sec, step load change of 10 kW was applied and as result the current increased while the voltage remained unchanged.

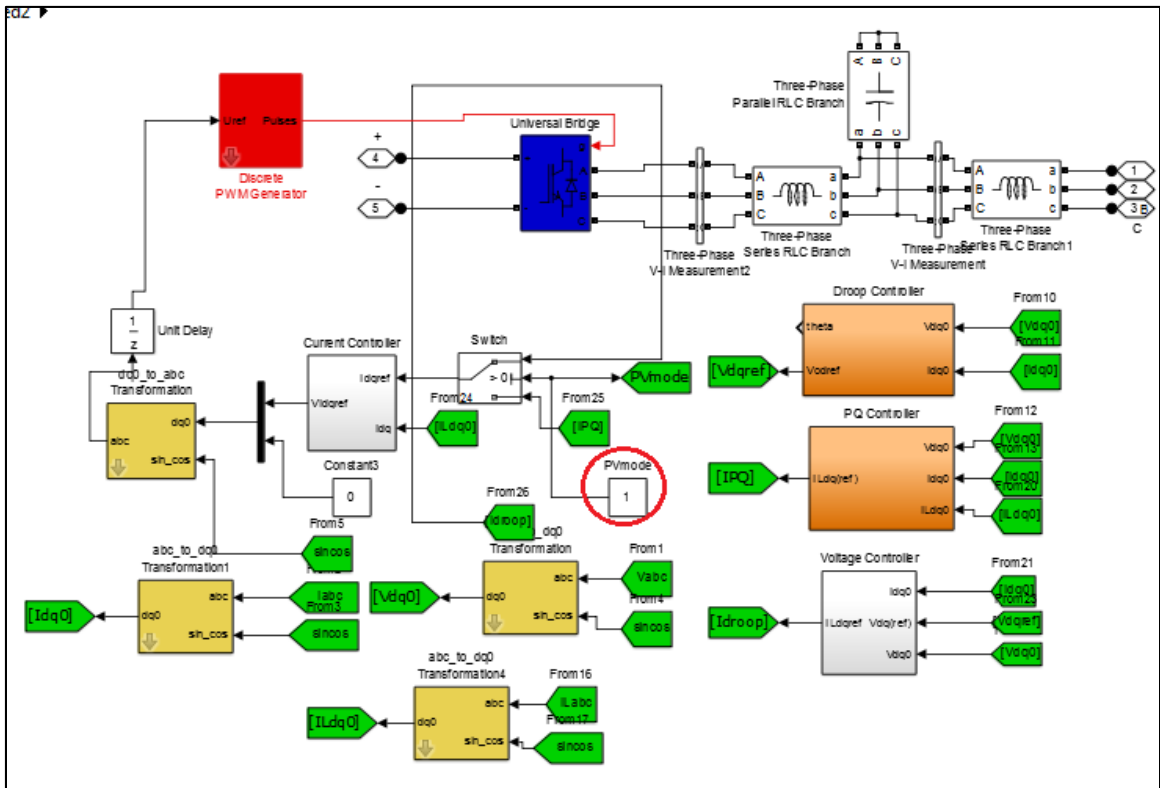


Figure 6-6 Simulink Model of Inverter and its Controllers

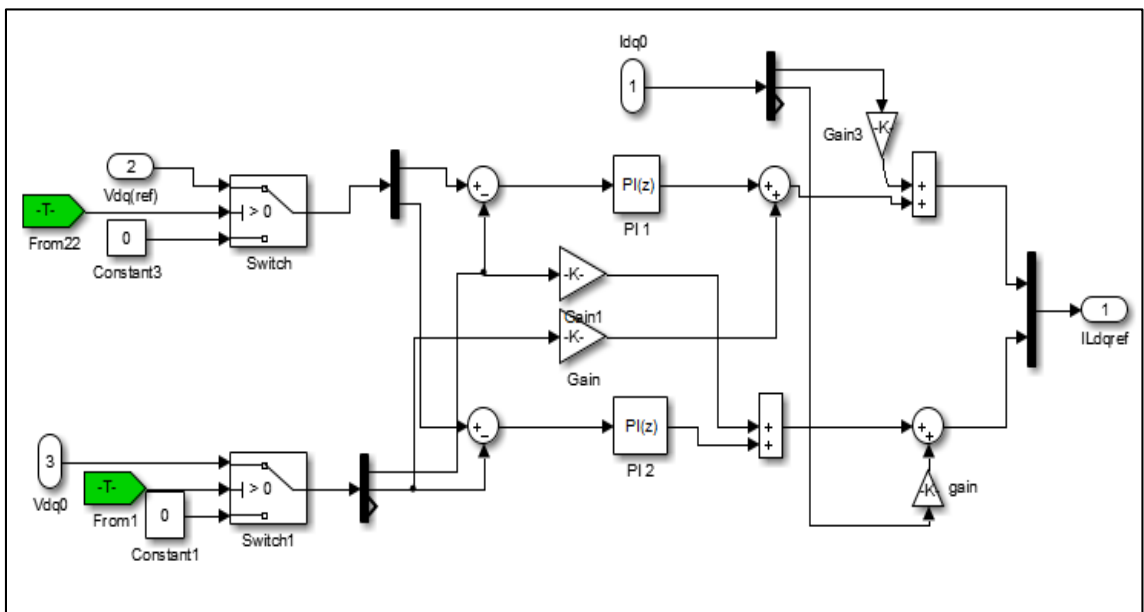


Figure 6-7 Simulink Model of Inverter Voltage controller

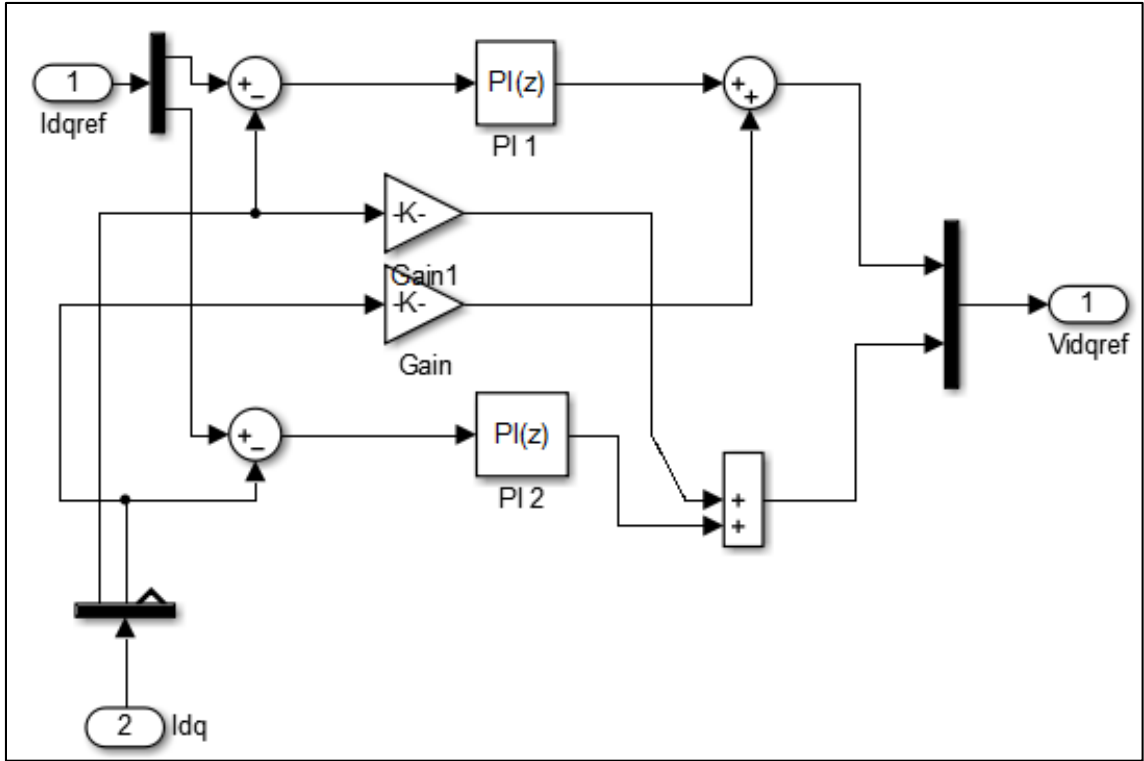


Figure 6-8 Simulink Model of Inverter Current Controller

Table 6-3 Inverter Test Parameters

Parameter	Value	Parameter	Value
f_s	10 KHz	m_p	-9.4×10^{-5}
L_f	1.35 mH	n_q	-1.3×10^{-3}
C_f	50 μ F	K_{pv}	0.05
r_f	0.1 Ω	K_{iv}	390
L_c	0.35 mH	K_{pc}	10.5
ω_c	31.41 rad/sec	K_{ic}	16000
r_{LC}	0.03 Ω	F	0.75

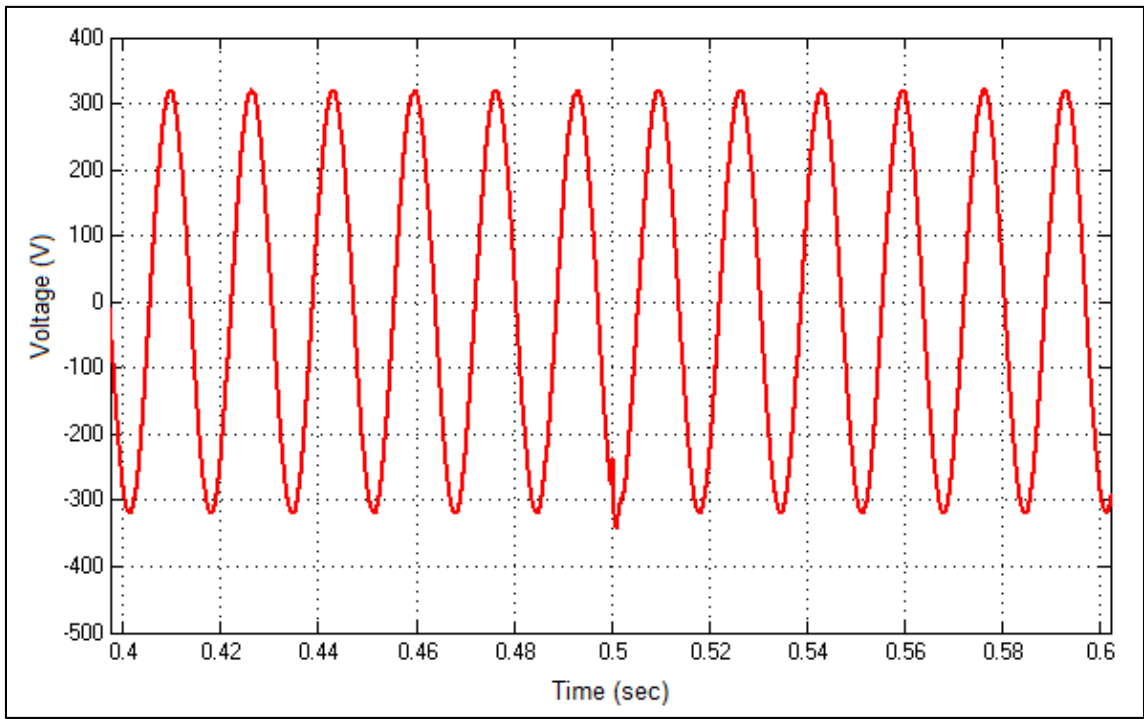


Figure 6-9 **Load Voltage Waveform**

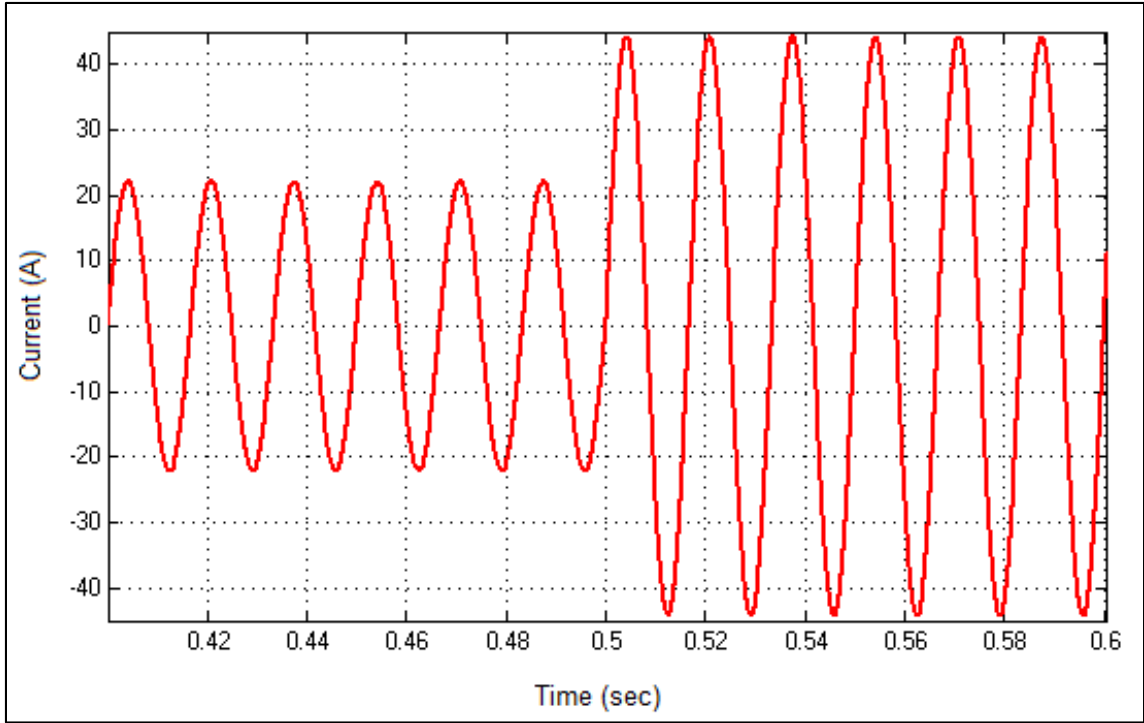


Figure 6-10 Load Current Waveform

6.2 Online Optimal Generation Schedule

24-hour generation schedule for June, 1st was obtained using online EMS. The optimization process was executed hour by hour. The data for solar irradiance were obtained via internet using the longitude and latitude coordination of Wadi Baisha dam where MH plant is supposed to be constructed. The solar irradiance data for a typical day in June are shown in Figure 6-11. The optimal daily generation schedule is illustrated in Figure 6-12. It can be noticed that MH alone completely electrify the load during night time, and early morning hours. While PV is able to autonomously supplying the total load from hour 12 to hour 17 during day time. BSS is charged when PV power is greater load demand, and discharged when PV power fall below load demand. In this case, the contribution of BSS is not great as the durations where PV power exceeds load demand

are short, and surplus power is small. However, this not the case always and the contribution of BSS can vary from season to another and even from day to another in the same season can noticed in Figure 6-14 which exposes the generation plan for another day in January. Obviously, the contribution of BSS is greater than previous one. The amount of stored power is considerable, and by discharging this power the amount of generated power by MH is diminished. BSS helps eliminating wasted power and saving water supply. The power contribution from different types of generation is shown in Table 6-4, while total energy supplied from different type of generators are depicted in Table 6-5. From the previous two cases it can be concluded that BSS is charged from PV power and never charged by MH. From cost perspective this seems to be logical. However, charging BSS from MH will lead to reducing working hours of MH which can beneficial in more than one way. Since reducing running hours of MH is accomplished by charging BSS from MH, low level MH generation is avoided in most hours increasing the efficiency of MH. Moreover, assuming that the discharged water is used for irrigation purposes, then it is better to have larger flow rate. Figure 6-15 shows the generation schedule for the same day as previous with reduced MH operational hours. Clearly charging BSS from MH yields to reducing MH working hours significantly. In addition to, the generation level of MH is increased. None of the previous case required committing diesel generator. However, during cloudy days, PV power is significantly reduced, and if MH cannot compensate for the power mismatch, then diesel generator must be operated. In spite the fact that the generation capacity of MH matches the load peak, the total energy that can be obtained from MH is limited by the potential energy of the water required for irrigation for one day. If there were no limitations on MH

generation, then there would be no need for PV in the first place. But PV was installed to support MH in electrifying the load. Another case where diesel is needed to be running is when a technical failure MH plant or irrigation system occurs. In that situation diesel has to back up the system.

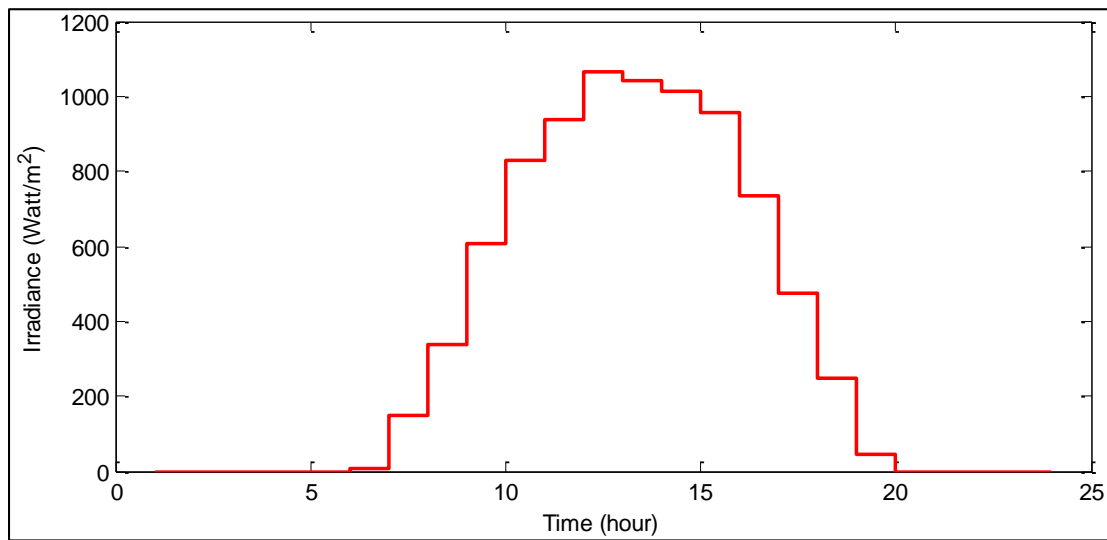


Figure 6-11 Solar Irradiance Curve for a Typical Day in summer

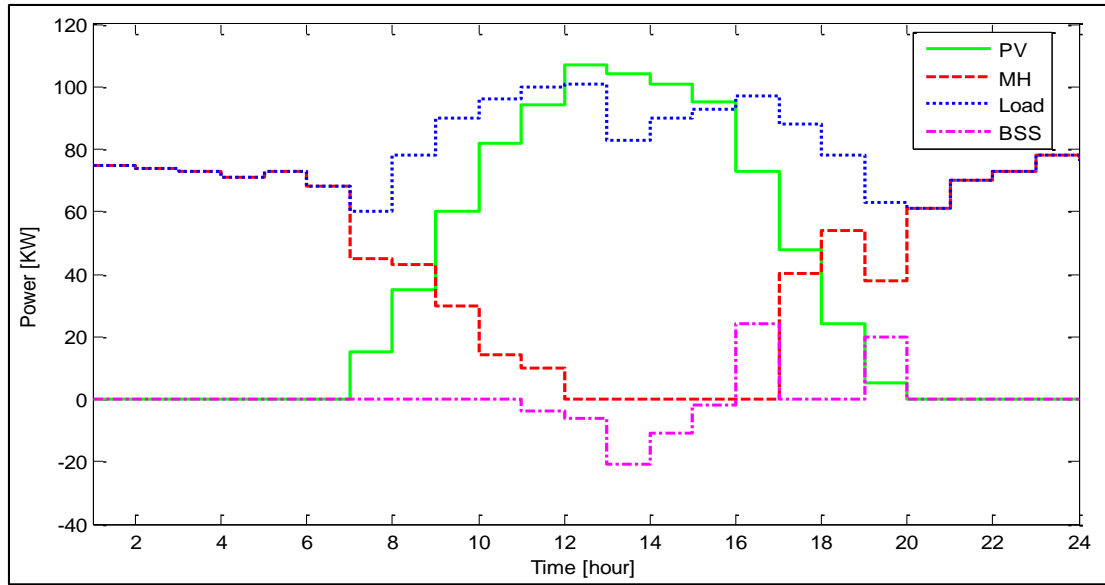


Figure 6-12 24 hours Generation Schedule for June, 1st Obtain from EMS

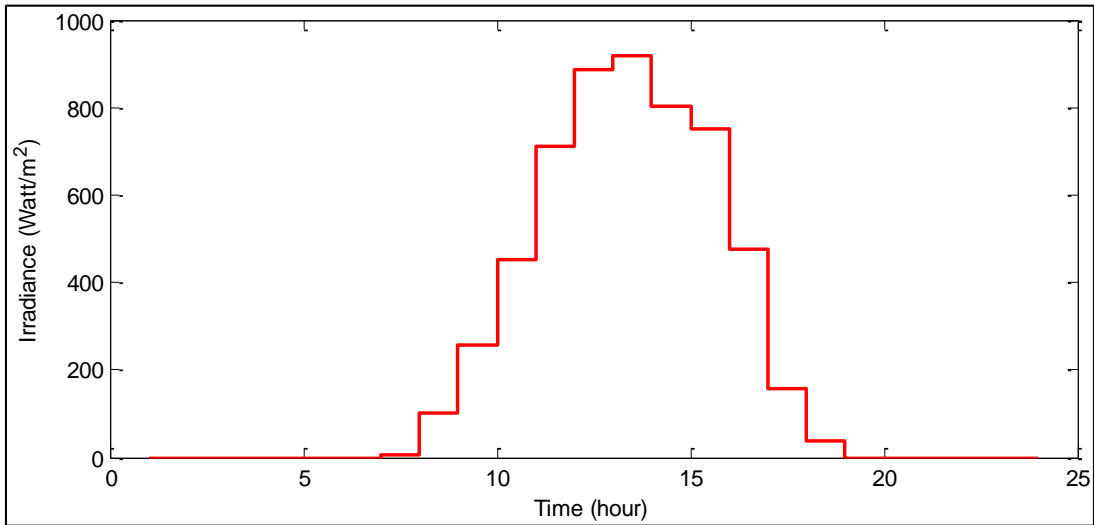


Figure 6-13 Solar Irradiance Curve for a Typical Day in winter

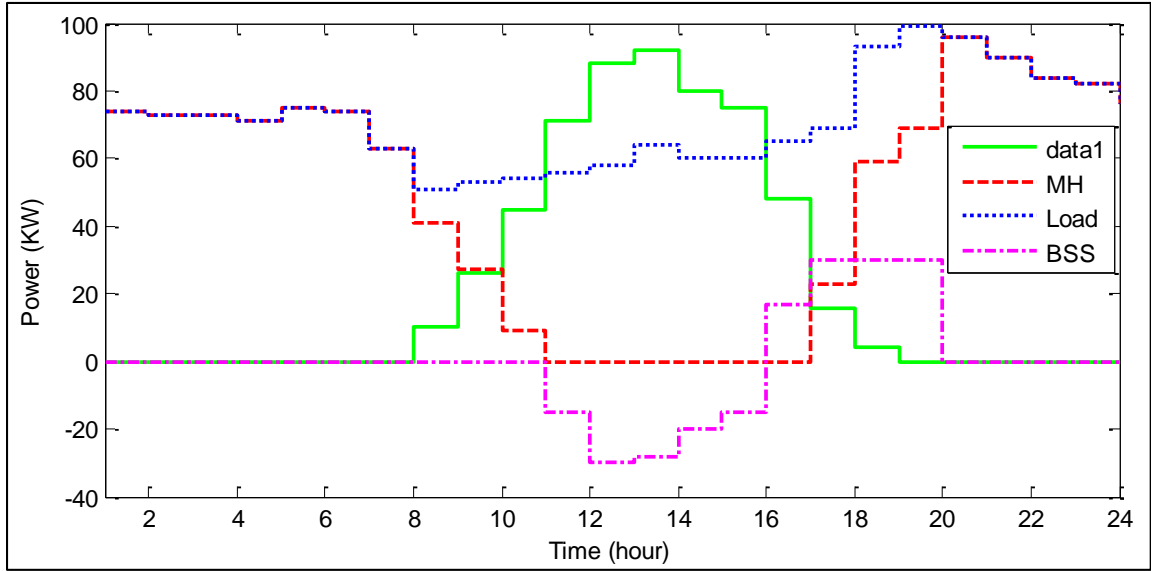


Figure 6-14 24 hours Generation Schedule for Jan, 1st Obtain from EMS

Table 6-4 Power Contribution Percentage from Different DGs

Hour	Power Contribution Percentage		
	MH	PV	BSS
1	100	0	0
2	100	0	0
3	100	0	0
4	100	0	0
5	100	0	0
6	100	0	0
7	100	0	0
8	80	20	0
9	51	49	0
10	17	83	0
11	0	127	-27
12	0	152	-52
13	0	144	-44
14	0	133	-33
15	0	125	-25
16	0	74	26
17	34	23	43
18	63	5	32
19	70	0	30
20	99	0	1
21	100	0	0
22	100	0	0
23	100	0	0
24	100	0	0

Table 6-5 Total Energy Supplied from Different DGs in One Day

Total Load Energy (KWh)	Total MH Supplied Energy (KWh)	Total PV Supplied Energy (KWh)	Total BSS Supplied Energy (KWh)
1713	1158	462	93

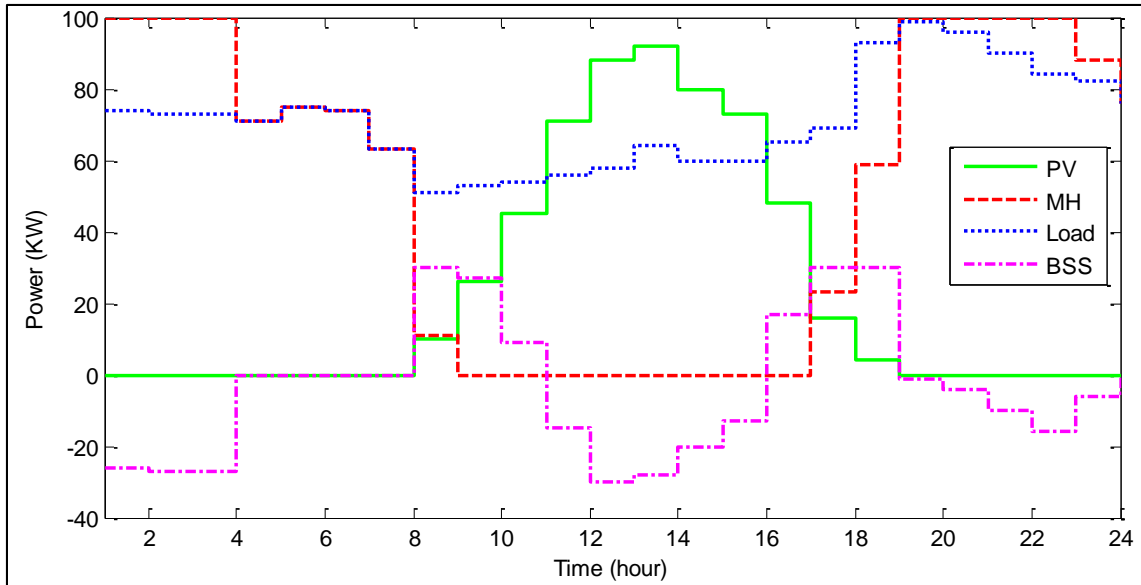


Figure 6-15 24 hours Generation Schedule for Jan, 1st Obtain from EMS with Reduced MH Working Hours

6.3 Simulation of MAS

Seven agents were created in JADE by generating Java code for each one, Each agent is represented by Java class and it is programmed to achieve set of goals. All agents were started in one container on the same PC. Although in reality, every agent will be located on remote host, for purpose of simulation it is enough to use one PC so the agents use local host IP to communicate. The modification required to work on multi-platforms is simplified by the option of searching online available in JADE. Once the agent created the GUI is launched showing the agents names as in Figure 6-16. The agents were given the names DG1-DG7. After building the agent they start the first sweep of communication to form the spanning tree as illustrated in Figure 6-17. At this stage, agents exchange messages with template type of REQUES and AGREE. Agent DG5 in particular, receives two request messages; one from DG3 and another from DG4. It chooses to agree on the request from agent DG4 and refuses the request from DG3. In the

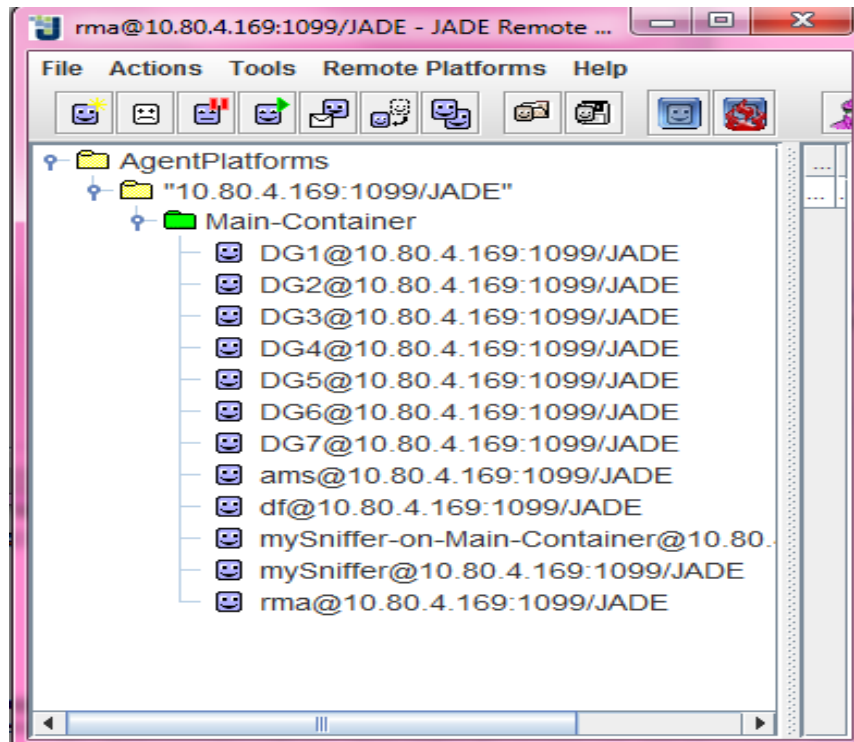


Figure 6-16 Snapshot of JADE GUI Showing Seven Agents created in Main container

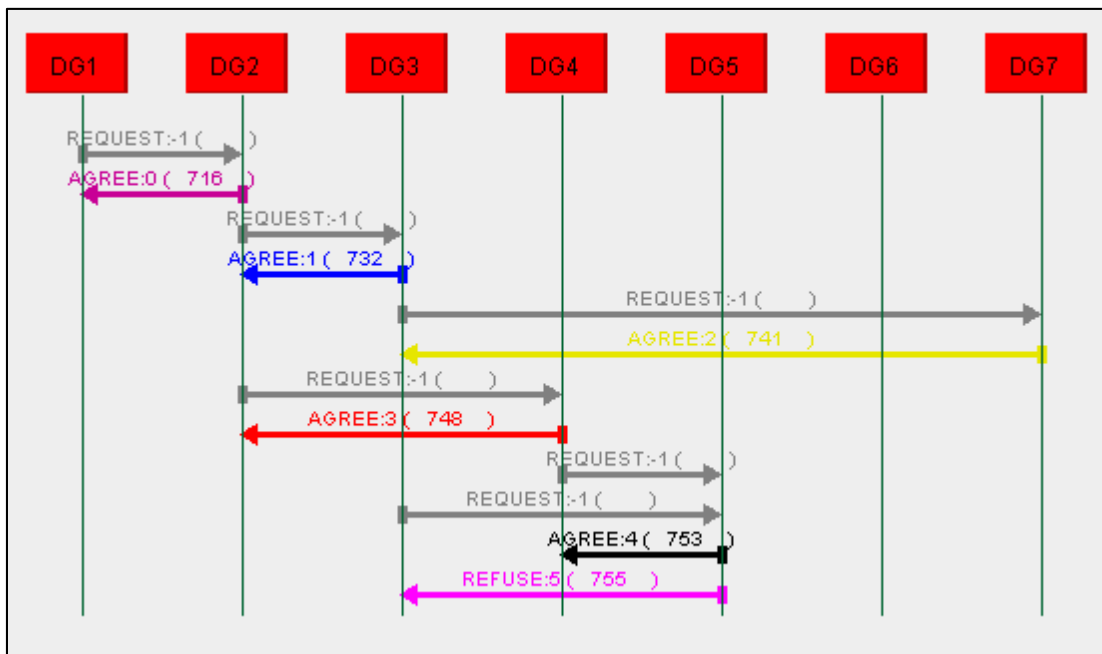


Figure 6-17 Snapshot from JADE Sniffer during Construction of Spanning Tree

After the completion of the first sweep, every agent knows its child and its parent. The results are shown as follows:

```
DG2 has Parent DG1@10.80.4.169:1099/JADE
DG1 has right child DG2@10.80.4.169:1099/JADE
DG3 has Parent DG2@10.80.4.169:1099/JADE
DG7 has Parent DG3@10.80.4.169:1099/JADE
DG 2 has right child DG3@10.80.4.169:1099/JADE
DG3 has right child DG7@10.80.4.169:1099/JADE
DG4 has Parent DG2@10.80.4.169:1099/JADE
DG 2 has left child DG4@10.80.4.169:1099/JADE
DG5 has Parent DG4@10.80.4.169:1099/JADE
DG4 has right child DG5@10.80.4.169:1099/JADE
```

The general structure of the agent name inside JADE environment has the format of:

<Local Name@IP address>

Next, in second sweep, the agents start flowing information and sending their local view (as received from MATLAB) of the system to their parents as shown in Figure 6-17.

When the starting agent has the complete view of the system it will process the information, take decisions, and issue the proposer commands. The information starts flowing in opposite direction of that for the second sweep (from parent to child). When any agents extract its information from the received message it sends it to MATLAB via UDP socket. MATLAB then, forward the information to controllers built in SIMULINK.

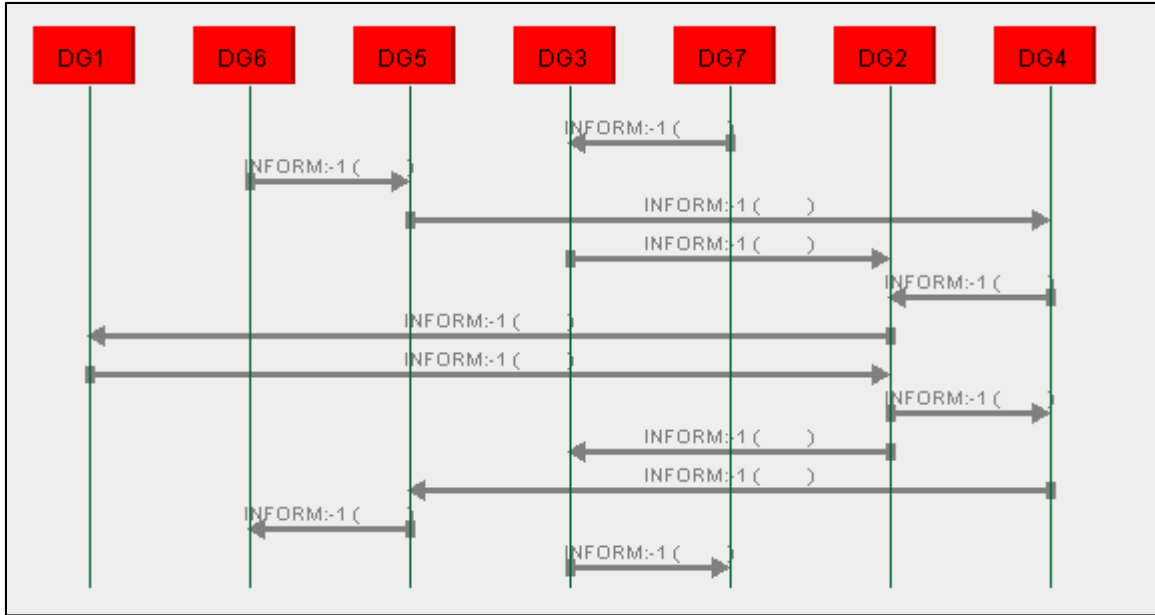


Figure 6-18 Information Flow between Agents

6.4 Simulation Complete Control and Management System

In order to simulate the two layer control (MAS and Local controller), Simulink and JADE are started together. JADE receive measurement and status signal from Simulink which represent the physical electrical network. Each bus in Simulink is bonded with on agent in JADE and the exchange information via UDP. To test the system capability of operating MG with minimum cost by maximizing the utilization of RES and BSS, the generation schedule was obtained for varying load and irradiance. The system was tested for different scenarios. In scenario 1 PV and BSS are autonomously supplying the load, and MH is committed at the end of simulation period. In the second scenario MH forms the grid and PV follows the grid. At the end of end of this scenario MH will be shut down leaving PV and BSS alone. In the third scenario interactive operation for diesel generator and PV generator are simulated. In summary the three scenarios are

Scenario 1: PV-BSS working autonomously and MH is committed when necessary

Scenario 2: MH generator is operated in parallel with PV-BSS and shut down when PV-BSS can supply the load

Scenario 3: The diesel is committed to back up PV-BSS system and shut down when no longer required

6.4.1 Simulation of Scenario 1

The sun irradiance curve is illustrated in Figure 6-19. The output of PV power, MH Power, and BSS were obtained as depicted in Figure 6-20. As can be seen from the plot, when the available power from PV exceeds the total connected load, the MAS send charging command to batteries along with the amount of charging power, and when PV power falls below the load, MAS instructs batteries to start discharging. The load continues to increase until it exceeds the maximum power from PV and batteries. At this point MAS decides to commit MH to compensate for the mismatch. When the MH is started PV inverter switches from VSI to PQ inverter. The load then increases further and so does the output of MH. Figure 6-21 shows the current of PV inverter when it starts to decrease at time =15 sec due drop in sun irradiance. The transient in PV inverter voltage when switching to PQ mode is exposed in Figure 6-22. Figures 6-23 and 6-24 are the plots of DC current for BSS-1 and BSS-2 respectively. The negative current indicates that the battery is charging. While positive current means that battery is being discharged. There three state of operation for BSS; off state, charging state, and discharging states. Figure 6-25 shows current during different transitions. Finally Figure 6-26 depicts the load current at bus 6 during load stepping up. In fact, in order to bring MH generator

online, the voltage of MH generator must be synchronized with MG voltage. So, the MH should be started first without closing its breaker, and after synchronizing is completed the breaker can be closed. In the simulation, since MH response is slow, it is kept running at low load without closing the breaker, and at the moment when MAS instruct MH to start up synchronization can be completed fast. Although in practical this not the case, here, since the simulation period is only few seconds, it was allowed for purpose of simulation only. As explained before the MG is running in SMO mode and when PV-BSS system is running autonomously then PV inverter acts as VSI and be responsible for regulating voltage and frequency of the MG. Figure 6-27 shows short term load following by PV inverter for fast changing load. When the MH generator is connected it regulates the frequency and follow load changes in short term as depicted in Figure 6-28.

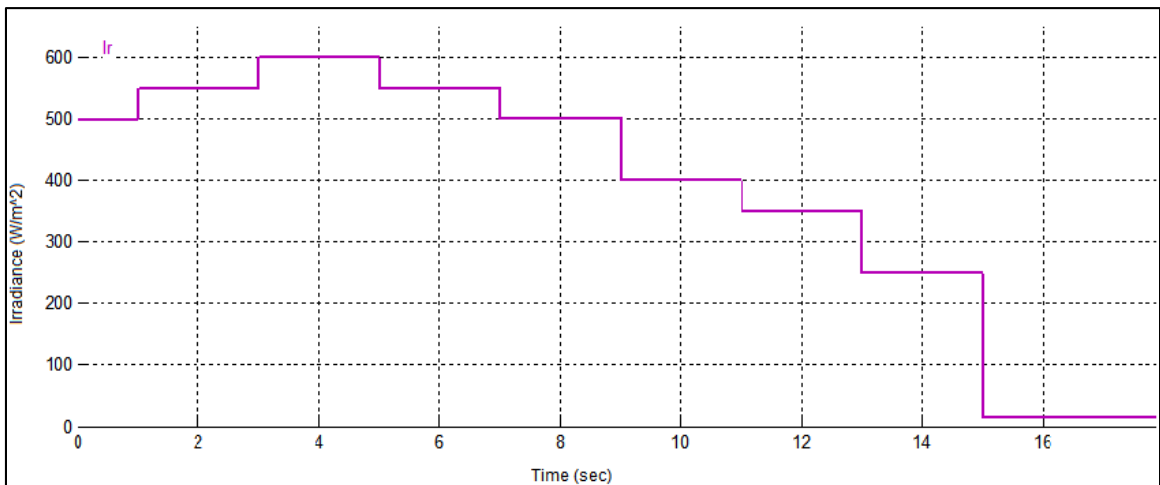


Figure 6-19 Irradiance Curve for Scenario 1

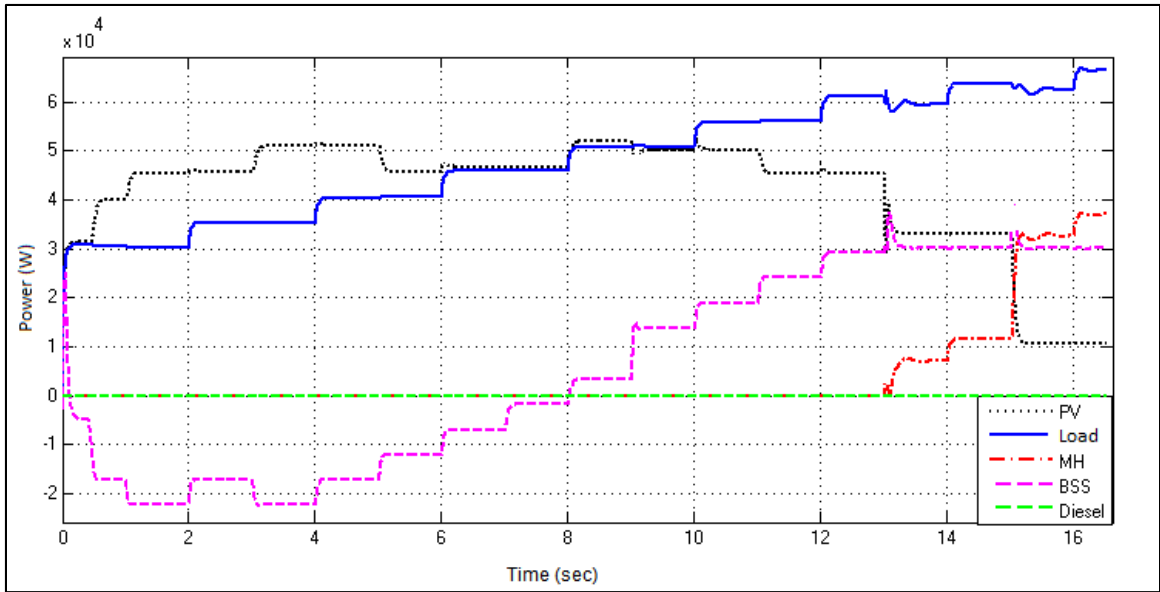


Figure 6-20 Generation Schedule using MAS for Scenario 1

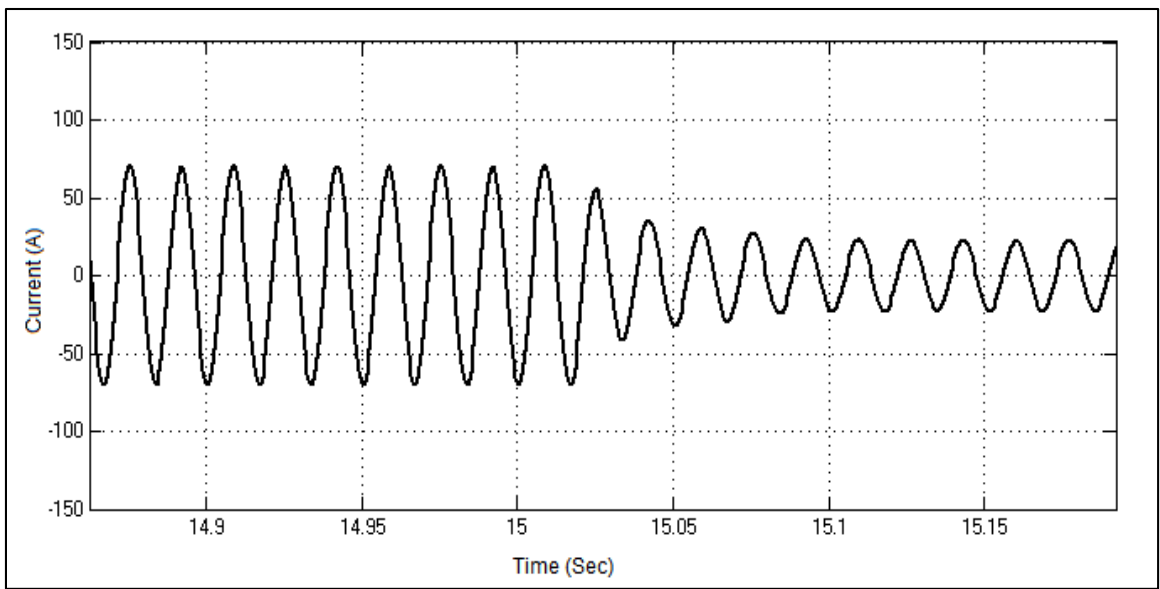


Figure 6-21 PV Inverter Current Waveform (Scenario 1)

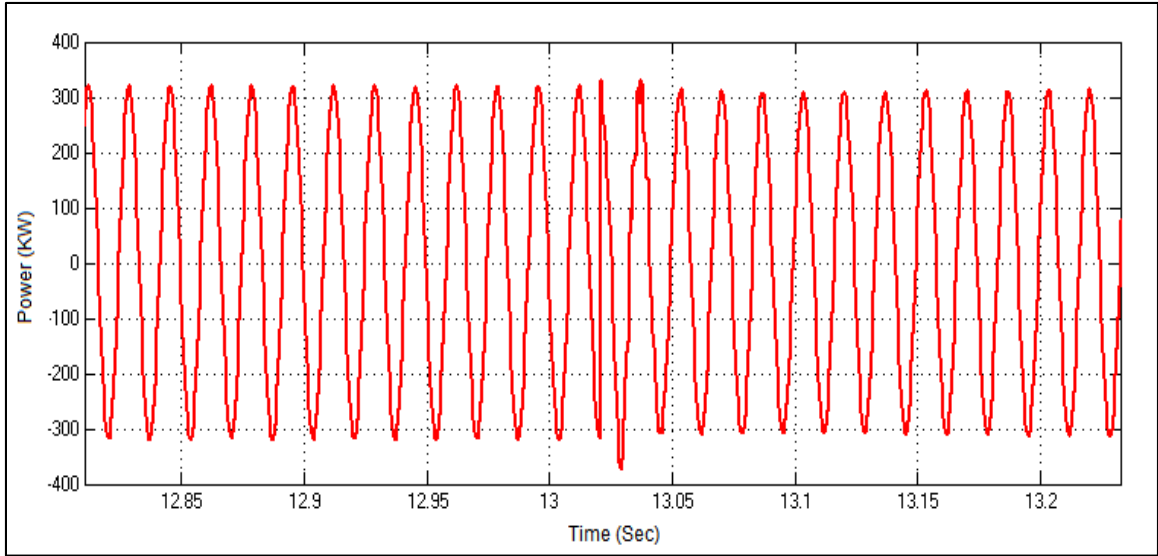


Figure 6-22 PV Generator Voltage during Transition from VSI Mode to PQ Mode (Scenario 1)

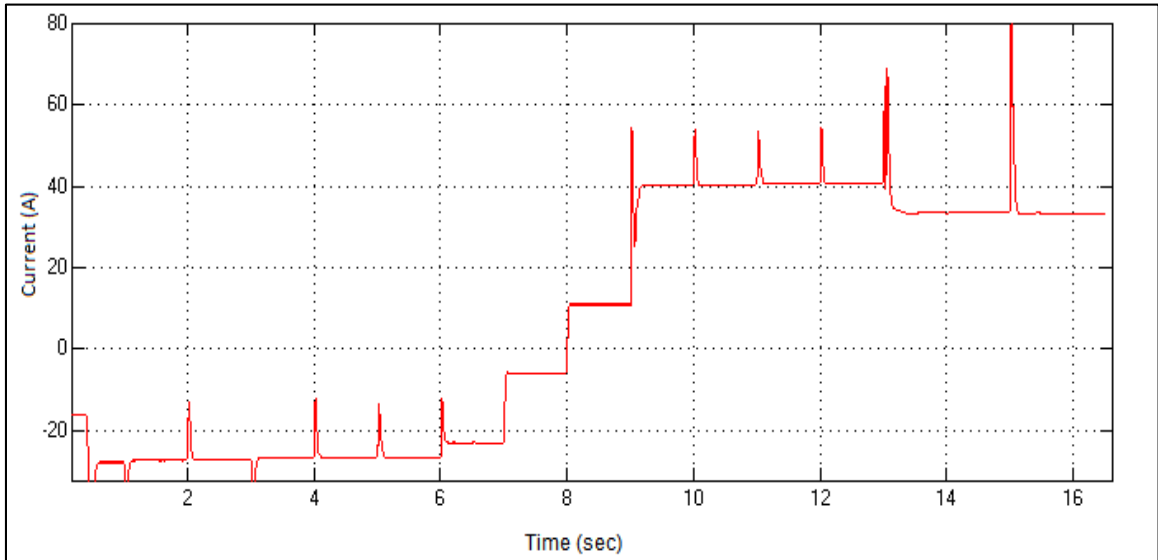


Figure 6-23 Battery-1 DC Current (Scenario 1)

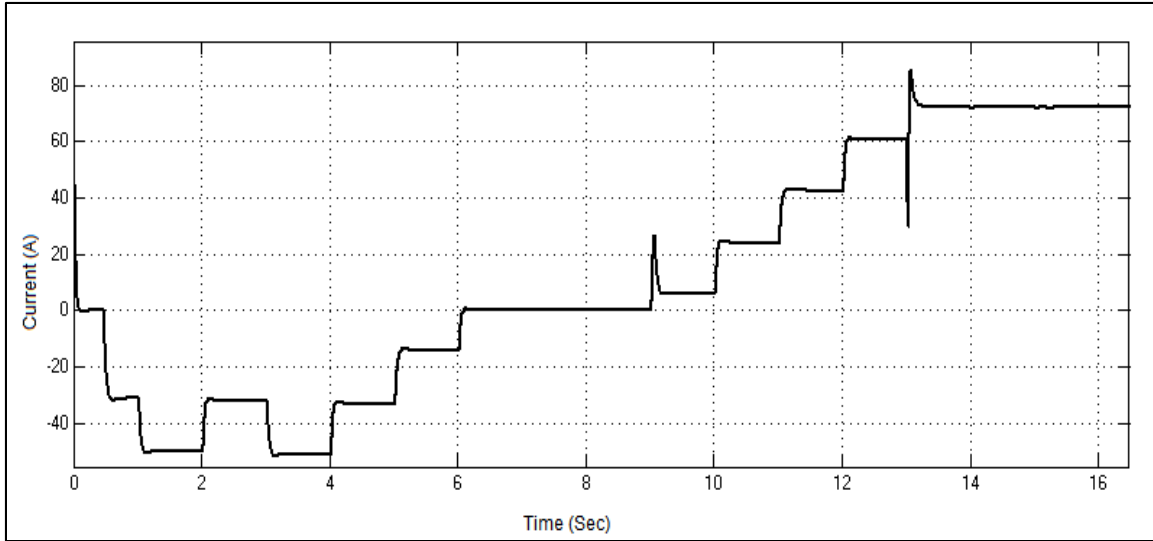


Figure 6-24 Battery-2 DC Current (Scenario 1)

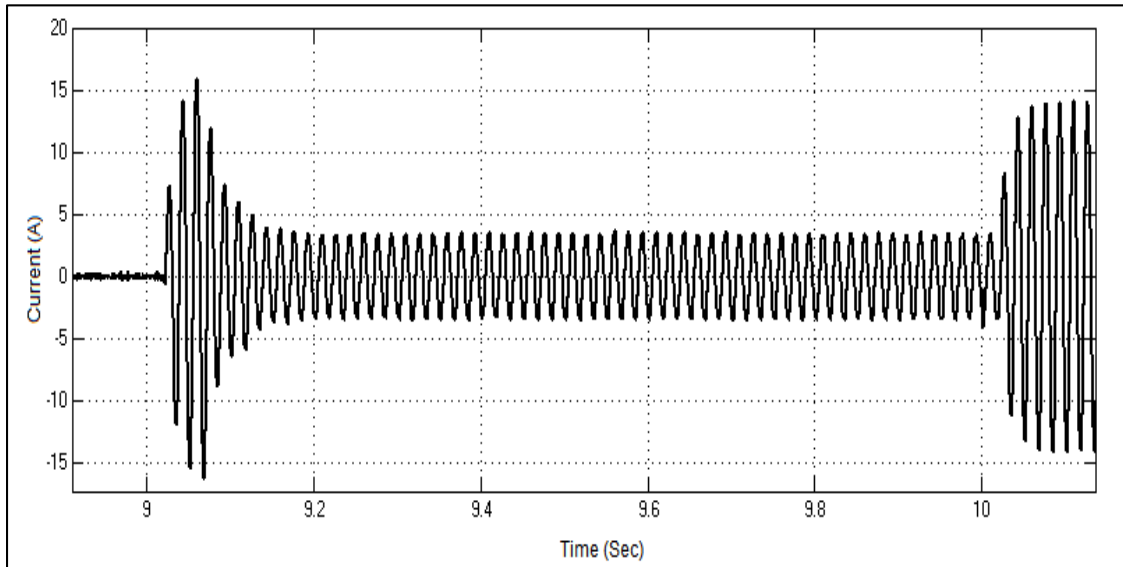


Figure 6-25 Battery Inverter Current during Transitions between Different States (Scenario 1)

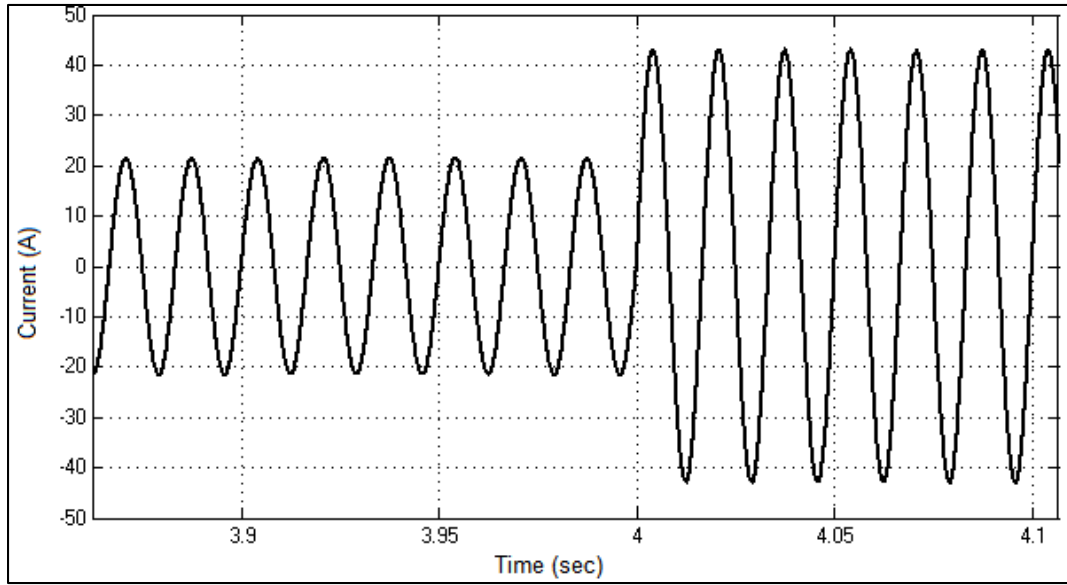


Figure 6-26 Load 3 Current Transition at Time =4 sec (Scenario 1)

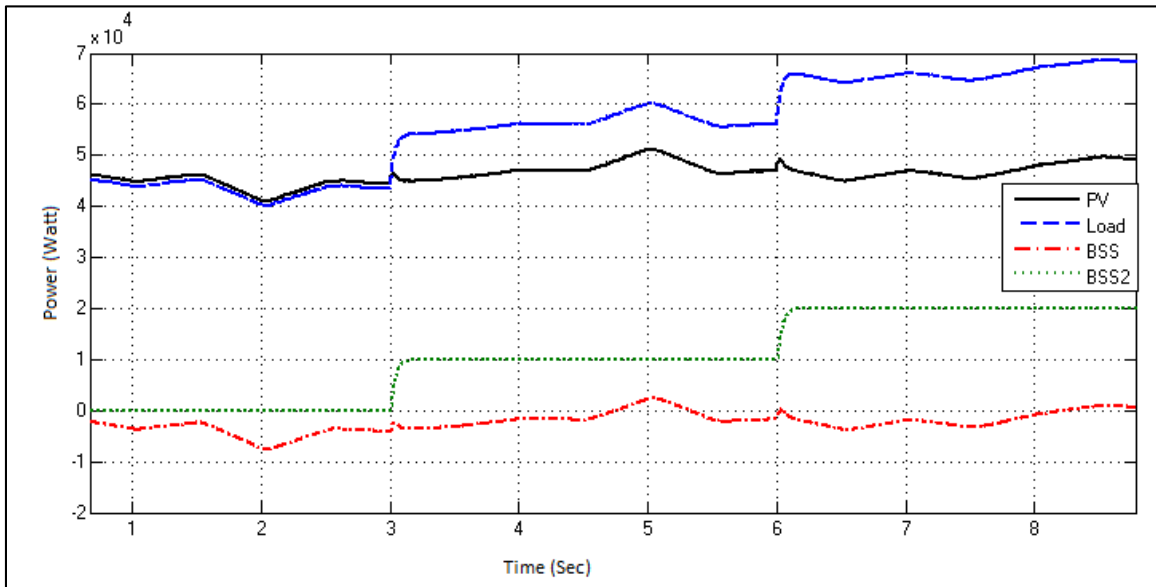


Figure 6-27 Load Flowing From PV Generator

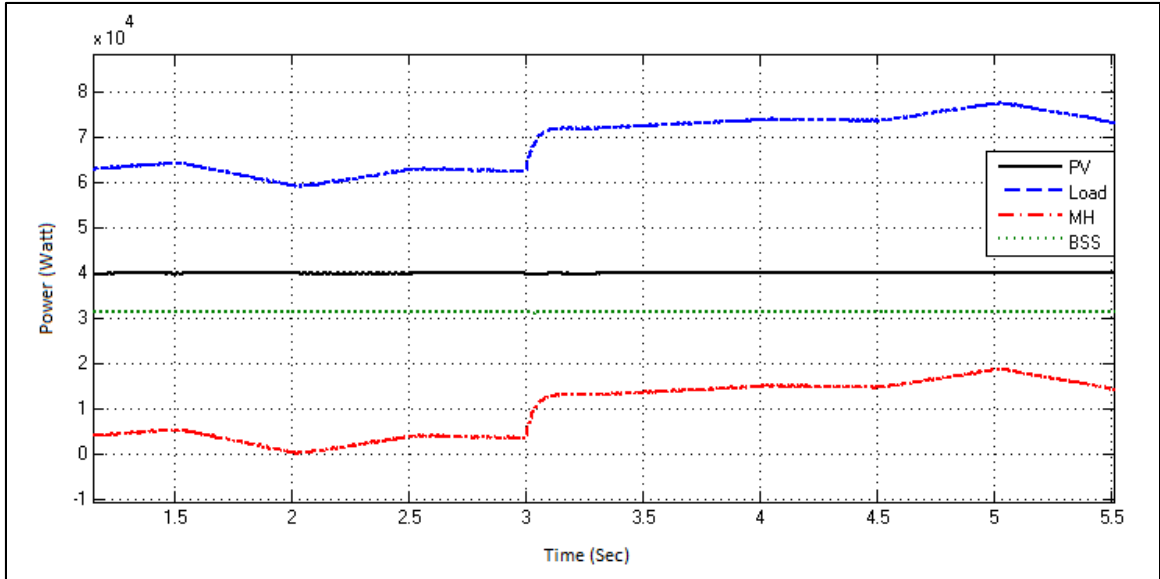


Figure 6-28 Load Following from HH Generator

6.4.2 Simulation of Scenario 2

In this scenario simulate morning time where PV power starts to increase till it can supply the total load alone. Due to limited data memory and huge amount of obtained data in addition to very slow simulation, the simulation time is in seconds, but the response of MH takes several seconds. So, we expect the bad frequency regulation when changing the load every two seconds. In order to simulate the systems in seconds, the starting time T_w of MH and the response time of SG were reduced to minimum values. In addition, 1 Hz fluctuation was tolerated. The fluctuation of frequency will results in bad transients when switching PV inverter to VSI inverter, and this will be disregarded.

The sun irradiance curve for this scenario is exposed in Figure 6-29. The output power from different DGs is shown in Figure 6-30. During the first 13 seconds, MH generator supplies the majority of the load, and any available solar power is injected to

the grid. During this period, MAS decide to leave both batteries in off state and save energy to support PV generator during day time. It is possible also to charge batteries in this period, but it assumed that batteries are fully charged. Of course, BSS-1 still needs to regulate the DC voltage at inverter voltage. At time = 13 seconds MAS finds that PV with aid of BSS can full supply the load. So, it instructs the Hydro to shut down. At the same time, MAS sends discharging commands to batteries to support PV. Figure 6-31, shows the voltage waveform of PV inverter during the switching from PQ inverter mode to VSI mode. Obviously the voltage distortion in this case is higher than distortion due to switching from VSI to PQ. This can be referred to two reasons; the frequency deviation that was permitted for simulation purpose and the sudden shut down operation. The current waveform of MH generator Current is depicted in Figure 6-32. In order to overcome the sudden shut down problem, the gradual shut down mechanism is used instead. The output power from MH generator and BSS generator during gradual shut down is illustrated in Figure 6-33. Apparently the power transients are eliminated and shut down process becomes smooth. The voltage of PV during mode transition is shown in Figure 6-34. The distortion in the voltage is minimized compared with the previous case. The current waveform of MH generator during shut down is depicted in Figure 6-35. The current are reduced in steps until it reaches zero. The DC current of BSS increases in steps with power increases as shown in Figure 6-36.

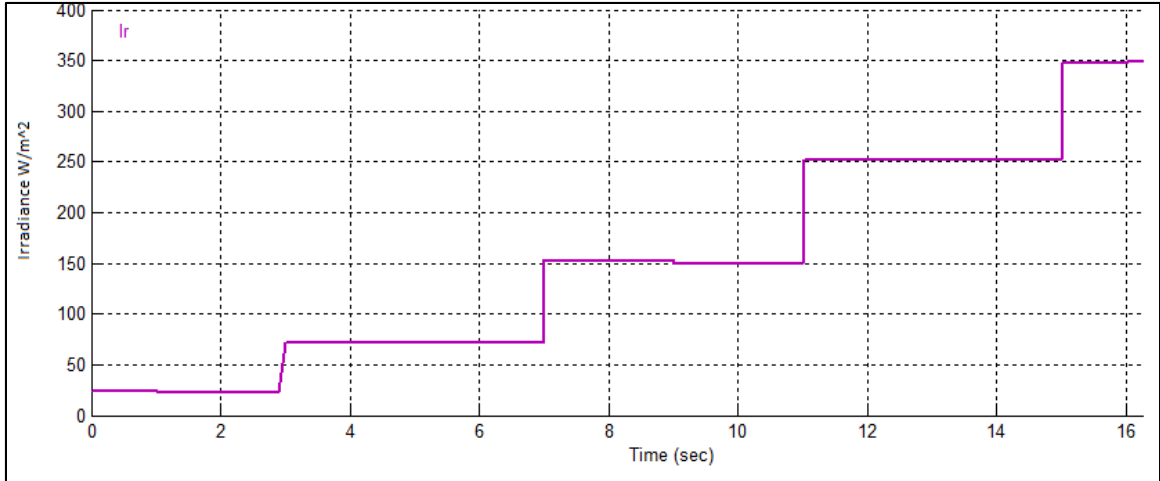


Figure 6-29 Sun Irradiance Curve (Scenario 2)

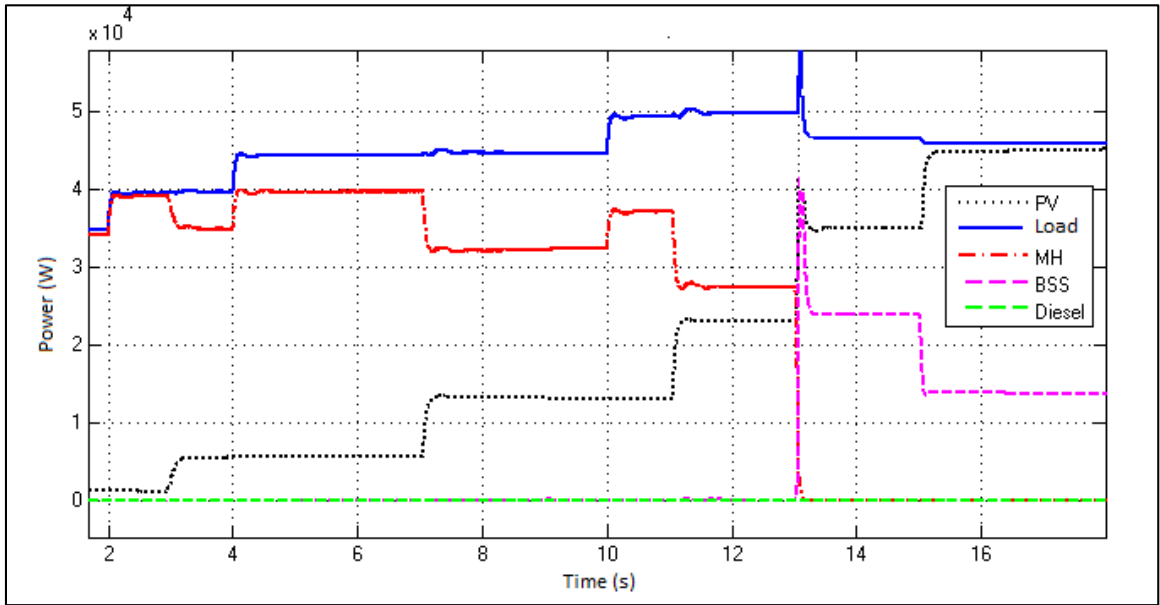


Figure 6-30 Output Power from Different DGs (Scenario 2)

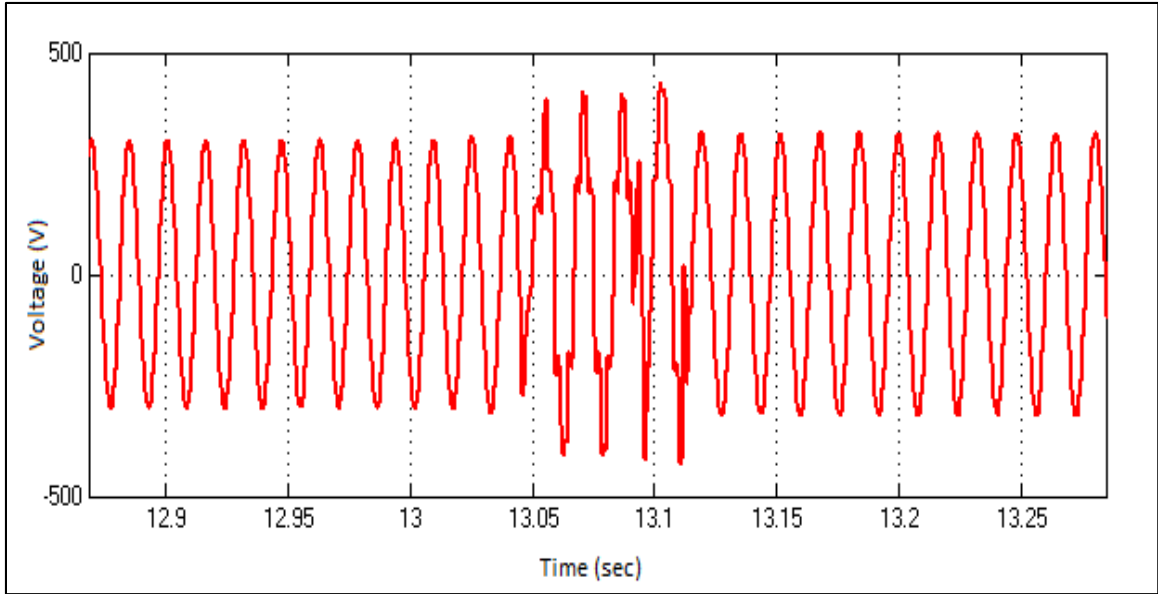


Figure 6-31 PV Inverter Voltage during Switching from PQ Mode to VSI Mode

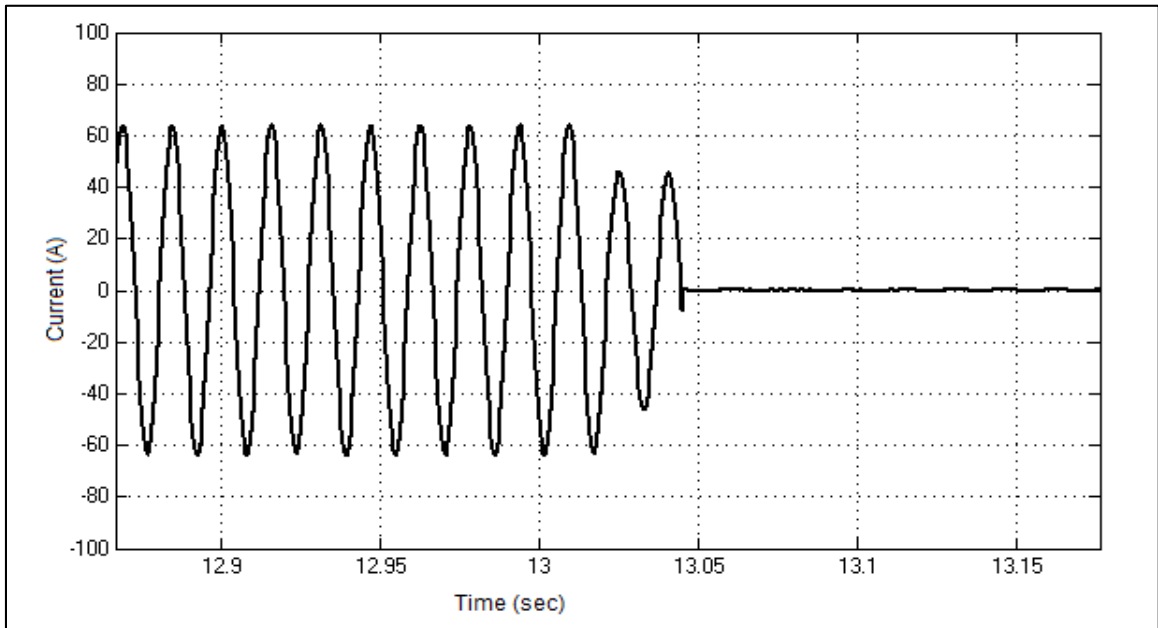


Figure 6-32 MH Generator Current during Shutting Down

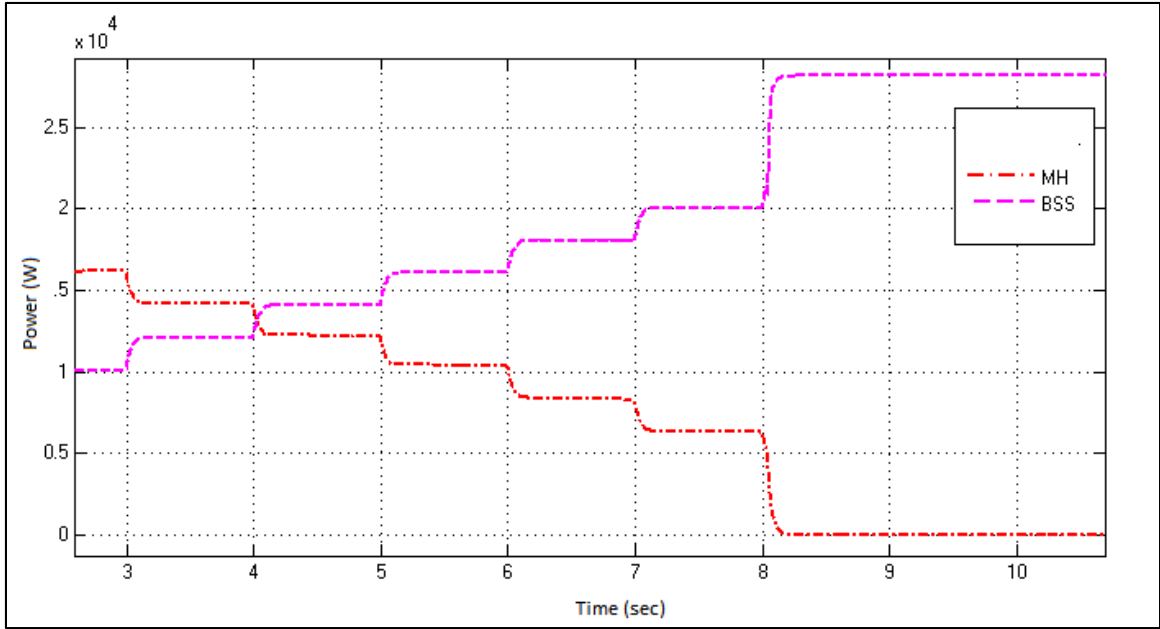


Figure 6-33 Generation Output of MH and PV during Gradual Shut Down

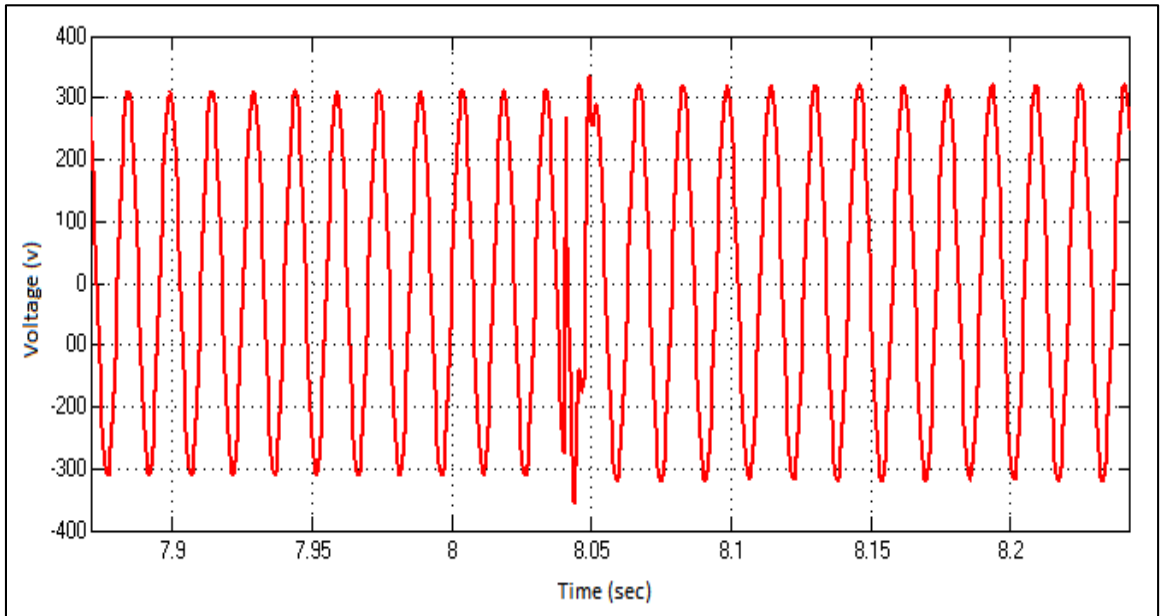


Figure 6-34 PV Generator Voltage during Transition from PQ Inverter to VSI in Gradual Shut Down

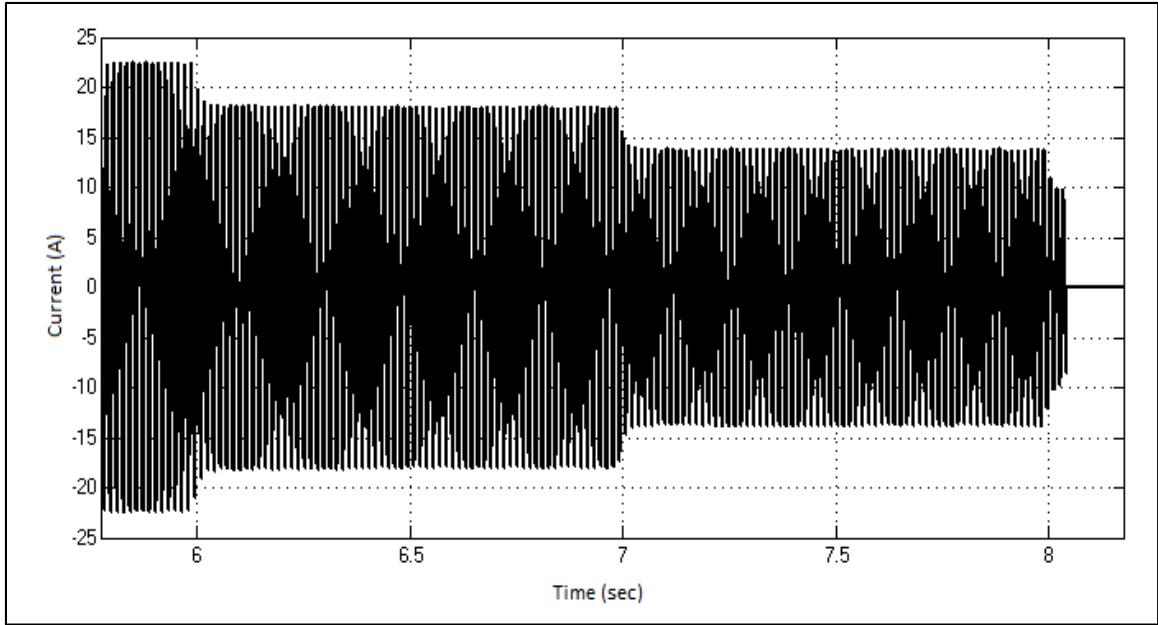


Figure 6-35 MH Generator Current during Gradual Shut Down

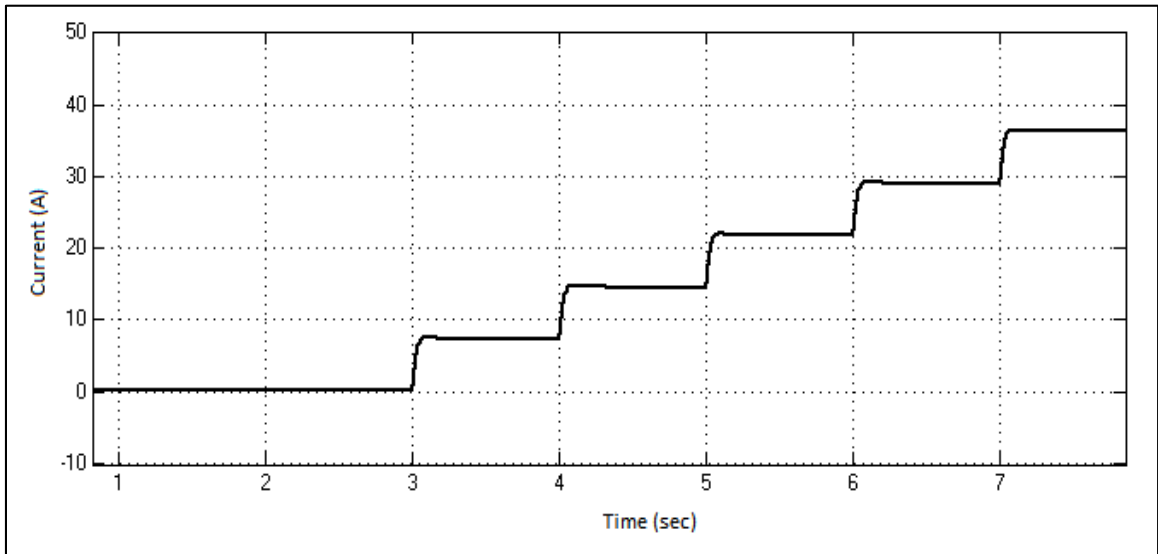


Figure 6-36 BSS DC Current during Gradual Shut Down

6.4.3 Simulation of Scenario 3

In this scenario, it is shown how diesel is gradually started up to back up PV-BSS system when the total capacity of PV-BSS cannot withstand the load, and MH generation is not available due to some technical failure. The sun irradiance curve for this scenario is illustrated in Figure 6-37. The output powers from different type of generators are depicted in Figure 6-38. Apparently, when the load demand exceeds the capacity of PV-BSS system, MAS instructs the diesel generator to start up. The output generation of the diesel is increased in steps and at the same time the BSS decreases its output. This will continue until BSS enters off state. The moment when the diesel is started PV inverter is switched to PQ inverter. The diesel generator governs the voltage and the frequency of MG as long as it runs. When MAS finds out that diesel generator is no longer needed and PV-BSS is capable of supplying the load autonomously, it commands diesel to start gradual shut down. Prior to opening of the diesel generator breaker, MAS convert PV inverter control mode to VSI. The current of diesel generator during gradual start up and gradual shut down is shown in Figures 6-39 and 6-40 respectively.

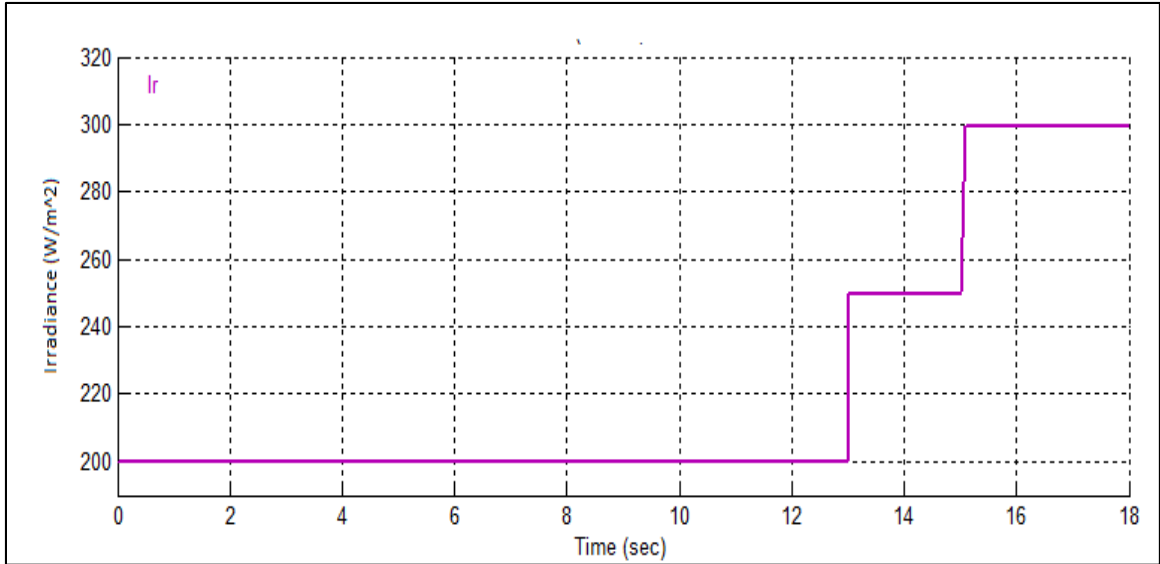


Figure 6-37 Sun Irradiance Curve (Scenario 3)

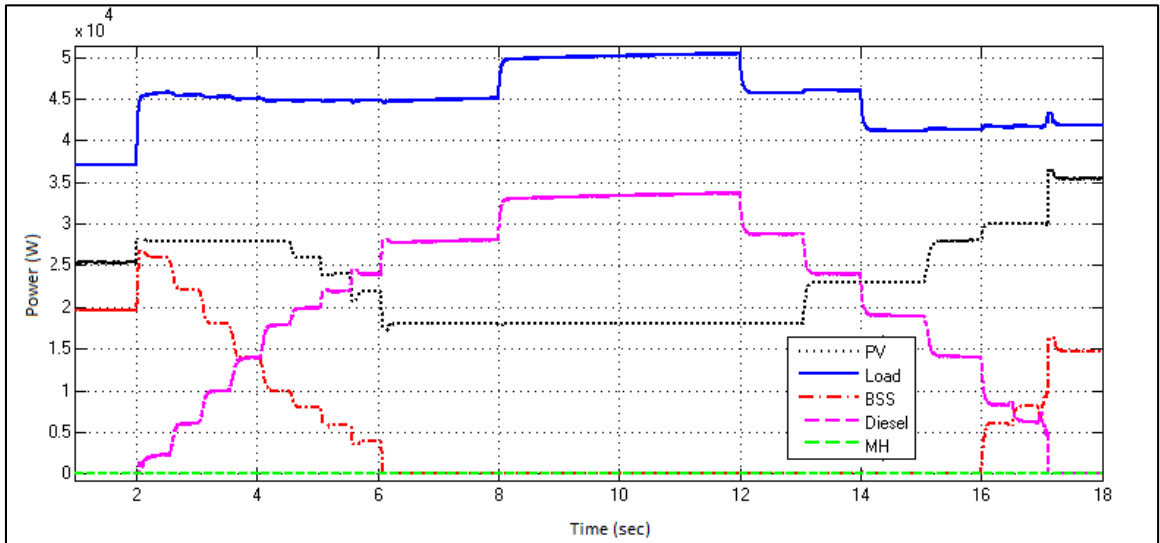


Figure 6-38 Output Generation from Different DGs (Scenario 3)

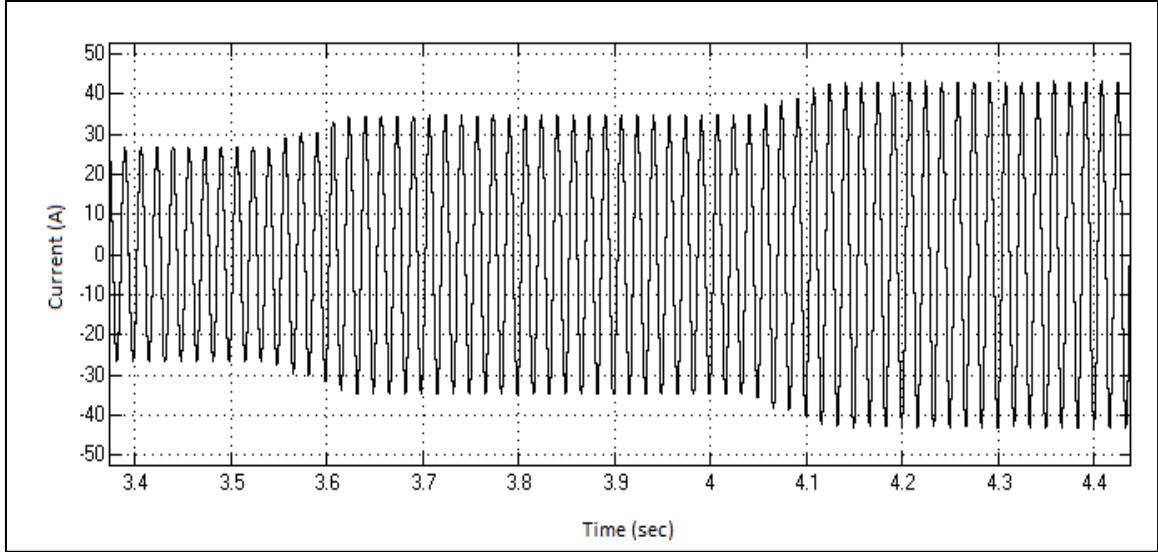


Figure 6-39 Diesel Generator Current during Start up (Scenario 3)

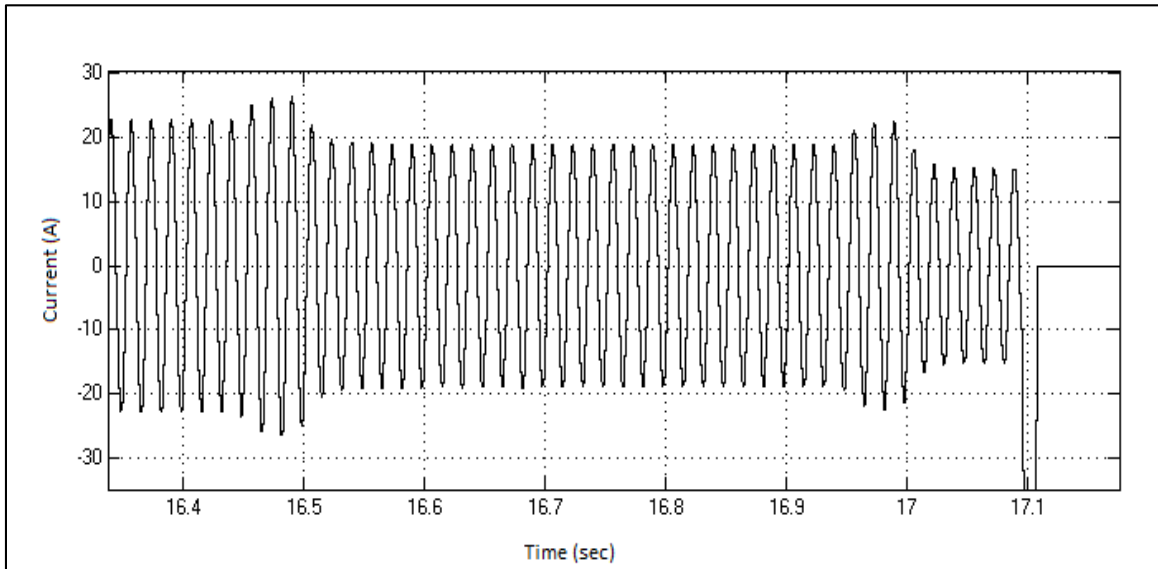


Figure 6-40 Diesel Generator Current during Shut down (Scenario 3)

6.5 Simulation of Zonal Control of MH

As discussed earlier, the small size of proposed MG won't allow flexibility in applying zonal control. Here one scenario simulated and that is when BA can't find parent to report to. Since BA has LA3 as a child agent, it acts as a starting agent for the two of

them. The only available plan for BA and LA is to fully or partially electrify the load corresponding to LA3 as long as it has energy stored in the BSS. The remaining agents including LA1, LA2, PVBA, DGA, and MHA will in turn form another zone, and choose the best options based on the available information. In fact, the plans of agents in different zones may conflict with each other; so, it is better for them to electrically isolate themselves from each other. The simulation results for the proposed scenario are shown in Figure 6-41 which expose the output power from different resources. The plots of Figure 6-41 are split into two sets of plots one for agents in first zone, and another for those agents in second zone. It can be clearly noticed from looking at Figure 6-42 that BA generation always following LA3 load demand. In other words, BA and LA3 are acting on their own. The other group of agent working without coordination with BA, and LA as depicted in Figure 6-43.

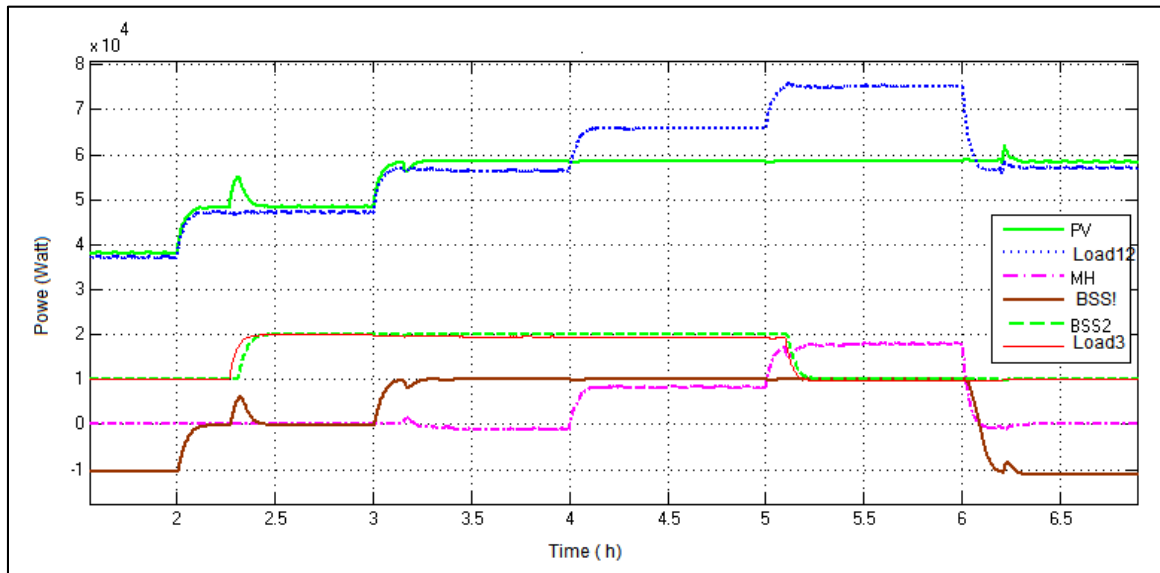


Figure 6-41 Load and Generation curves in Zonal Control

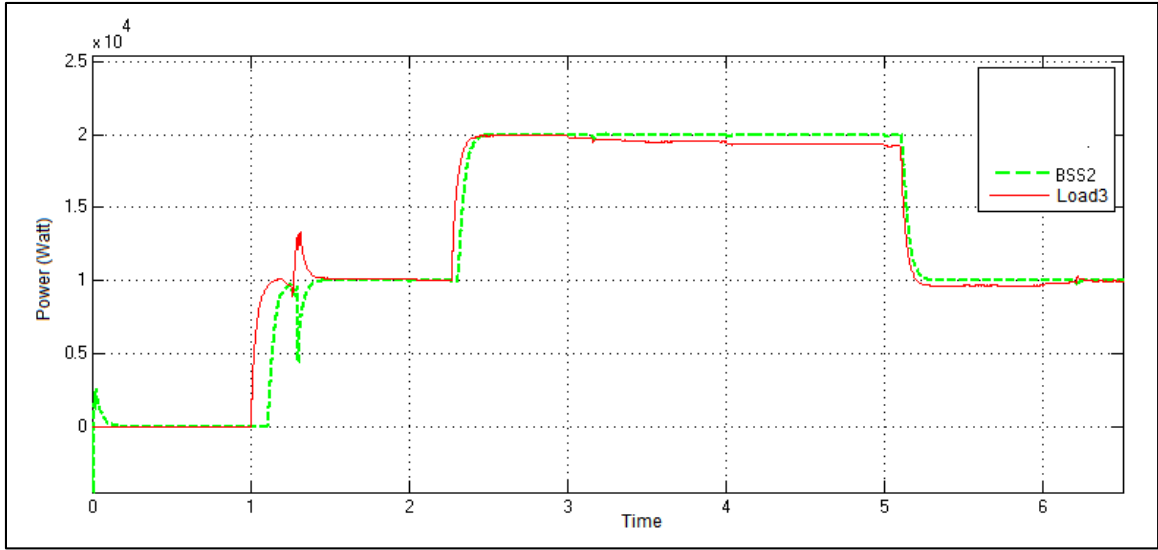


Figure 6-42 Plots of LA3 Load and BA Generation in zone 1

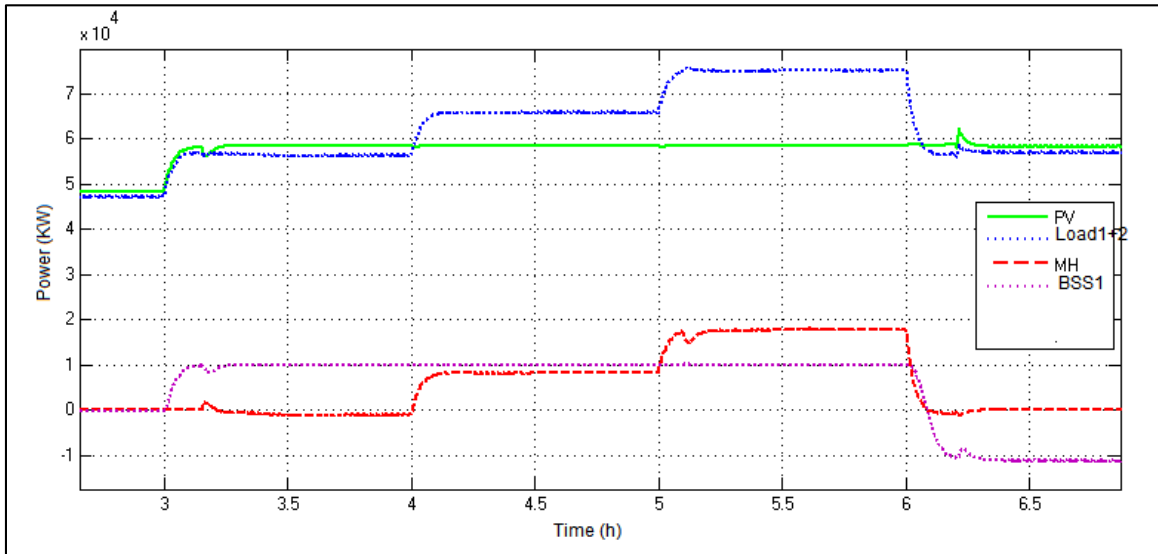


Figure 6-43 Load and Generation plots for Agents in Zone 2

CHAPTER 7

CONCLUSION AND FUTURE WORK

7.1 Conclusion

In this thesis, two level energy management and control strategy based on MAS were proposed, designed, and simulated. The proposed strategy was applied on MG containing PV, MH, diesel generator, and BSS. The main achievements of this thesis can be summarized in the following points:

- A Complete dynamic model for MG containing PV, MH generator, diesel generator, and BSS was developed and simulated in MATLAB.
- The optimal generation schedule was obtained for the considered system using online management.
- MAS-based online energy management and control system was designed and simulated in JADE. The MAS was linked to MG network to supervise it and provide it with control settings that lead to optimal operation.
- The proposed MAS has shown the capability of running MG in optimal operation by fully utilizing RES.
- The Proposed MAS was responsible for reconfiguration of MG and operation mode transitions including switching of inverter control mode from PQ inverter and VSI and vice versa, and Switching battery between charging state, off state, and discharging state.

- Interactive operation of MH generator and PV generator was managed in decentralized manner using MAS
- The Proposed MAS can handle unit commitment operation and it has the feature of smooth unit start up and shut down.
- A new information flow and communication system has been proposed to enable different agents with different types in the system to coordinate with each other
- MAS-based zonal control approach has been proposed to deal with power and communication failure in the system.

7.2 Future Work

As a future work, the following can be done to extend the work of this thesis:

- The proposed system can be simulated in RTDS to obtain real time measurements and verify its validity.
- More type of generator such as wind and fuel cell can be integrated with system to give more variety and flexibility in generation system.
- The design MAS can be improved to incorporate more features and tasks such as protection.

APPENDIX A

The data for Wadi Baisha Dam are shown in Figure A-1 and the data for hydraulic turbine and speed governor are illustrated in Table A-2.

Table 0-1 Data for Wadi Baisha Dam

Location	S (17 ⁰ 39' 56" N, and 42 ⁰ 39' 27" E)
Crest Elevation	339 m a.s.l
Riverbed Elevation	265 m a.s.l
Foundation Elevation	233 m a.s.l
Height Above Foundation	106 m
Catchment Area is about	4600 km ²
Mean Annual Flow	74.5 MCM
Maximum Flood	9864 m ³ /sec
Maximum Reservoir Level	337.5 m a.s.
Reservoir Level for Dead Storage	308.5 m a.s.l
Volume of Reservoir at a Level of Spillway Crest	193.6 MCM

Table 0-2 Hydraulic Turbine and Speed Controller Parameters

Parameter	Value
Water starting time (T_w)	0.874 sec
Speed controller proportional gain (K_p)	1.163
Speed controller integral gain (K_i)	0.105
Permanent droop gain (R_p)	0.01
Servo motor gain (K_a)	3.3
Servo motor time constant (T_G)	.07 sec

Table A-3 shows the data for diesel generator. Figure A-1 depicts a typical fuel consumption curve for 120 KV diesel generators.

Table 0-3 Diesel Generator Parameters

Parameter	Value
Speed controller time constants [T_{C1} T_{C2} T_{C3}]	[0.2 0.00002 0.01] sec
Speed controller gain K	40
Actuator time constants [T_{A1} T_{A2} T_{A3}]	[0.25 0.009 0.0384] sec
Engine time delay (T_d)	0.024 sec

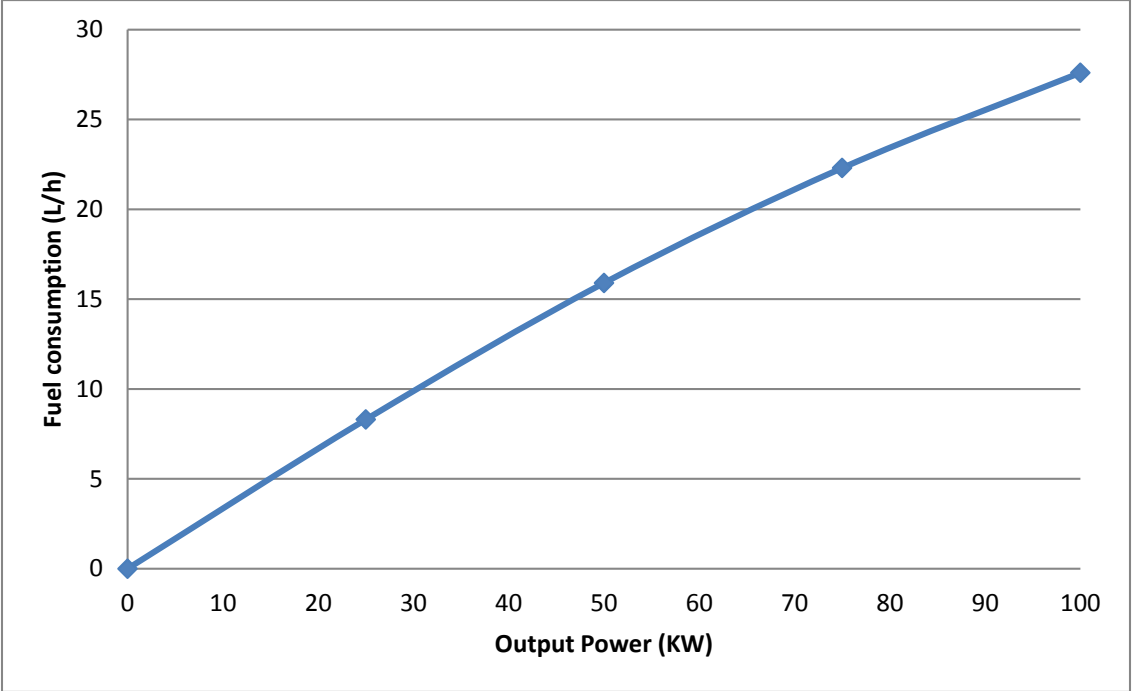


Figure 0-1 **Typical Fuel Consumption Curve for 120 KVA Diesel Generator**

References

- [1] A. Colet-Subirachs, A. Ruiz-Alvarez, O. Gomis-Bellmunt, F. Alvarez-Cuevas-Figuerola, and A. Sudria-Andreu, "Centralized and distributed active and reactive power control of a utility connected microgrid using IEC61850," *Systems Journal, IEEE*, vol. 6, pp. 58-67, 2012.
- [2] Y.-J. Kim, S.-J. Ahn, P.-I. Hwang, G.-C. Pyo, and S.-I. Moon, "Coordinated control of a DG and voltage control devices using a dynamic programming algorithm," *IEEE Transactions on Power Systems*, vol. 28, pp. 42-51, 2013.
- [3] S. Conti, R. Nicolosi, S. Rizzo, and H. Zeineldin, "Optimal dispatching of distributed generators and storage systems for MV islanded microgrids," *IEEE Transactions on Power Delivery*, vol. 27, pp. 1243-1251, 2012.
- [4] A. K. Basu, A. Bhattacharya, S. Chowdhury, and S. Chowdhury, "Planned scheduling for economic power sharing in a CHP-based micro-grid," *IEEE Transactions on Power Systems*, vol. 27, pp. 30-38, 2012.
- [5] A. G. Tsikalakis and N. D. Hatziargyriou, "Centralized control for optimizing microgrids operation," in *Power and Energy Society General Meeting, 2011 IEEE*, 2011, pp. 1-8.
- [6] O. Gomis-Bellmunt, A. Sumper, A. Colet-Subirachs, A. Ruiz-Alvarez, F. Alvarez-Cuevas-Figuerola, and A. Sudria-Andreu, "A utility connected microgrid based on power emulators," in *Power and Energy Society General Meeting, 2011 IEEE*, 2011, pp. 1-6.
- [7] D. E. Olivares, C. A. Cañizares, and M. Kazerani, "A centralized optimal energy management system for microgrids," in *Power and Energy Society General Meeting, 2011 IEEE*, 2011, pp. 1-6.
- [8] X. Wang, J. M. Guerrero, F. Blaabjerg, and Z. Chen, "Secondary voltage control for harmonics suppression in islanded microgrids," in *Power and Energy Society General Meeting, 2011 IEEE*, 2011, pp. 1-8.
- [9] M. N. Ambia, A. Al-Durra, and S. Mueeen, "Centralized power control strategy for AC-DC hybrid micro-grid system using multi-converter scheme," in *IECON 2011-37th Annual Conference on IEEE Industrial Electronics Society*, 2011, pp. 843-848.
- [10] A. Ruiz-Alvarez, A. Colet-Subirachs, F. Alvarez-Cuevas Figuerola, O. Gomis-Bellmunt, and A. Sudria-Andreu, "Operation of a utility connected microgrid using an IEC 61850-based multi-level management system," *IEEE Transactions on Power Systems*, vol. 3, pp. 858-865, 2012.
- [11] K. Tan, X. Peng, P. L. So, Y. C. Chu, and M. Chen, "Centralized control for parallel operation of distributed generation inverters in microgrids," *IEEE Transactions on Smart Grid* vol. 3, pp. 1977-1987, 2012.
- [12] M. Hassan and M. Abido, "Optimal design of microgrids in autonomous and grid-connected modes using particle swarm optimization," *IEEE Transactions on Power Electronics*, vol. 26, pp. 755-769, 2011.

- [13] Z. Miao, A. Domijan, and L. Fan, "Investigation of microgrids with both inverter interfaced and direct ac-connected distributed energy resources," *IEEE Transactions on Power Delivery* vol. 26, pp. 1634-1642, 2011.
- [14] W. C. Sheng, L. Hua, Y. Z. Long, W. Y. Bo, P. Y. Chang, and X. H. Hua, "Research on control strategies of small-hydro/PV hybrid power system," in *Sustainable Power Generation and Supply, 2009. SUPERGEN'09. International Conference on*, 2009, pp. 1-5.
- [15] I. J. Balaguer, Q. Lei, S. Yang, U. Supatti, and F. Z. Peng, "Control for grid-connected and intentional islanding operations of distributed power generation," *IEEE Transactions on Industrial Electronics* vol. 58, pp. 147-157, 2011.
- [16] N. Pogaku, M. Prodanovic, and T. C. Green, "Modeling, analysis and testing of autonomous operation of an inverter-based microgrid," *Power Electronics, IEEE Transactions on*, vol. 22, pp. 613-625, 2007.
- [17] H. H. Zeineldin, "A Q-f droop curve for facilitating islanding detection of inverter-based distributed generation," *IEEE transactions on power electronics*, vol. 24, pp. 665-673, 2009.
- [18] C. K. Sao and P. W. Lehn, "Control and power management of converter fed microgrids," *IEEE Transactions on Power Systems* vol. 23, pp. 1088-1098, 2008.
- [19] J.-W. Kim, H.-S. Choi, and B. H. Cho, "A novel droop method for converter parallel operation," *IEEE Transactions on Power Electronics*, vol. 17, pp. 25-32, 2002.
- [20] M. N. Marwali, J.-W. Jung, and A. Keyhani, "Control of distributed generation systems-Part II: Load sharing control," *IEEE Transactions on Power Electronics*, vol. 19, pp. 1551-1561, 2004.
- [21] J. C. Vasquez, J. M. Guerrero, A. Luna, P. Rodríguez, and R. Teodorescu, "Adaptive droop control applied to voltage-source inverters operating in grid-connected and islanded modes," *IEEE Transactions on Industrial Electronics* vol. 56, pp. 4088-4096, 2009.
- [22] Y. Mohamed and E. F. El-Saadany, "Adaptive decentralized droop controller to preserve power sharing stability of paralleled inverters in distributed generation microgrids," *IEEE Transactions on Industrial Electronics* vol. 23, pp. 2806-2816, 2008.
- [23] J. Kim, J. M. Guerrero, P. Rodriguez, R. Teodorescu, and K. Nam, "Mode adaptive droop control with virtual output impedances for an inverter-based flexible AC microgrid," *IEEE Transactions on Power Electronics*, vol. 26, pp. 689-701, 2011.
- [24] E. Rokrok and M. Golshan, "Adaptive voltage droop scheme for voltage source converters in an islanded multibus microgrid," *IET generation, transmission & distribution*, vol. 4, pp. 562-578, 2010.
- [25] N. Soni, S. Doolla, and M. C. Chandorkar, "Improvement of Transient Response in Microgrids Using Virtual Inertia," *IEEE Transactions on Power Delivery* vol. 28, 2013.
- [26] C. Rowe, T. Summers, and R. Betz, "Arctan power frequency droop for power electronics dominated microgrids," in *Universities Power Engineering Conference (AUPEC), 2010 20th Australasian*, 2010, pp. 1-6.

- [27] C. N. Rowe, T. J. Summers, R. E. Betz, D. J. Cornforth, and T. G. Moore, "Arctan Power–Frequency Droop for Improved Microgrid StabilityMicrogrid Stability," *IEEE transactions on power electronics*, vol. 28, NO.8, pp. 3747-3759, AUGUST 2013.
- [28] C.-T. Lee, C.-C. Chu, and P.-T. Cheng, "A new droop control method for the autonomous operation of distributed energy resource interface converters," in *Energy Conversion Congress and Exposition (ECCE), 2010 IEEE*, 2010, pp. 702-709.
- [29] C.-T. Lee, R.-P. Jiang, and P.-T. Cheng, "A grid synchronization method for droop controlled distributed energy resources converters," in *Energy Conversion Congress and Exposition (ECCE), 2011 IEEE*, 2011, pp. 743-749.
- [30] E. Barklund, N. Pogaku, M. Prodanovic, C. Hernandez-Aramburo, and T. C. Green, "Energy management in autonomous microgrid using stability-constrained droop control of inverters," *IEEE Transactions on Power Electronics* vol. 23, pp. 2346-2352, 2008.
- [31] G. Diaz, C. Gonzalez-Moran, J. Gomez-Aleixandre, and A. Diez, "Scheduling of droop coefficients for frequency and voltage regulation in isolated microgrids," *IEEE Transactions on Power Electronics*, vol. 25, pp. 489-496, 2010.
- [32] J. M. Guerrero, P. C. Loh, T.-L. Lee, and M. Chandorkar, "Advanced control architectures for intelligent microgrids—Part II: Power quality, energy storage, and AC/DC microgrids," *IEEE Transactions on Industrial Electronics*, vol. 60, pp. 1263-1270, 2013.
- [33] J. M. Guerrero, J. Matas, L. G. de Vicuña, M. Castilla, and J. Miret, "Decentralized control for parallel operation of distributed generation inverters using resistive output impedance," *IEEE Transactions on Industrial Electronics* vol. 54, pp. 994-1004, 2007.
- [34] K. De Brabandere, B. Bolsens, J. Van den Keybus, A. Woyte, J. Driesen, and R. Belmans, "A voltage and frequency droop control method for parallel inverters," *IEEE Transactions on Power Electronics*, vol. 22, pp. 1107-1115, 2007.
- [35] Y. Li, "Decoupled power control for an inverter based low voltage microgrid in autonomous operation," in *Power Electronics and Motion Control Conference, 2009. IPEMC'09. IEEE 6th International*, 2009, pp. 2490-2496.
- [36] J. Beerten and R. Belmans, "Analysis of Power Sharing and Voltage Deviations in Droop-Controlled DC Grids," *IEEE transactions on power system*, vol. 28, NO. 4, pp. 4588-4597, NOVEMBER 2013.
- [37] T. L. Vandoorn, B. Meersman, L. Degroote, B. Renders, and L. Vandeveldel, "A control strategy for islanded microgrids with dc-link voltage control," *IEEE Transactions on Smart Grid*, vol. 26, pp. 703-713, 2011.
- [38] T. L. Vandoorn, B. Meersman, J. D. De Kooning, and L. Vandeveldel, "Analogy between conventional grid control and islanded microgrid control based on a global DC-link voltage droop," *IEEE Transactions on Smart Grid*, vol. 27, pp. 1405-1414, 2012.
- [39] T.-F. Wu, Y.-K. Chen, and Y.-H. Huang, "3C strategy for inverters in parallel operation achieving an equal current distribution," *IEEE Transactions on Smart Grid*, vol. 47, pp. 273-281, 2000.

- [40] S. Chiang, C. Lin, and C. Yen, "Current limitation control technique for parallel operation of UPS inverters," in *Power Electronics Specialists Conference, 2004. PESC 04. 2004 IEEE 35th Annual*, 2004, pp. 1922-1926.
- [41] H. Van Der Broeck and U. Boeke, "A simple method for parallel operation of inverters," in *Telecommunications Energy Conference, 1998. INTELEC. Twentieth International*, 1998, pp. 143-150.
- [42] Y. Pei, G. Jiang, X. Yang, and Z. Wang, "Auto-master-slave control technique of parallel inverters in distributed AC power systems and UPS," in *Power Electronics Specialists Conference, 2004. PESC 04. 2004 IEEE 35th Annual*, 2004, pp. 2050-2053.
- [43] X. Sun, Y.-S. Lee, and D. Xu, "Modeling, analysis, and implementation of parallel multi-inverter systems with instantaneous average-current-sharing scheme," *IEEE Transactions on Power Electronics*, vol. 18, pp. 844-856, 2003.
- [44] Y. Zhang, H. Ma, G. Zhao, and J. Guo, "A current-sharing method based on networked control for three-phase parallel inverter," in *IECON 2012-38th Annual Conference on IEEE Industrial Electronics Society*, 2012, pp. 57-61.
- [45] Y. Xing, L. Huang, S. Sun, and Y. Yan, "Novel control for redundant parallel UPSs with instantaneous current sharing," in *Power Conversion Conference, 2002. PCC Osaka 2002. Proceedings of the*, 2002, pp. 959-963.
- [46] A. M. Roslan, K. H. Ahmed, S. J. Finney, and B. W. Williams, "Improved instantaneous average current-sharing control scheme for parallel-connected inverter considering line impedance impact in microgrid networks," *IEEE Transactions on Power Electronics*, vol. 26, pp. 702-716, 2011.
- [47] R. G. Wandhare, S. Thale, and V. Agarwal, "Reconfigurable hierarchical control of a microgrid developed with PV, wind, micro-hydro, fuel cell and ultra-capacitor," in *Applied Power Electronics Conference and Exposition (APEC), 2013 Twenty-Eighth Annual IEEE*, 2013, pp. 2799-2806.
- [48] C. Hou, X. Hu, and D. Hui, "Hierarchical control techniques applied in microgrid," in *Power System Technology (POWERCON), 2010 International Conference on*, 2010, pp. 1-5.
- [49] J. M. Guerrero, J. C. Vasquez, J. Matas, L. G. de Vicuña, and M. Castilla, "Hierarchical control of droop-controlled AC and DC microgrids—a general approach toward standardization," *IEEE Transactions on Industrial Electronics*, vol. 58, pp. 158-172, 2011.
- [50] C.-X. Dou and B. Liu, "Multi-Agent Based Hierarchical Hybrid Control for Smart Microgrid," *IEEE Transactions on Smart Grid*, vol. 4, 2013.
- [51] J. Guerrero, P. Loh, M. Chandorkar, and T. Lee, "Advanced Control Architectures for Intelligent MicroGrids?? Part I: Decentralized and Hierarchical ControlAdvanced Control Architectures for Intelligent Microgrids?? Part II: Power Quality, Energy Storage, and AC/DC Microgrids," 2013.
- [52] T. Vandoorn, B. Zwaenepoel, J. De Kooning, B. Meersman, and L. Vandeveld, "Smart microgrids and virtual power plants in a hierarchical control structure," in *Innovative Smart Grid Technologies (ISGT Europe), 2011 2nd IEEE PES International Conference and Exhibition on*, 2011, pp. 1-7.

- [53] C. Dou, X. Jia, Z. Bo, D. Liu, and F. Zhao, "Hybrid control for micro-grid based on hybrid system theory," in *Power and Energy Society General Meeting, 2011 IEEE*, 2011, pp. 1-11.
- [54] Y.-R. Mohamed and A. A. Radwan, "Hierarchical control system for robust microgrid operation and seamless mode transfer in active distribution systems," *IEEE Transactions on Smart Grid*, vol. 2, pp. 352-362, 2011.
- [55] A. Bidram and A. Davoudi, "Hierarchical structure of microgrids control system," *Smart Grid, IEEE Transactions on*, vol. 3, pp. 1963-1976, 2012.
- [56] T. L. Vandoorn, B. Renders, L. Degroote, B. Meersman, and L. Vandeveldel, "Active load control in islanded microgrids based on the grid voltage," *IEEE Transactions on Smart Grid*, vol. 2, pp. 139-151, 2011.
- [57] M. Meiqin, D. Wei, and L. Chang, "Multi-agent based simulation for microgrid energy management," in *Power Electronics and ECCE Asia (ICPE & ECCE), 2011 IEEE 8th International Conference on*, 2011, pp. 1219-1223.
- [58] T. Funabashi, G. Fujita, K. Koyanagi, and R. Yokoyama, "Field tests of a microgrid control system," in *Universities Power Engineering Conference, 2006. UPEC'06. Proceedings of the 41st International*, 2006, pp. 232-236.
- [59] T. Logenthiran, D. Srinivasan, A. Khambadkone, and H. Aung, "Multi-Agent System (MAS) for short-term generation scheduling of a microgrid," in *Sustainable Energy Technologies (ICSET), 2010 IEEE International Conference on*, 2010, pp. 1-6.
- [60] T. Logenthiran, D. Srinivasan, A. Khambadkone, and H. Aung, "Scalable Multi-Agent System (MAS) for operation of a microgrid in islanded mode," in *Power Electronics, Drives and Energy Systems (PEDES) & 2010 Power India, 2010 Joint International Conference on*, 2010, pp. 1-6.
- [61] C.-x. Dou and B. Liu, "Hierarchical management and control based on MAS for distribution grid via intelligent mode switching," *International Journal of Electrical Power & Energy Systems*, vol. 54, pp. 352-366, 2014.
- [62] C. Dou, B. Liu, and J. M. Guerrero, "MAS based event-triggered hybrid control for smart microgrids," in *Industrial Electronics Society, IECON 2013-39th Annual Conference of the IEEE*, 2013, pp. 1712-1717.
- [63] N. Cai and J. Mitra, "A decentralized control architecture for a microgrid with power electronic interfaces," in *North American Power Symposium (NAPS), 2010*, 2010, pp. 1-8.
- [64] N. Cai and J. Mitra, "A multi-level control architecture for master-slave organized microgrids with power electronic interfaces," *Electric Power Systems Research*, vol. 109, pp. 8-19, 2014.
- [65] F. Ren, M. Zhang, and D. Sutanto, "A multi-agent solution to distribution system management by considering distributed generators," *Power Systems, IEEE Transactions on*, vol. 28, pp. 1442-1451, 2013.
- [66] A. L. Dimeas and N. D. Hatziargyriou, "Agent based Control for Microgrids," presented at the IEEE Power Engineering Society General Meeting, Tampa, USA, 2007.
- [67] A. Dimeas and N. Hatziargyriou, "A MAS architecture for microgrids control," in *Intelligent Systems Application to Power Systems, 2005. Proceedings of the 13th International Conference on*, 2005, p. 5 pp.

- [68] A. Dimeas and N. Hatziargyriou, "Multi-agent reinforcement learning for microgrids," in *Power and Energy Society General Meeting, 2010 IEEE*, 2010, pp. 1-8.
- [69] S. Chatzivasiliadis, N. Hatziargyriou, and A. Dimeas, "Development of an agent based intelligent control system for microgrids," in *Power and Energy Society General Meeting-Conversion and Delivery of Electrical Energy in the 21st Century, 2008 IEEE*, 2008, pp. 1-6.
- [70] Z. Jiang, "Agent-based control framework for distributed energy resources microgrids," in *Intelligent Agent Technology, 2006. IAT'06. IEEE/WIC/ACM International Conference On*, 2006, pp. 646-652.
- [71] M. Cirrincione, M. Cossentino, S. Gaglio, V. Hilaire, A. Koukam, M. Pucci, . . . G. Vitale, "Intelligent energy management system," in *Industrial Informatics, 2009. INDIN 2009. 7th IEEE International Conference on*, 2009, pp. 232-237.
- [72] C. Colson and M. H. Nehrir, "Comprehensive real-time microgrid power management and control with distributed agents," 2013.
- [73] Z. Xiaoyan, L. Tianqi, and L. Xueping, "Multi-Agent based Microgrid Coordinated Control," *Energy Procedia*, vol. 14, pp. 154-159, 2012.
- [74] Z. Jian, A. Qian, J. Chuanwen, W. Xingang, Z. Zhanghua, and G. Chenghong, "The application of multi agent system in microgrid coordination control," in *Sustainable Power Generation and Supply, 2009. SUPERGEN'09. International Conference on*, 2009, pp. 1-6.
- [75] I.-Y. Chung, W. Liu, D. A. Cartes, E. G. Collins, and S.-I. Moon, "Control methods of inverter-interfaced distributed generators in a microgrid system," *Industry Applications, IEEE Transactions on*, vol. 46, pp. 1078-1088, 2010.
- [76] M. Pipattanasomporn, H. Feroze, and S. Rahman, "Multi-agent systems in a distributed smart grid: Design and implementation," in *Power Systems Conference and Exposition, 2009. PSCE'09. IEEE/PES*, 2009, pp. 1-8.
- [77] M. Pipattanasomporn, H. Feroze, and S. Rahman, "Securing critical loads in a PV-based microgrid with a multi-agent system," *Renewable Energy*, vol. 39, pp. 166-174, 2012.
- [78] J. Rocabert, G. Azevedo, G. Vazquez, I. Candela, P. Rodriguez, and J. Guerrero, "Intelligent control agent for transient to an island grid," in *Industrial Electronics (ISIE), 2010 IEEE International Symposium on*, 2010, pp. 2223-2228.
- [79] K. Manickavasagam, M. Nithya, K. Priya, J. Shruthi, S. Krishnan, S. Misra, and S. Manikandan, "Control of distributed generator and smart grid using multi-agent system," in *Electrical Energy Systems (ICEES), 2011 1st International Conference on*, 2011, pp. 212-217.
- [80] X. Zhou, Y. Gu, Y. Ma, L. Cui, and S. Liu, "Hybrid operation control method for micro-grid based on MAS," in *Progress in Informatics and Computing (PIC), 2010 IEEE International Conference on*, 2010, pp. 72-75.
- [81] W.-D. Zheng and J.-D. Cai, "A multi-agent system for distributed energy resources control in microgrid," in *Critical Infrastructure (CRIS), 2010 5th International Conference on*, 2010, pp. 1-5.
- [82] D. Shao, Q. Wei, and T. Nie, "A Multi-Agent control strategy in microgrid island mode," in *Strategic Technology (IFOST), 2011 6th International Forum on*, 2011, pp. 429-432.

- [83] G. Zheng and N. Li, "Multi-Agent Based Control System for Multi-Microgrids," in *Computational Intelligence and Software Engineering (CiSE), 2010 International Conference on*, 2010, pp. 1-4.
- [84] C. Colson, M. Nehrir, and R. Gunderson, "Distributed multi-agent microgrids: a decentralized approach to resilient power system self-healing," in *Resilient Control Systems (ISRCS), 2011 4th International Symposium on*, 2011, pp. 83-88.
- [85] H. Dagdougui and R. Sacile, "Decentralized Control of the Power Flows in a Network of Smart Microgrids Modeled as a Team of Cooperative Agents."
- [86] T. Logenthiran, D. Srinivasan, and T. Z. Shun, "Multi-agent system for demand side management in smart grid," in *Power Electronics and Drive Systems (PEDS), 2011 IEEE Ninth International Conference on*, 2011, pp. 424-429.
- [87] H. Kumar Nunna, S. Doolla, and A. Shukla, "Multi-agent application for demand response in microgrids," in *Industrial Electronics Society, IECON 2013-39th Annual Conference of the IEEE*, 2013, pp. 7629-7634.
- [88] V. Di Lecce, A. Quarto, A. Galiano, M. Dassisti, and M. Chimienti, "An auction based agency for demand side management system: An evaluation," in *Instrumentation and Measurement Technology Conference (I2MTC), 2013 IEEE International*, 2013, pp. 77-82.
- [89] I. Dusparic, C. Harris, A. Marinescu, V. Cahill, and S. Clarke, "Multi-agent residential demand response based on load forecasting," in *Technologies for Sustainability (SusTech), 2013 1st IEEE Conference on*, 2013, pp. 90-96.
- [90] M. Deindl, C. Block, R. Vahidov, and D. Neumann, "Load shifting agents for automated demand side management in micro energy grids," in *Self-Adaptive and Self-Organizing Systems, 2008. SASO'08. Second IEEE International Conference on*, 2008, pp. 487-488.
- [91] H. Kumar Nunna and S. Doolla, "Energy Management in Microgrids Using Demand Response and Distributed Storage—A Multiagent Approach," 2013.
- [92] A. K. Abdelsalam, A. M. Massoud, S. Ahmed, and P. N. Enjeti, "High-performance adaptive perturb and observe MPPT technique for photovoltaic-based microgrids," *Power Electronics, IEEE Transactions on*, vol. 26, pp. 1010-1021, 2011.
- [93] T. Bennett, A. Zilouchian, and R. Messenger, "Perturb and Observe versus Incremental Conductance MPPT Algorithms."
- [94] N. Femia, G. Petrone, G. Spagnuolo, and M. Vitelli, "Optimizing duty-cycle perturbation of P&O MPPT technique," in *Power Electronics Specialists Conference, 2004. PESC 04. 2004 IEEE 35th Annual*, 2004, pp. 1939-1944.
- [95] N. Femia, G. Petrone, G. Spagnuolo, and M. Vitelli, "Optimizing sampling rate of P&O MPPT technique," in *Power Electronics Specialists Conference, 2004. PESC 04. 2004 IEEE 35th Annual*, 2004, pp. 1945-1949.
- [96] N. Femia, G. Petrone, G. Spagnuolo, and M. Vitelli, "Perturb and observe MPPT technique robustness improved," in *Industrial Electronics, 2004 IEEE International Symposium on*, 2004, pp. 845-850.
- [97] N. Femia, G. Petrone, G. Spagnuolo, and M. Vitelli, "Optimization of perturb and observe maximum power point tracking method," *Power Electronics, IEEE Transactions on*, vol. 20, pp. 963-973, 2005.

- [98] G. Petrone, G. Spagnuolo, and M. Vitelli, "A multivariable perturb-and-observe maximum power point tracking technique applied to a single-stage photovoltaic inverter," *Industrial Electronics, IEEE Transactions on*, vol. 58, pp. 76-84, 2011.
- [99] L. Piegari and R. Rizzo, "Adaptive perturb and observe algorithm for photovoltaic maximum power point tracking," *Renewable Power Generation, IET*, vol. 4, pp. 317-328, 2010.
- [100] D. Sera, L. Mathe, T. Kerekes, S. Spataru, and R. Teodorescu, "On the Perturb-and-Observe and Incremental Conductance MPPT methods for PV systems," *IEEE Journal of Photovoltaics*, 2013.
- [101] M. A. Elgendy, B. Zahawi, and D. J. Atkinson, "Assessment of the Incremental Conductance Maximum Power Point Tracking Algorithm," 2012.
- [102] G.-C. Hsieh, H.-I. Hsieh, C.-Y. Tsai, and C.-H. Wang, "Photovoltaic power-increment-aided incremental-conductance MPPT with two-phased tracking," *Power Electronics, IEEE Transactions on*, vol. 28, pp. 2895-2911, 2013.
- [103] K. Kachhiya, M. Lokhande, and M. Patel, "MATLAB/Simulink model of solar PV module and MPPT algorithm," in *Proceedings of the National Conference on Recent Trends in Engineering and Technology*, 2011.
- [104] F. Kazan, S. Karaki, R. A. Jabr, and M. Mansour, "Maximum power point tracking using ripple correlation and incremental conductance," in *Universities Power Engineering Conference (UPEC), 2012 47th International*, 2012, pp. 1-6.
- [105] G. Kish, J. Lee, and P. Lehn, "Modelling and control of photovoltaic panels utilising the incremental conductance method for maximum power point tracking," *IET Renewable Power Generation*, vol. 6, pp. 259-266, 2012.
- [106] F. Liu, S. Duan, F. Liu, B. Liu, and Y. Kang, "A variable step size INC MPPT method for PV systems," *Industrial Electronics, IEEE Transactions on*, vol. 55, pp. 2622-2628, 2008.
- [107] A. Safari and S. Mekhilef, "Simulation and hardware implementation of incremental conductance MPPT with direct control method using Cuk converter," *Industrial Electronics, IEEE Transactions on*, vol. 58, pp. 1154-1161, 2011.
- [108] Z. Xuesong, S. Daichun, M. Youjie, and C. Deshu, "The simulation and design for MPPT of PV system Based on Incremental Conductance Method," in *Information Engineering (ICIE), 2010 WASE International Conference on*, 2010, pp. 314-317.
- [109] Y. Yusof, S. H. Sayuti, M. Abdul Latif, and M. Z. C. Wanik, "Modeling and simulation of maximum power point tracker for photovoltaic system," in *Power and Energy Conference, 2004. PECon 2004. Proceedings. National*, 2004, pp. 88-93.
- [110] W. Xiao, M. G. Lind, W. G. Dunford, and A. Capel, "Real-time identification of optimal operating points in photovoltaic power systems," *Industrial Electronics, IEEE Transactions on*, vol. 53, pp. 1017-1026, 2006.
- [111] J. Alonso-Martínez and S. Arnaltes, "A Three-Phase Grid-Connected Inverter for Photovoltaic Application Using Fuzzy MPPT," in *International Conference on Renewable Energies and Power Quality (ICREPQ)*, 2006.
- [112] E. Karatepe and T. Hiyama, "Artificial neural network-polar coordinated fuzzy controller based maximum power point tracking control under partially shaded conditions," *Renewable Power Generation, IET*, vol. 3, pp. 239-253, 2009.

- [113] J. Li and H. Wang, "Maximum power point tracking of photovoltaic generation based on the fuzzy control method," in *Sustainable Power Generation and Supply, 2009. SUPERGEN'09. International Conference on*, 2009, pp. 1-6.
- [114] W.-M. Lin, C.-M. Hong, and C.-H. Chen, "Neural-network-based MPPT control of a stand-alone hybrid power generation system," *Power Electronics, IEEE Transactions on*, vol. 26, pp. 3571-3581, 2011.
- [115] T. Noguchi and H. Matsumoto, "Maximum-Power-Point Tracking Method of Photovoltaic Using Only Single Current Sensor," *EPE2003, Toulouse*, p. 8, 2003.
- [116] K. Tse, M. Ho, H.-H. Chung, and S. Hui, "A novel maximum power point tracker for PV panels using switching frequency modulation," *Power Electronics, IEEE Transactions on*, vol. 17, pp. 980-989, 2002.
- [117] A. W. Leedy, L. Guo, and K. A. Aganah, "A constant voltage MPPT method for a solar powered boost converter with DC motor load," in *Southeastcon, 2012 Proceedings of IEEE*, 2012, pp. 1-6.
- [118] Y. Zhihao and W. Xiaobo, "Compensation loop design of a photovoltaic system based on constant voltage MPPT," in *Power and Energy Engineering Conference, 2009. APPEEC 2009. Asia-Pacific*, 2009, pp. 1-4.
- [119] A. Pandey, N. Dasgupta, and A. K. Mukerjee, "A simple single-sensor MPPT solution," *Power Electronics, IEEE Transactions on*, vol. 22, pp. 698-700, 2007.
- [120] O. Lopez-Lapena, M. T. Penella, and M. Gasulla, "A new MPPT method for low-power solar energy harvesting," *Industrial Electronics, IEEE Transactions on*, vol. 57, pp. 3129-3138, 2010.
- [121] T. Wegiel and D. Borkowski, "Variable speed small hydropower plant," in *Power Electronics for Distributed Generation Systems (PEDG), 2012 3rd IEEE International Symposium on*, 2012, pp. 167-174.
- [122] S. Adhau, "A comparative study of micro hydro power schemes promoting self sustained rural areas," in *Sustainable Power Generation and Supply, 2009. SUPERGEN'09. International Conference on*, 2009, pp. 1-6.
- [123] F. H. Schwartz and M. Shahidehpour, "Small hydro as green power," in *EIC Climate Change Technology, 2006 IEEE*, 2006, pp. 1-6.
- [124] L. Wang, D.-J. Lee, L.-Y. Chen, J.-Y. Yu, S.-R. Jan, S.-J. Chen, . . . Y.-C. Li, "A micro hydro power generation system for sustainable microgrid development in rural electrification of Africa," in *Power & Energy Society General Meeting, 2009. PES'09. IEEE*, 2009, pp. 1-8.
- [125] Y.-C. Wang, M.-J. Chen, W. Huang, and Y.-J. Lin, "Dynamic analysis of a grid-linked small-hydro induction generation system," in *Electrotechnical Conference, 2004. MELECON 2004. Proceedings of the 12th IEEE Mediterranean*, 2004, pp. 1021-1024.
- [126] L. G. Scherer and R. F. de Camargo, "Frequency and voltage control of micro hydro power stations based on hydraulic turbine's linear model applied on induction generators," in *Power Electronics Conference (COBEP), 2011 Brazilian*, 2011, pp. 546-552.
- [127] L. G. Scherer and R. F. de Camargo, "Control of micro hydro power stations using nonlinear model of hydraulic turbine applied on microgrid systems," in *Power Electronics Conference (COBEP), 2011 Brazilian*, 2011, pp. 812-818.

- [128] L. Giuliani Scherer, R. Figueiredo de Camargo, H. Pinheiro, and C. Rech, "Advances in the modeling and control of micro hydro power stations with induction generators," in *Energy Conversion Congress and Exposition (ECCE), 2011 IEEE*, 2011, pp. 997-1004.
- [129] C. B. Tischer, F. C. Posser, L. G. Scherer, C. M. Franchi, and R. F. de Camargo, "Hybrid method for control of voltage regulation applied in micro hydro power station," in *IECON 2012-38th Annual Conference on IEEE Industrial Electronics Society*, 2012, pp. 1013-1018.
- [130] I. Tamrakar, L. Shilpakar, B. Fernandes, and R. Nilsen, "Voltage and frequency control of parallel operated synchronous generator and induction generator with STATCOM in micro hydro scheme," *Generation, Transmission & Distribution, IET*, vol. 1, pp. 743-750, 2007.
- [131] C. Ion and C. Marinescu, "Control of parallel operating micro hydro power plants," in *Optimization of Electrical and Electronic Equipment (OPTIM), 2010 12th International Conference on*, 2010, pp. 1204-1209.
- [132] I. Ducar and C. Ion, "Design of a PMSG for micro hydro power plants," in *Optimization of Electrical and Electronic Equipment (OPTIM), 2012 13th International Conference on*, 2012, pp. 712-717.
- [133] L. Belhadji, S. Bacha, and D. Roje, "Modeling and control of variable-speed micro-hydropower plant based on Axial-flow turbine and permanent magnet synchronous generator (MHPP-PMSG)," in *IECON 2011-37th Annual Conference on IEEE Industrial Electronics Society*, 2011, pp. 896-901.
- [134] D. Borkowski and T. Wegiel, "Small Hydropower Plant With Integrated Turbine-Generators Working at Variable Speed," *IEEE Transactions on Energy Conversion*, vol. 28, pp. 452 - 459, 2013.
- [135] D. Fodorean, L. Szabo, and A. Miraoui, "Generator solutions for stand alone pico-electric power plants," in *Electric Machines and Drives Conference, 2009. IEMDC'09. IEEE International*, 2009, pp. 434-438.
- [136] C. Marinescu and C. Ion, "Optimum control for an autonomous micro hydro power plant with induction generator," in *PowerTech, 2009 IEEE Bucharest*, 2009, pp. 1-6.
- [137] B. Singh and V. Rajagopal, "Neural-Network-Based Integrated Electronic Load Controller for Isolated Asynchronous Generators in Small Hydro Generation," *Industrial Electronics, IEEE Transactions on*, vol. 58, pp. 4264-4274, 2011.
- [138] V. Rajagopal, B. Singh, and G. Kasal, "Electronic load controller with power quality improvement of isolated induction generator for small hydro power generation," *IET renewable power generation*, vol. 5, pp. 202-213, 2011.
- [139] B. Singh and V. Rajagopal, "Digital control of voltage and frequency of induction generator in isolated small hydro system," in *Power Electronics, Drives and Energy Systems (PEDES), 2012 IEEE International Conference on*, 2012, pp. 1-7.
- [140] S. Doolla and T. Bhatti, "Load frequency control of an isolated small-hydro power plant with reduced dump load," *Power Systems, IEEE Transactions on*, vol. 21, pp. 1912-1919, 2006.
- [141] A. A. Ghadimi and H. Rastegar, "Optimal control and management of distributed generation units in an islanded microgrid," in *Integration of Wide-Scale*

- Renewable Resources Into the Power Delivery System, 2009 CIGRE/IEEE PES Joint Symposium, 2009, pp. 1-7.*
- [142] J.-Y. Kim, J.-H. Jeon, S.-K. Kim, C. Cho, J. H. Park, H.-M. Kim, and K.-Y. Nam, "Cooperative control strategy of energy storage system and microsourses for stabilizing the microgrid during islanded operation," *Power Electronics, IEEE Transactions on*, vol. 25, pp. 3037-3048, 2010.
 - [143] N. Kroutikova, C. Hernandez-Aramburo, and T. Green, "State-space model of grid-connected inverters under current control mode," *IET Electric Power Applications*, vol. 1, pp. 329-338, 2007.
 - [144] J. He and Y. W. Li, "Hybrid Voltage and Current Control Approach for DG-Grid Interfacing Converters With filters," *Industrial Electronics, IEEE Transactions on*, vol. 60, pp. 1797-1809, 2013.
 - [145] T. L. Vandoorn, B. Meersman, J. D. De Kooning, and L. Vandeveld, "Transition from islanded to grid-connected mode of microgrids with voltage-based droop control," *IEEE Transactions on Power System*, vol. 28, pp. 2545 - 2553, 2013.
 - [146] Y.-Y. Hong, M.-C. Hsiao, Y.-R. Chang, Y.-D. Lee, and H.-C. Huang, "Multiscenario Underfrequency Load Shedding in a Microgrid Consisting of Intermittent Renewables," *IEEE Transactions on Power Delivery* vol. 28, pp. 1610 - 1617, 2013.
 - [147] P. Mahat, Z. Chen, and B. Bak-Jensen, "Underfrequency load shedding for an islanded distribution system with distributed generators," *IEEE Transactions on Power Delivery*, vol. 25, pp. 911-918, 2010.
 - [148] F. Caseo, L. Trindade, and W. Freitas, "Smart load shedding for the formation of microgrids fed by synchronous generators," in *Innovative Smart Grid Technologies Latin America (ISGT LA), 2013 IEEE PES Conference On*, 2013, pp. 1-6.
 - [149] J. Bloemink and M. Iravani, "Control of a Multiple Source Microgrid With Built-in Islanding Detection and Current Limiting," *IEEE Transactions on Power Delivery*, vol. 27, pp. 2122-2132, 2012.
 - [150] C. Cho, J.-H. Jeon, J.-Y. Kim, S. Kwon, K. Park, and S. Kim, "Active synchronizing control of a microgrid," *IEEE Transactions on Power Electronics*, vol. 26, pp. 3707-3719, 2011.
 - [151] M. Datta, T. Senjyu, A. Yona, T. Funabashi, and C.-H. Kim, "A frequency-control approach by photovoltaic generator in a PV–diesel hybrid power system," *Energy Conversion, IEEE Transactions on*, vol. 26, pp. 559-571, 2011.
 - [152] M. G. Villalva and J. R. Gazoli, "Comprehensive approach to modeling and simulation of photovoltaic arrays," *Power Electronics, IEEE Transactions on*, vol. 24, pp. 1198-1208, 2009.
 - [153] A. Durgadevi, S. Arulselvi, and S. Natarajan, "Photovoltaic modeling and its characteristics," in *Emerging Trends in Electrical and Computer Technology (ICTECT), 2011 International Conference on*, 2011, pp. 469-475.
 - [154] D. Canever, G. Dudgeon, S. Massucco, J. McDonald, and F. Silvestro, "Model validation and coordinated operation of a photovoltaic array and a diesel power plant for distributed generation," in *Power Engineering Society Summer Meeting, 2001*, 2001, pp. 626-631.

- [155] M. Datta, H. Ishikawa, H. Naitoh, and T. Senjyu, "Frequency control improvement in a PV-diesel hybrid power system with a virtual inertia controller," in *7th IEEE Conference on Industrial Electronics and Applications, ICIEA 2012*, 2012, pp. 1167-1172.
- [156] Z. Yang, C. Wu, H. Liao, Y. Wang, and H. Wang, "Research on hydro/photovoltaic hybrid generating system," in *Power System Technology (POWERCON), 2010 International Conference on*, 2010, pp. 1-6.
- [157] P. Maes, "Artificial life meets entertainment: lifelike autonomous agents," *Communications of the ACM*, vol. 38, pp. 108-114, 1995.
- [158] M. Wooldridge and G. Weiss, "Intelligent agents. Multiagent Systems," *A modern approach to Distributed Artificial Intelligence*, pp. 27-77, 1999.
- [159] S. J. Russell, P. Norvig, J. F. Canny, J. M. Malik, and D. D. Edwards, *Artificial intelligence: a modern approach* vol. 2: Prentice hall Englewood Cliffs, 1995.
- [160] S. D. McArthur, E. M. Davidson, V. M. Catterson, A. L. Dimeas, N. D. Hatziargyriou, F. Ponci, and T. Funabashi, "Multi-agent systems for power engineering applications—Part I: Concepts, approaches, and technical challenges," *Power Systems, IEEE Transactions on*, vol. 22, pp. 1743-1752, 2007.
- [161] F. L. Bellifemine, G. Caire, and D. Greenwood, *Developing multi-agent systems with JADE* vol. 7: John Wiley & Sons, 2007.
- [162] G. Caire, "JADE Tutorial: JADE programming for Beginners," *Documentación de JADE*, vol. 3, 2003.

Vitae

Name	:Tawfiq Naji Kameel
Nationality	:Jordanian
Date of Birth	:7/30/1986
Email	:Tawfiq188@gmail.com
Address	:KFUPM, Student Campus, Dhahran
Academic Background	:Electrical Engineering

Thesis Outcomes

1. T.N. Kameel and M.A. Abido, "Potential of standalone hybrid micro-hydro/PV/diesel microgrid in Saudi Arabia," *Saudi Arabia Smart Grid Conference 2013*
2. T.N. Kameel and M.A. Abido, "Multi-agents system (MAS) applications in microgrid: A Review" (under preparation)
3. T.N. Kameel and M.A. Abido, "Multi-agent based energy management and control system applied for PV/ micro-hydro/ diesel/ battery generations system" (under preparation)
4. T.N. Kameel and M.A. Abido, "A dynamic communication and Zonal control of microgrid using multi-agents system," (under preparation)

Experience

Electrical Engineer: Manifa Project CPF (ARAMCO Project)

Modern Arab Construction Ltd | Khobar | Saudi Arabia *June-2009 > June-2010*

Responsibilities and Duties:

- Installation of Low Voltage Switch Gears and Control Gears
- Installation of Transformers
- Laying of High and Low Voltage Cables above and under ground
- Grounding

Electrical Engineer: Tanajib Water Treatment Plant (ARAMCO Project)

Modern Arab Construction Ltd | Khobar | Saudi Arabia *June-2010 > December-2011*

Responsibilities and Duties:

- Supervisor for electrical activities inside 4.16 KV substation including installation of power transformers, switchgear, MCC, power and control panels
- Leader for testing and pre-commissioning team
- Troubleshooter for control system
- HVAC power and control system
- Preparing the energizing packages for the equipment in substation
- Testing for MV and LV motors in the plants
- Perform no load and full load run for field MV and LV motors

Research Assistant

Center of Engineering Research (CER) at KFUPM | Saudi Arabia

Responsibilities and Duties:

- Carry out researches on pumped storage system in KSA
- Carry out researches on potential of micro hydro and PV generation in KSA
- Translate technical documents from English to Arabic
- Attending workshops arrange by CER.